ON THIN SHALLOW ELASTIC SHELLS OVER POLYGONAL BASES

ON THIN SHALLOW ELASTIC SHELLS
OVER POLYGONAL BASES

by

DOUGLAS S. WALKINSHAW, B. ENG.

A Thesis

Submitted to the Faculty of Graduate Studies

in Partial Fulfilment of the Requirements

for the Degree

Master of Engineering

McMaster University

October 1965

MASTER OF ENGINEERING (1965)

TITLE: On Thin Shallow Elastic Shells Over Polygonal Bases

AUTHOR: Douglas S. Walkinshaw, B.Eng. (McMaster University)

SUPERVISOR: Professor G. Æ. Oravas

NUMBER OF PAGES: viii, 141

SCOPE AND CONTENTS:

This thesis proposes to demonstrate, by means of numerical examples, the applicability of the approximate solution for shallow, spherical, calotte shells enclosing polygonal bases for the purposes of practical design.

The theoretical solution is based on a collocation procedure by means of which prescribed boundary conditions are satisfied at discrete boundary points and is derived from the general theory of MUSHTARI and VLASOV in which the transverse shear deformation of the shell is neglected in comparison with its transverse bending and extensional surface deformation.

ACKNOWLEDGMENTS

The writer wishes to express sincere gratitude to his research supervisor, Dr. G. Æ. Oravas, for his invaluable guidance throughout this investigation.

Grateful acknowledgment is due to Professor J. N. Siddal for his assistance in the execution of the experimental analysis, and also to G. E. Riley and T. E. Michels for their important contributions to this work.

TABLE OF CONTENTS

NOMENCLATURE

u_n	Normal displacement
F	VLASOV's stress function
$\bar{F}_1(\sigma)$, $\bar{F}_2(\sigma)$	Stress resultants per unit length of parametric lines in middle surface of shell
$F_{rr}(\sigma)$, $F_{\theta\theta}(\sigma)$	Normal components of stress resultants in middle surface of shell
$F_{r\theta}(\sigma)$, $F_{\theta r}(\sigma)$	Tangential shear components of stress resultants in middle surface of shell
$F_{rn}(\sigma)$, $F_{\theta n}(\sigma)$	Components of transverse shear stress resultants to middle surface
$\bar{M}_1(\sigma)$, $\bar{M}_2(\sigma)$	Stress couples per unit length of parametric lines in middle surface of shell
$M_{r\theta}(\sigma)$, $M_{\theta r}(\sigma)$	Flexural components of stress couples
$M_{rr}(\sigma)$, $M_{\theta\theta}(\sigma)$	Torsional components of stress couples
$\bar{p}$	Load intensity per unit area of middle surface of shell
p_n	Load intensity component per unit area normal to middle surface of shell

D	Flexural rigidity of shell
E	Modulus of elasticity of shell
λ, μ	CAUCHY-LAMÉ elastic constants
ν	POISSON's ratio
h	Shell's thickness
R	Radius of curvature of middle surface of spherical shell
r	Radial parametric coordinate of shell
$\bar{r} = \bar{r}_o + \bar{\pi}$	Radius vector to arbitrary point in shell
$\bar{r}_o$	Radius vector to middle surface of shell
$\bar{\pi}$	Radius vector of arbitrary point in shell's surface relative to middle surface
$\nabla^2 \equiv \frac{d}{d\bar{r}_o} \cdot \frac{d}{d\bar{r}_o}$	EULER - LAPLACE differential operator
α_1, α_2	Parametric coordinates in middle surface of shell
α_n	Parametric coordinate normal to middle surface of shell
ds_i	Infinitesimal line segment along parametric coordinate α_i

ϵ_{ss}	Middle surface strain parallel to shell's boundary
$\epsilon_{rr}, \epsilon_{\theta\theta}$	Direct middle surface strain
$\bar{e}_r, \bar{e}_\theta$	Unit base vectors in shell's middle surface
$\bar{e}_n$	Unit base vector normal to shell's middle surface
$\bar{e}_s$	Unit vector in surface of shell tangent to shell's boundary
$\bar{n}$	Unit vector in surface of shell normal to shell's boundary
$J_n(x)$	Standardized n-th order BESSELL function of first kind of argument x
$Y_n(x)$	Standardized n-th order BESSELL function of second kind of argument x
$I_n(x)$	Standardized n-th order modified BESSEL function of first kind of argument x
$K_n(x)$	Standardized n-th order modified BESSEL function of second kind of argument x
$ber_n(x)$, $bei_n(x)$	n-th order KELVIN functions of first kind of argument x
$ker_n(x)$, $Kei_n(x)$	n-th order KELVIN functions of second kind of argument x
$i = \sqrt{-1}$	Imaginary unit

$ber'_n(x)$, $bei'_n(x)$	First derivatives of n-th order KELVIN functions of first kind with respect to argument x
$ber''_n(x)$, $bei''_n(x)$	Second derivatives of n-th order KELVIN functions of first kind with respect to argument x

CHAPTER I

INTRODUCTION

The purpose of this investigation was to show that the approximate theoretical solution for shallow, thin, calotte shells of spherical middle surface, subjected to isothermal deformation by uniform normal pressure, given initially by ORAVAS in 1957 (1)* and further studied by him in 1958 and later by RILEY in 1964, will give reliable results for practical design.

TÖLKE's Boundary Collocation Method forms the basis of this solution whereby a rigorous satisfaction of the prescribed boundary conditions is collocated for a number of discrete points located on the boundary of one of the shell's rotationally periodic segments. The solution obtained for the characteristic segment of the shell is applicable to the entire shell since in the Semi-Direct BERNOULLI's Method of solution of the partial differential equations, the rotationally periodic symmetry of the shell's comportment was anticipated in the choice of the direct part of the functional form of the solution series.

RILEY's investigation raised certain fundamental

---

*References are given chronologically in the BIBLIOGRAPHY.

questions pertaining to the extent of the applicability of the collocative boundary value problem to thin shells and the general nature of its numerical accuracy.

It was subsequently established that the number and location of the collocation points are not of such paramount significance to the practical reliability of the results as was initially believed to be the case. Instead, the reliability of the results is largely dependent upon the degree of accuracy employed in the numerical calculations. Therefore McMaster University's I.B.M. 7040 computer was used to perform the extensive numerical computations required for the requisite high degree of accuracy in the solution of the polygonal spherical shell problem.

KELVIN functions, $ber_n(x)$ and $bei_n(x)$, constitute an important part of the truncated series in the collocative solution of the spherical calotte shell problem. The wide range of the orders of magnitude of $ber_n(x)$ and $bei_n(x)$ over their functional order n, produces widely ranging orders of magnitude for the coefficients of the linear collocation equations. A satisfactory solution of these equations as well as subsequent computations required machine computation by double precision techniques which employed 17 figure accuracy.

Theoretical solutions by the collocation method were obtained for spherical shells enclosing hexagonal, rectangular and triangular bases. The distribution of normal displacements, stress resultants and stress couples along radial lines are graphically depicted for the characteristic segments of the three calotte shells.

Comparison of the theoretical and experimental results for the spherical shell enclosing an hexagonal base revealed that the theoretical solution by the collocation method is of acceptable accuracy in view of the unavoidable geometric imperfections in the structure of the experimental shell and of the differences between the actual and theoretically convenient boundary conditions.

The results obtained for the spherical shell over a rectangular base were compared with a solution by another method first given by DIKOVICH in 1960. There are certain differences in the results of the two solutions, some of which, no doubt, were caused by the fact that the boundary conditions of the two shells were not entirely identical. It was observed that while the stress resultants of both solutions were of comparable magnitudes, the normal displacement and the stress couples were of considerably larger magnitudes for the solution by the collocation method.

The solution for the shell over a triangular base has been given without comparison, as no other theoretical solutions are known to exist for such shells.

CHAPTER II

SHELL ENCLOSING HEXAGONAL BASE

The experimental results given by RILEY in 1964 for the shallow spherical shell enclosing an hexagonal base were used for the purpose of verifying the reliability of the theoretical solution by the collocation method. Since this method satisfies prescribed edge conditions only at a set of discrete points on the shell's boundary known as collocation points, there should be some minimum number of points for which the solution will become sufficiently accurate for practical design. Logically, an increase in the number of collocation points above this minimum number should only cause an insignificant increase in the accuracy of the practical solution.

This section gives a thorough comparison of the sectional resultants obtained experimentally and theoretically for various number and distribution of collocation points (see FIGURE 7). The distribution of sectional resultants $F_{rr}(\sigma)$, $F_{\theta\theta}(\sigma)$, $M_{r\theta}(\sigma)$ and $M_{\theta r}(\sigma)$ and normal displacement u_n are depicted graphically along radial lines emanating from the shell's apex (see FIGURE 6).

A vectorial representation of the sectional resultants is given in FIGURE 1. For a spherical shell, coordinates 1 and 2 become the cylindrical coordinates r and θ.

For this shallow polygonal spherical shell of 6-ply periodicity, the boundary conditions

$$F(\sigma)_{nn} = 0 \qquad \text{(II-1)}$$

$$\delta\left(\frac{\partial u_n}{\partial n}\right) = 0 \qquad \text{(II-2)}$$

$$u_n = 0 \qquad \text{(II-3)}$$

$$\epsilon_{ss} = 0 \qquad \text{(II-4)}$$

were used for all the collocation points except at the shell's corners since the strain was certainly not zero at the corner points of the shell structure. Therefore the boundary condition $\epsilon_{ss} = 0$ has been omitted at that point. The boundary conditions (II-1) to (II-4) appear as linear boundary equations of the coefficients of the truncated series solution and are given in APPENDIX A.

It was found that there were some incongruities between theoretical and experimental results especially near the shell's boundary. The theoretical boundary conditions were not rigorously satisfied since the shell structure exhibited some constraint against normal displacement and some rotation of the boundary. Better over-all consistency between the experimental and theoretical results was obtained by introducing the observed experimental average normal boundary stress resultant and average boundary rotation

$$F_{nn}(\sigma) = -240 \text{ lb./in.}$$
$$\delta\left(\frac{\partial u_n}{\partial n}\right) = 0.00055 \text{ rad.}$$

in the boundary equations (II-1) and (II-2) respectively. These modified boundary equations are denoted by (II-1*) and (II-2*) respectively. Part of the deviation between the theoretical and experimental results, near the re-entrant corners of the shell, was due to the stress concentration brought about by the discontinuity of the boundary members at the shell's corners.

A typical I.B.M. 7040 computer programme by which the theoretical solution may be obtained is now given.

Computer Programme

```
$IBFTC
C       BØUNDARY CØLLØCATIØN FØR SECTIØNAL RESULTANTS
        DØUBLE PRECISIØN  FR(20,53),FI(20,53),U(20),E(20),BERØ(20),BEIØ(
       120),BER(20,14),BEI(20,14),BERI(20,7),BEII(20,7),BERII(20,7),
       2BEIII(20,7),H(20),Ø(20),AA(20),RR(27),D(27),
       3R(20),ZZ(10),Z(10),A(27,27),QQ(10),Q(10),CØ(27),CI(27),DIS(15),
       4RØT(15),UN(7,20),FRR(7,20),FØØ(7,20),BMRØ(7,20),BMØR(7,20),ARG(20)
       5,FK,CC,Y,CK,B,ZZZ(10),SID(10)
       6,C,DY,DZ,X,T,PRESS,RAD,V,DD,W,BB,CT,ZØ,API,RØ,CK1,CK2,C2K1,C2K2,
       7C2K,FK1,FK2,F4K,F4K2,EF
        DIMENSIØN NI(108),WØRK(54)
        L=7
        LU=9+L
        LC=9+L
        LL=L+1
        LO=L-1
        READ 2,(ARG(J),J=1,LC)
        READ 3,(AA(J),J=1,LC)
        READ 1,(BERØ(J),J=1,LU)
        READ 1,(BEIØ(J),J=1,LU)
        READ 1,(BERI(K,1),K=1,LC)
        READ 1,(BEII(K,1),K=1,LC)
        READ 5,(QQ(I),I=1,7)
    1   FØRMAT (1D20.14)
    2   FØRMAT (1D7.2)
    3   FØRMAT (1D7.0)
    5   FØRMAT (7D7.1)
        EF=1.D+7
        PRESS=-20.D0
        RAD=64.D0
        V=.33D0
        DD= EF      *.375D0**3/(12.D0*(1.D0-(V**2)))
        W=(12.D0*(1.D0-(V**2)))**.5D0/((EF     ) *(.375D0**2))
        BB=((12.D0*(1.D0-(V**2)))**.5D0/(64.D0*.375D0))**.5D0
        API=3.14159265359D0
        ZØ=API/6.D0
        RØ=25.0D0*DCØS(ZØ)
        DØ 773 I=1,LU
  773   R(I)=ARG(I)/BB
        DØ 774 I=1,L
        IF (R(I)-RØ) 771,771,772
  771   R(I)=RØ
  772   SID(I)=(R(I)**2-RØ**2)**0.5D0
  774   CØNTINUE
        DØ 775 I=1,L
  775   ZZZ(I)=SID(I)/RØ
        DØ 776 I=1,L
  776   Z(I)=DATAN(ZZZ(I))
        DØ 777 I=1,L
  777   ZZ(I)=Z(I)*(180.D0/API)
        PRINT 150,ZØ
        PRINT 150,RØ
        PRINT 6,(R(I),I=1,LU)
        PRINT 7,(ZZ(I),I=1,L)
    6   FØRMAT (6E18.8/6E18.8/6E18.8/6E18.8/3E18.8)
```

```
    7 FØRMAT (7D18.10)
      NN=51
      N1=NN+1
      N2=NN+2
      NN1=NN-1
      NN2=NN-2
      NN3=NN-3
      NN4=NN-4
      C=NN
      DØ 8 I=1,7
    8 Q(I)=(API/180.DO)*QQ(I)
      DØ 9 J=1,LU
      U(J)=-ARG(J)/2.DO**0.5DO
      E(J)=ARG(J)/2.DO**0.5DO
    9 CØNTINUE
      DZ=1.DO
      DY=2.DO
      DØ 10 J=1,LU
      X=2.DO/(U(J)**2+E(J)**2)
      FR(J,1)=0.0
      FI(J,1)=0.0
      FR(J,2)=AA(J)
      FI(J,2)=0.0
      FR(J,3)=X*(C-DZ)*U(J)*AA(J)
      FI(J,3)=-X*(C-DZ)*E(J)*AA(J)
      FR(J,4)=X*(C-DY)*U(J)*FR(J,3)-AA(J)+X*(C-DY)*E(J)*FI(J,3)
      FI(J,4)=-X*(C-DY)*E(J)*FR(J,3)+X*(C-DY)*U(J)*FI(J,3)
   10 CØNTINUE
      DØ 11 J=1,LU
      DØ 11 I=1,NN3
      Y=NN2-I
      T=(2.DO/(U(J)**2+E(J)**2))*Y
      FR(J,I+4)=T*U(J)*FR(J,I+3)-FR(J,I+2)+T*E(J)*FI(J,I+3)
      FI(J,I+4)=T*U(J)*FI(J,I+3)-FI(J,I+2)-T*E(J)*FR(J,I+3)
   11 CØNTINUE
      DØ 12 J=1,LU
      H(J)=(FR(J,N1)*BERØ(J)+FI(J,N1)*BEIØ(J))/(BERØ(J)**2+BEIØ(J)**2)
      Ø(J)=(-FR(J,N1)*BEIØ(J)+FI(J,N1)*BERØ(J))/(BERØ(J)**2+BEIØ(J)**2)
   12 CØNTINUE
      DØ 13 J=1,LU
      DØ 13 I=16,N1,6
      LM=N2-I
      LN=((LM-1)/6)+1
      BER(J,LN)=(FI(J,I)*Ø(J)+H(J)*FR(J,I))/(H(J)**2+Ø(J)**2)
      BEI(J,LN)=(-FR(J,I)*Ø(J)+H(J)*FI(J,I))/(H(J)**2+Ø(J)**2)
   13 CØNTINUE
      DØ 778 J=1,LU
      DØ 778 I=17,NN4,6
      LM=N2-I
      LN=LM/6+7
      BER(J,LN)=(FI(J,I)*Ø(J)+H(J)*FR(J,I))/(H(J)**2+Ø(J)**2)
      BEI(J,LN)=(-FR(J,I)*Ø(J)+H(J)*FI(J,I))/(H(J)**2+Ø(J)**2)
  778 CØNTINUE
      DØ 14 K=1,LC
      DØ 14 M=1,6
```

```
      I=M+7
      B=6*M
      BERI(K,M+1)=-(1.D0/2.D0**.5D0)*(BER(K,I)+BEI(K,I))-(B*BER(K,M+1))
     1/ARG(K)
      BEII(K,M+1)=(1.D0/2.D0**.5D0)*(BER(K,I)-BEI(K,I))-( B*BEI(K,M+1))
     1/ARG(K)
   14 CØNTINUE
      DØ 15  K=1,LC
      DØ 15 M=1,7
      CC=ABS(6*(M-1))
      BERII(K,M)=-(DZ/ARG(K))*BERI(K,M)+((CC/ARG(K))**DY)*BER(K,M)-BEI
     1(K,M)
      BEIII(K,M)=-(DZ/ARG(K))*BEII(K,M)+((CC/ARG(K))**DY)*BEI(K,M)+BER(
     1K,M)
   15 CØNTINUE
      PRINT 150,BB
      PRINT 150,W
      PRINT 150,DD
      PRINT 150,(BER(1,1))
      PRINT 150,(BEI(1,1))
  150 FØRMAT (1D20.12)
      N=4*L-1
      LLL=2*L+1
      LLLL=3*L+1
      L2=2*L
      L3=3*L
      LL0=L+3
      LL1=L+2
      LL2=2*L+2
      LL3=3*L+2
      CT=1.D-20
      DØ 20 J=1,L
      I=J
      A(J,1)=(DZ/W)*(BB/R(I))*BEII(I,1)*(DCØS(Z(I))**2)*CT
     1+((BB**2)/W)*BEIII(I,1)*(DSIN(Z(I))**2)*CT
      A(J,2)=-(DZ/W)*(BB/R(I))*BERI(I,1)*(DCØS(Z(I))**2)*CT
     1+((BB**2)/W)*BERII(I,1)*(DSIN(Z(I))**2)*CT
      A(J,3)=0.0
   20 CØNTINUE
      DØ 21 J=LL,L2
      I=J-L
      A(J,1)=-BB*BERI(I,1)*(DCØS(Z(I)))*CT
      A(J,2)=-BB*BEII(I,1)*(DCØS(Z(I)))*CT
      A(J,3)=0.0
   21 CØNTINUE
      DØ 22 J=LLL,L3
      I=J-2*L
      A(J,1) =BER(I,1)*CT
      A(J,2) =BEI(I,1) *CT
      A(J,3)=1.D0*CT
   22 CØNTINUE
      DØ 23 J=LLLL,N
      I=J-3*L
      A(J,1)=(((DZ/W)*(BB/R(I))*BEII(I,1)-V*((BB**2)/W)*BEIII(I,1))*
     1(DSIN(Z(I))**2)+(((BB**2)/W)*BEIII(I,1)-(V/W)*(BB/R(I))*BEII(I,1))
```

```
      2*(DCØS(Z(I))**2))*CT
       A(J,2)=((V*((BB**2)/W)*BERII(I,1)-BB/( W*R(I))*BER(I,1))*(DSIN(Z(I
      1))**2)+((V/W)*(BB/R(I))*BERI(I,1)-((BB**2)/W)*BERII(I,1))
      2*(DCØS(Z(I))**2))*CT
       A(J,3)=0.0
   23 CØNTINUE
       DØ 25 K=4,LL1
       DØ 25 J=1,L
       M=K-3+1
       I=J
       CK=FLØAT (6*(K-3))
       CK1=CK-1.D0
       CK2=CK-2.D0
       A(J,K)=((((DZ/W)*(BB/R(I))*BEII(I,M)-(DZ/W)*((CK/R(I))**2)*BEI(I,M
      1))*(DCØS(Z(I))**2)+((BB**2)/W)*BEIII(I,M)*((DSIN(Z(I)))**2))*
      2(DCØS(CK*Z(I)))+((-CK/W)*(BB/R(I))*BEII(I,M)+(CK/W)*(DZ/(R(I)**2))
      3*BEI(I,M))*(DSIN(2.D0*Z(I)))*(DSIN(CK*Z(I))))*CT
   25 CØNTINUE
       DØ 26 K=4,LL1
       DØ 26 J=LL,L2
       M=K-3+1
       I=J-L
       CK=FLØAT (6*(K-3))
       CK1=CK-1.D0
       CK2=CK-2.D0
       A(J,K)=(-(BB*BERI(I,M)*(DCØS(Z(I)))*(DCØS(CK*Z(I))))-(CK/R(I)*
      1BER(I,M)*(DSIN(Z(I)))*DSIN(CK*Z(I)))))*CT
   26 CØNTINUE
       DØ 27 K=4,LL1
       DØ 27 J=LLL,L3
       M=K-3+1
       I=J-2*L
       CK=FLØAT (6*(K-3))
       CK1=CK-1.D0
       CK2=CK-2.D0
       A(J,K)=(BER(I,M))*(DCØS(CK*Z(I)))*CT
   27 CØNTINUE
       DØ 28 K=4,LL1
       DØ 28 J=LLLL,N
       M=K-3+1
       I=J-3*L
       CK=FLØAT (6*(K-3))
       CK1=CK-1.D0
       CK2=CK-2.D0
       A(J,K)=((((DZ/W)*(BB/R(I))*BEII(I,M)-(DZ/W)*((CK/R(I))**2)*BEI(I,M
      1)-V*((BB**2)/W)*BEIII(I,M))*((DSIN(Z(I)))**2)+(((BB**2)/W)*BEIII(I
      2,M)-(V/W)*(BB/R(I))*BEII(I,M)+(V/W)*((CK/R(I))**2)*BEI(I,M))*((
      3DCØS(Z(I)))**2))*(DCØS(CK*Z(I)))+((DZ+V)*(CK/W)*((BB/R(I))*BEII(I,
      4M)-(DZ/R(I)**2)*BEI(I,M))*(DSIN(DY*Z(I))))*(DSIN(CK*Z(I))))*CT
   28 CØNTINUE
       DØ 29 K=LL0,LLL
       DØ 29 J=1,L
       M=K-3-L0+1
       I=J
       CK=FLØAT (6*(K-3-L0))
```

```
      CK1=CK-1.D0
      CK2=CK-2.D0
      A(J,K)=((((-DZ/W)*(BB/R(I))*BERI(I,M)+(DZ/W)*((CK/R(I))**2)*BER
     1(I,M))*(DCØS(Z(I))**2)-((BB**2)/W)*BERII(I,M)*((DSIN(Z(I)))**2))*
     2(DCØS(CK*Z(I)))+((CK/W)*(BB/R(I))*BERI(I,M)-(CK/W)*(DZ/(R(I)**2))
     3*BER(I,M))*(DSIN(DY*Z(I)))*(DSIN(CK*Z(I))))*CT
   29 CØNTINUE
      DØ 30 K=LLO,LLL
      DØ 30 J=LL,L2
      M=K-3-LO+1
      I=J-L
      CK=FLØAT (6*(K-3-LO))
      CK1=CK-1.D0
      CK2=CK-2.D0
      A(J,K)=(-(BB*BEII(I,M)*(DCØS(Z(I)))))*(DCØS(CK*Z(I)))-((CK/R(I))*BE
     1I(I,M)*(DSIN(Z(I)))))*(DSIN(CK*Z(I)))))*CT
   30 CØNTINUE
      DØ 31 K=LLO,LLL
      DØ 31 J=LLL,L3
      M=K-3-LO+1
      I=J-2*L
      CK=FLØAT (6*(K-3-LO))
      CK1=CK-1.D0
      CK2=CK-2.D0
      A(J,K)=(BEI(I,M))*(DCØS(CK*Z(I)))*CT
   31 CØNTINUE
      DØ 32 K=LLO,LLL
      DØ 32 J=LLLL,N
      M=K-3-LO+1
      I=J-3*L
      CK=FLØAT (6*(K-3-LO))
      CK1=CK-1.D0
      CK2=CK-2.D0
      A(J,K)=(((BB/(W*R(I))*BERI(I,M)+(DZ/W)*((CK/R(I))**2)*BER(I,M)
     1+V*((BB**2)/W)*BERII(I,M))*((DSIN(Z(I)))**2)+(-((BB**2)/W)*BERII(I
     2,M)+(V/W)*(BB/R(I)) *BERI(I,M)-(V/W)*((CK/R(I))**2)*BER(I,M))*
     3(DCØS(Z(I))**2))*(DCØS(CK*Z(I)))-((DZ+V)*(CK/W)*(-(DZ/(R(I)**2))
     4*BER(I,M)+(BB/R(I))*BER(I,M)))*(DSIN(DY*Z(I)))*(DSIN(CK*Z(I))))*CT
   32 CØNTINUE
      DØ 33 K=LL2,L3
      DØ 33 J=1,L
      M=K-3-2*LO+1
      I=J
      A(J,K)=0.0
   33 CØNTINUE
      DØ 34 K=LL2,L3
      DØ 34 J=LL,L2
      M=K-3-2*LO+1
      I=J-L
      CK=FLØAT (6*(K-3-2*LO))
      CK1=CK-1.D0
      CK2=CK-2.D0
      C2K1=CK1/2.D0
      A(J,K)=-CK*(R(I)**C2K1)*CT*(R(I)**C2K1)*DCØS(Z(I))*DCØS(CK*Z(I))
     1         -CK*(R(I)**C2K1)*CT*(R(I)**C2K1)*DSIN(Z(I))*DSIN(CK*Z(I))
```

```
   34 CØNTINUE
      DØ 35 K=LL2,L3
      DØ 35 J=LLL,L3
      M=K-3-2*LO+1
      I=J-2*L
      CK=FLØAT (6*(K-3-2*LO))
      CK1=CK-1.DO
      CK2=CK-2.DO
      C2K=CK/2.DO
      A(J,K)=(R(I)**C2K)*CT*(R(I)**C2K)*DCØS(CK*Z(I))
   35 CØNTINUE
      DØ 36 K=LL2,L3
      DØ 36 J=LLLL,N
      M=K-3-2*LO+1
      I=J-3*L
      A(J,K)=0.0
   36 CØNTINUE
      DØ 37 K=LLLL,N
      DØ 37 J=1,L
      M=K-3-3*LO+1
      I=J
      CK=FLØAT (6*(K-3-3*LO))
      CK1=CK-1.DO
      CK2=CK-2.DO
      C2K2=CK2/2.DO
      A(J,K)=(R(I)**C2K2)*CT*(R(I)**C2K2)*CK*(CK1/W)*((((DSIN(Z(I)))**2)
     1-((DCØS(Z(I)))**2))*(DCØS(CK*Z(I)))-(DSIN(DY*Z(I)))*(DSIN(CK*Z(I))
     2))
   37 CØNTINUE
      DØ 38 K=LLLL,N
      DØ 38 J=LL,L2
      M=K-3-3*LO+1
      I=J-L
      A(J,K)=0.0
   38 CØNTINUE
      DØ 39 K=LLLL,N
      DØ 39 J=LLL,L3
      M=K-3-3*LO+1
      I=J-2*L
      A(J,K)=0.0
   39 CØNTINUE
      DØ 40 K=LLLL,N
      DØ 40 J=LLLL,N
      M=K-3-3*LO+1
      I=J-3*L
      CK=FLØAT (6*(K-3-3*LO))
      CK1=CK-1.DO
      CK2=CK-2.DO
      C2K2=CK2/2.DO
      A(J,K)=(R(I)**C2K2)*CT*(R(I)**C2K2)*((DZ+V)/W)*CK*CK1*((((DCØS(Z(I
     1)))**2)-((DSIN(Z(I)))**2))*(DCØS(CK*Z(I)))+(DSIN(DY*Z(I)))*(DSIN(
     2CK*Z(I))))
   40 CØNTINUE
      CØ(1 )=1.D 13
      CØ(2 )=1.D 13
```

```
      CØ(3  )=1.D 15
      CØ(4  )=1.D 14
      CØ(5  )=1.D 16
      CØ(6  )=1.D 19
      CØ(7  )=1.D 23
      CØ(8  )=1.D 27
      CØ(9  )=1.D 31
      CØ(10)=1.D 14
      CØ(11)=1.D 16
      CØ(12)=1.D 19
      CØ(13)=1.D 23
      CØ(14)=1.D 28
      CØ(15)=1.D 32
      CØ(16)=1.D 07
      CØ(17)=1.D-02
      CØ(18)=1.D-10
      CØ(19)=1.D-18
      CØ(20)=1.D-26
      CØ(21)=1.D-34
      CØ(22)=1.D 07
      CØ(23)=1.D-02
      CØ(24)=1.D-11
      CØ(25)=1.D-19
      CØ(26)=1.D-27
      CØ(27)=1.D-35
      PRINT 150,BB
      PRINT 150,W
      PRINT 150,DD
      DØ 42 I=1,N
      DØ 42 J=1,N
      A(I,J)=A(I,J)*CØ(J)
   42 CØNTINUE
      DØ 80 I=1,L
   80 CI(I)=DZ
      DØ 81 I=LL,L3
   81 CI(I)=1.D+5
      DØ 82 I=LLLL,N
   82 CI(I)=DZ
      DØ 43 J=1,N
      DØ 43 I=1,N
   43 A(I,J)=A(I,J)*CI(I)
      PRINT 150,(BER(1,1))
      PRINT 150,(BEI(1,1))
   52 FØRMAT (7E18.8/7E18.8/7E18.8/6E18.8//)
   41 CALL DMINVS (A,27,N,O.,IERR,NI,WØRK)
      PRINT 150,BB
      PRINT 150,W
      PRINT 150,DD
      PRINT 150,(BER(1,1))
      PRINT 150,(BEI(1,1))
      DØ 56 I=1,N
      DØ 56 J=1,N
      A(I,J)=A (I,J)*CI(J)
   56 CØNTINUE
      DØ 45 J=1,L
```

```
   45 D(J)=-PRESS*RAD/DY-240.D0
      DØ 46 J=LL,L2
   46 D(J)=0.00055D0
      DØ 47 J=LLL,L3
   47 D(J)=-PRESS*(RAD **2)/(EF*0.375D0)
      DØ 48 J=LLLL,N
   48 D(J)=-(DZ-V)*PRESS*RAD/DY
      DØ 49 I=1,N
   49 RR(I)=0.0
      DØ 50 I=1,N
      DØ 50 J=1,N
   50 RR(I)=RR(I)+A(I,J)*D(J)
      DØ 57 I=1,N
      RR(I)=RR(I)*CØ(I)
   57 CØNTINUE
      PRINT 51,(RR(I),I=1,N)
   51 FØRMAT (5X,8E15.8//5X,8E15.8//5X,8E15.8//5X,3E15.8//)
      DØ 163 I=1,1
      DØ 163 J=1,1
      PRINT 158
  158 FØRMAT (//5X,9HDISP CØMP/)
      PRINT 150,(BER(1,1))
      PRINT 150,(BEI(1,1))
      PRINT 150,CT
      PRINT 150,RR(1)
      PRINT 150,RR(2)
      DIS(1)=PRESS*(RAD**2)/(EF*.375D0)
      PRINT159,(DIS(1))
      DIS(1)=RR(2)*BEI(J,1)*CT
      PRINT159,(DIS(1))
      DIS(1)=RR(1)*BER(J,1)*CT
      PRINT159,(DIS(1))
      DIS(1)=RR(3)*CT
      PRINT159,(DIS(1))
      DØ 160 K=1,LO
      K6=K+1
      FK=6*K
      FK1=FK-1.D0
      FK2=FK-2.D0
      K3=3+K
      KL3=3+LO+K
      KLL3=3+2*LO+K
      KLLL3=3+3*LO+K
      F4K=FK/4.D0
      F4K2=FK2/4.D0
      DIS(K)=RR(KL3)*BEI(J,K6)*CT*DCØS(FK*Q(I))
      PRINT 159,(DIS(K))
      DIS(K)=RR(K3)*BER(J,K6)*CT*DCØS(FK*Q(I))
      PRINT 159,(DIS(K))
      DIS(K)=((((RR(KLL3)*R(J)**F4K)*R(J)**F4K)*R(J)**F4K)*CT)*R(J)**F4K
     1*DCØS(FK*Q(I))
      PRINT 159,(DIS(K))
  159 FØRMAT (5X,1E18.8/)
  160 CØNTINUE
      PRINT 161
```

```
  161 FØRMAT (//5X,8HRØT CØMP/)
      RØT(1)=PRESS*RAD*((R(J)**2)/4.D0)
      PRINT 159,(RØT(I))
      RØT(1)=(DZ/W)*RR(1)*BEI(J,1)*CT
      PRINT 159,(RØT(I))
      RØT(1)=-(DZ/W)*RR(2)*BER(J,1)*CT
      PRINT 159,(RØT(I))
      DØ 162 K=1,LO
      K6=K+1
      FK=6*K
      FK1=FK-1.D0
      FK2=FK-2.D0
      K3=3+K
      KL3=3+LO+K
      KLL3=3+2*LO+K
      KLLL3=3+3*LO+K
      F4K=FK/4.D0
      F4K2=FK2/4.D0
      RØT(K)=(DZ/W)*(RR(K3)*BEI(J,K6))*CT*DCØS(FK*Q(I))
      PRINT 159,(RØT(K))
      RØT(K)=-(DZ/W)*(RR(KL3)*BER(J,K6))*CT*DCØS(FK*Q(I))
      PRINT 159,(RØT(K))
      RØT(K)=(DZ/W)*((((RR(KLLL3)*R(J)**F4K)*R(J)**F4K)*R(J)**F4K)*CT)
     1*R(J)**F4K*DCØS(FK*Q(I))
      PRINT 159,(RØT(K))
  162 CØNTINUE
  163 CØNTINUE
      DØ 60 I=1,7
      DØ 60 J=LL,LC
      UN(I,J)=PRESS*(RAD**2)/(EF        *.375D0)+(RR(2)*BEI(J,1)
     1+RR(1)*BER(J,1)+RR(3))*CT
      FRR(I,J)=PRESS*RAD/DY+(RR(1)*(BB/(W*R(J)))*BEII(J,1)
     1-RR(2)*(BB/(W*R(J)))*BERI(J,1))*CT
      FØØ(I,J)=PRESS*RAD/DY+(RR(1)*((BB**2)/W)*BEIII(J,1)-RR(2)*((BB**2)
     1/W)*BERII(J,1))*CT
      BMRØ(I,J)=DD*(-RR(1)*((BB**2)*BERII(J,1)+V*(BB/R(J))*BERI(J,1))
     1-RR(2)*((BB**2)*BEIII(J,1)+V*(BB/R(J))*BEII(J,1)))*CT
      BMØR(I,J)=DD*(RR(1)*((BB/R(J))*BERI(J,1)+V*(BB**2)*BERII(J,1))+RR(
     12)*((BB/R(J))*BEII(J,1)+V*(BB**2)*BEIII(J,1)))*CT
   60 CØNTINUE
      PRINT 150,BB
      PRINT 150,W
      PRINT 150,DD
      DØ 61 I=1,7
      DØ 61 J=LL,LC
      DØ 61 K=1,LO
      K6=K+1
      FK=6*K
      FK1=FK-1.D0
      FK2=FK-2.D0
      K3=3+K
      KL3=3+LO+K
      KLL3=3+2*LO+K
      KLLL3=3+3*LO+K
      F4K=FK/4.D0
```

```
      F4K2=FK2/4.D0
      UN(I,J)=UN(I,J)+((RR(KL3)*BEI(J,K6)+RR(K3)*BER(J,K6))*CT
     1+((((RR(KLL3)*R(J)**F4K)*R(J)**F4K)*R(J)**F4K)*CT)*R(J)**F4K)
     2*DCØS(FK*Q(I))
      FRR(I,J)=FRR(I,J)+((RR(K3)*((-DZ/W)*((FK/R(J))**2)*BEI(J,K6)
     1+(BB/(W*R(J)))*BEII(J,K6))+RR(KL3)*((DZ/W)*((FK/R(J))**2)*
     2BER(J,K6)-(BB/(W*R(J)))*BERI(J,K6)))*CT
     3-FK*(FK1/W)*((((RR(KLLL3)*R(J)**F4K2)*R(J)**F4K2)*R(J)**F4K2)*CT)
     4*R(J)**F4K2)*DCØS(FK*Q(I))
      FØØ(I,J)=FØØ(I,J)+((RR(K3)*(((BB**2)/W)*BEIII(J,K6))-RR(KL3)*(((
     1BB**2)/W)*BERII(J,K6)))*CT
     2+FK*(FK1/W)*((((RR(KLLL3)*R(J)**F4K2)*R(J)**F4K2)*R(J)**F4K2)*CT)
     3*R(J)**F4K2)*DCØS(FK*Q(I))
      BMRØ(I,J)=BMRØ(I,J)+DD*((RR(K3)*((-BB**2)*BERII(J,K6)+V*((FK/R(J))
     1**2)*BER(J,K6)-V*(BB/R(J))*BERI(J,K6))+RR(KL3)*(-(BB**2)*BEIII(J,
     2K6)+V*((FK/R(J))**2)*BEI(J,K6)-V*(BB/R(J))*BEII(J,K6)))*CT
     3-(DZ-V)*FK*FK1*((((RR(KLL3)*R(J)**F4K2)*R(J)**F4K2)*R(J)**F4K2)
     4*CT)*R(J)**F4K2)*DCØS(FK*Q(I))
      BMØR(I,J)=BMØR(I,J)+DD*((RR(K3)*(-((FK/R(J))**2)*BER(J,K6)+(BB/
     1R(J))*BERI(J,K6)+V*(BB**2)*BERII(J,K6))+RR(KL3)*(-((FK/R(J))**2)*
     2BEI(J,K6)+(BB/R(J))*BEII(J,K6)+V*(BB**2)* BEIII(J,K6)))*CT
     3-(DZ-V)*FK*FK1*((((RR(KLLL3)*R(J)**F4K2)*R(J)**F4K2)*R(J)**F4K2)*
     4 CT)*R(J)**F4K2)*DCØS(FK*Q(I))
   61 CØNTINUE
      DØ 400 J=1,L
      I=J
      UN(I,J)=PRESS*(RAD**2)/(EF      *.375D0)+(RR(2)*BEI(J,1)
     1+RR(1)*BER(J,1)+RR(3))*CT
      FRR(I,J)=PRESS*RAD/DY+(RR(1)*(BB/(W*R(J)))*BEII(J,1)
     1-RR(2)*(BB/(W*R(J)))*BERI(J,1))*CT
      FØØ(I,J)=PRESS*RAD/DY+(RR(1)*((BB**2)/W)*BEIII(J,1)-RR(2)*((BB**2)
     1/W)*BERII(J,1))*CT
      BMRØ(I,J)=DD*(-RR(1)*((BB**2)*BERII(J,1)+V*(BB/R(J))*BERI(J,1))
     1-RR(2)*((BB**2)*BEIII(J,1)+V*(BB/R(J))*BEII(J,1)))*CT
      BMØR(I,J)=DD*(RR(1)*((BB/R(J))*BERI(J,1)+V*(BB**2)*BERII(J,1))+RR(
     12)*((BB/R(J))*BEII(J,1)+V*(BB**2)*BEIII(J,1)))*CT
  400 CØNTINUE
      PRINT 150,BB
      PRINT 150,W
      PRINT 150,DD
      DØ 402 J=1,L
      DØ 402 K=1,LO
      I=J
      K6=K+1
      FK=6*K
      FK1=FK-1.D0
      FK2=FK-2.D0
      K3=3+K
      KL3=3+LO+K
      KLL3=3+2*LO+K
      KLLL3=3+3*LO+K
      F4K=FK/4.D0
      F4K2=FK2/4.D0
      UN(I,J)=UN(I,J)+((RR(KL3)*BEI(J,K6)+RR(K3)*BER(J,K6))*CT
     1+((((RR(KLL3)*R(J)**F4K)*R(J)**F4K)*R(J)**F4K)*CT)*R(J)**F4K)
```

```
      2*DCØS(FK*Z(I))
       FRR(I,J)=FRR(I,J)+((RR(K3)*((-DZ/W)*((FK/R(J))**2)*BEI(J,K6)
      1+(BB/(W*R(J)))*BEII(J,K6))+RR(KL3)*((DZ/W)*((FK/R(J))**2)*
      2BER(J,K6)-(BB/(W*R(J)))*BERI(J,K6)))*CT
      3-FK*(FK1/W)*((((RR(KLLL3)*R(J)**F4K2)*R(J)**F4K2)*R(J)**F4K2)*CT)
      4*R(J)**F4K2)*DCØS(FK*Z(I))
       FØØ(I,J)=FØØ(I,J)+((RR(K3)*(((BB**2)/W)*BEIII(J,K6))-RR(KL3)*(((
      1BB**2)/W)*BERII(J,K6)))*CT
      2+FK*(FK1/W)*((((RR(KLLL3)*R(J)**F4K2)*R(J)**F4K2)*R(J)**F4K2)*CT)
      3*R(J)**F4K2)*DCØS(FK*Z(I))
       BMRØ(I,J)=BMRØ(I,J)+DD*((RR(K3)*((-BB**2)*BERII(J,K6)+V*((FK/R(J))
      1**2)*BER(J,K6)-V*(BB/R(J))*BERI(J,K6))+RR(KL3)*(-(BB**2)*BEIII(J,
      2K6)+V*((FK/R(J))**2)*BEI(J,K6)-V*(BB/R(J))*BEII(J,K6)))*CT
      3-(DZ-V)*FK*FK1*((((RR(KLL3)*R(J)**F4K2)*R(J)**F4K2)*R(J)**F4K2)
      4*CT)*R(J)**F4K2)*DCØS(FK*Z(I))
       BMØR(I,J)=BMØR(I,J)+DD*((RR(K3)*(-((FK/R(J))**2)*BER(J,K6)+(BB/
      1R(J))*BERI(J,K6)+V*(BB**2)*BERII(J,K6))+RR(KL3)*(-((FK/R(J))**2)*
      2BEI(J,K6)+(BB/R(J))*BEII(J,K6)+V*(BB**2)* BEIII(J,K6)))*CT
      3-(DZ-V)*FK*FK1*((((RR(KLLL3)*R(J)**F4K2)*R(J)**F4K2)*R(J)**F4K2)*
      4 CT)*R(J)**F4K2)*DCØS(FK*Z(I))
  402 CØNTINUE
      PRINT 85,(ZZ(J),J=1,L)
      PRINT 63
   63 FØRMAT (28X,6HNØRMAL,2X,12HDISPLACEMENT//)
      PRINT 62,((UN(I,J),I=1,7),J=LL,LC)
      PRINT 85,(UN   (I,I),I=1,L)
      PRINT 64
   64 FØRMAT (26X,6HRADIAL,2X,6HSTRESS,2X,9HRESULTANT//)
      PRINT 62,((FRR(I,J),I=1,7),J=LL,LC)
      PRINT 85,(FRR (I,I),I=1,L)
      PRINT 65
   65 FØRMAT (26X,6HCIRCUM,2X,6HSTRESS,2X,9HRESULTANT//)
      PRINT 62,((FØØ(I,J),I=1,7),J=LL,LC)
      PRINT 85,(FØØ (I,I),I=1,L)
      PRINT 66
   66 FØRMAT (24X,6HCIRCUM,2X,6HTRANSV,2X,6HSTRESS,2X,6HCØUPLE//)
      PRINT 62,((BMRØ(I,J),I=1,7),J=LL,LC)
      PRINT 85,(BMRØ(I,I),I=1,L)
      PRINT 67
   67 FØRMAT (24X,6HRADIAL,2X,6HTRANSV,2X,6HSTRESS,2X,6HCØUPLE//)
      PRINT 62,((BMØR(I,J),I=1,7),J=LL,LC)
      PRINT 85,(BMØR(I,I),I=1,L)
   62 FØRMAT (5X,7E18.8)
   85 FØRMAT (//5X,7E18.8)
      STØP
      END
```

1. LEGEND AND OUTLINE

(a) COLLOCATION POINTS

. L = 7

(b) SHELL PARAMETERS

π - API

shell periodicity - k = 6

shell base circle - 25 in. radius

central angle of characteristic segment - ZØ = API/6

shell radius - RAD = 64 in.

coefficient of elasticity, E - EF = 10^7 lb./in.^{2} (aluminium)

POISSON's ratio, ν - V = 0.33

normal pressure, p_n - PRESS = -20 p.s.i.

(c) KELVIN FUNCTIONS

constant a - AA(I)

function F_n, $\Re[F_n(\lambda r)]$ - FR(I,J)
$\Im[F_n(\lambda r)]$ - FI(I,J)

constant α, α_r - H(I)
α_i - Ø(I)

KELVIN functions of the first kind

zero order $\mathrm{ber}_o\,(\lambda r)$ - BERØ(I)
$\mathrm{bei}_o\,(\lambda r)$ - BEIØ(I)

order n $\mathrm{ber}_n\,(\lambda r)$ - BER(I,J)
$\mathrm{bei}_n\,(\lambda r)$ - BEI(I,J)

first derivative $\mathrm{ber}_n'\,(\lambda r)$ - BERI(I,J)
$\mathrm{bei}_n'\,(\lambda r)$ - BEII(I,J)

second derivative $\quad ber''_n(\lambda r)$ - BERII(I,J)

$bei''_n(\lambda r)$ - BEIII(I,J)

where

I represents the argument λr

and J represents the order n .

(d) SIMULTANEOUS EQUATIONS SATISFYING BOUNDARY EQUATIONS

These equations are set up in the form

$$A(I,J) \times RR(J) = D(I) \qquad \text{(II-5)}$$

where

I represents row subscripts ,

J represents column subscripts ,

A(I,J) represents the coefficients φ,

RR(J) represents the constants A_o^1, A_o^2, E_o^1, A_{6n}^1, A_{6n}^2, C_{6n}^1, C_{6n}^2 ,

and D(I) represents the non-homogeneous constants in the simultaneous boundary equations.

Each row of the array given by (II-5) represents a boundary equation. Since each boundary equation must be satisfied at each collocation point except at the corner (i.e. $\theta = 30^\circ$), there will be

$$4L - 1 = N$$

equations containing N unknown coefficients RR(J).

For L=7 these coefficients are

$$
\begin{aligned}
RR(1) &= A_0^1 \\
RR(2) &= A_0^2 \\
RR(3) &= E_0^1 \\[6pt]
RR(4) &= A_6^1 \\
RR(5) &= A_{12}^1 \\
&\vdots \\
RR(9) &= A_{36}^1 \\[6pt]
RR(10) &= A_6^2 \\
RR(11) &= A_{12}^2 \\
&\vdots \\
RR(15) &= A_{36}^2 \\[6pt]
RR(16) &= C_6^1 \\
RR(17) &= C_{12}^1 \\
&\vdots \\
RR(21) &= C_{36}^1 \\[6pt]
RR(22) &= C_6^2 \\
RR(23) &= C_{12}^2 \\
&\vdots \\
RR(27) &= C_{36}^2
\end{aligned}
$$

The first three constants A_o^1, A_o^2, E_o^1, are the same for any number of collocation points, while the remainder are divided into four consecutive sets of order L-1 (in this case sets of six constants).

The coefficients φ, are given by A(I,J) and form an N x N matrix. This portion of the programme commences after ISN (statement) 15 and ends at ISN 40.

The matrix A(I,J) is then inverted (ISN 41) and once the constants D(I) have been given (ISN-45, 46, 47, 48), the unknown constants RR(I) may be calculated from

RR(I) = A^{-1}(I,J) x D(J)

(e) NORMAL DISPLACEMENT AND SECTIONAL RESULTANTS

u_n - UN(I,J)

$F(\sigma)_{rr}$ - FRR(I,J)

$F(\sigma)_{\theta\theta}$ - FØØ(I,J)

$M(\sigma)_{r\theta}$ - BMRØ(I,J)

$M(\sigma)_{\theta r}$ - BMØR(I,J)

where I represents radial lines defined by θ = constant,

J represents arguments λr

and the constants

D - DD
ω - W
λ - BB

2. REFINEMENTS FOR RETENTION OF ACCURACY AND OVERMASTERY OF COMPUTER LIMITATIONS

Double precision techniques were used throughout the numerical calculations. Limitations on the amount of machine memory storage available were overcome by computing and storing KELVIN functions of order kn only, where n = o, 1..., (L-1) and k represents the rotational periodicity of the shell.

N.A.S.A. tables by LOWELL in 1959 gave zero order KELVIN functions to 12-14 figure accuracy for arguments containing only two decimal places. In order to insure the accuracy of the zero order KELVIN functions employed in the programme, it was essential to use only those arguments which were tabulated by LOWELL. Consequently once λ was computed, radii r were calculated from the arguments λr - ARG (I).

The radii r - R(I), which described the collocation points, were then used to determine corresponding angles θ - ZZ(I) such that in this case

$$r\cos\theta = 25.0 \quad \cos \pi/6$$

Unique constants a-AA(I) were used for each KELVIN function calculated by the "Backward Recurrence Technique" in order to prevent both computer underflow (numbers smaller than 10^{-38}) and overflow (numbers greater than 10^{+38}).

A constant CT = $1. \times 10^{-20}$ was introduced in the calculation of the coefficients φ, to prevent computer overflow. It was not removed until the calculation of the sectional resultants was completed.

The rows and columns of the matrix A(I,J) were multiplied by constants CI(I) and CØ(J) respectively, in order to reduce the elements to comparable orders of magnitude with a maximum range of approximately 10^{+4}. This step was essential to produce accuracy in the inversion calculation which employs the "GAUSS Pivotal

Technique". These constants were removed after the inversion was completed.

The accuracy of the matrix inversion was checked by multiplying the matrix by its inverse

i.e. $A \times A^{-1} = I$

where I is the unit diagonal matrix having off-diagonal elements of zero magnitude. A "perfect" inversion using double precision techniques produces off-diagonal elements whose magnitudes are of the order 10^{-16}.

3. CHANGES IN PROGRAMME FOR DIFFERENT SPHERICAL SHELLS OVER POLYGONAL BASE.

The shell parameters given in section (1-a) must be changed for each particular shallow shell.

In addition, the following changes may be necessary with respect to:

(a) PERIODICITY

- (i) New KELVIN functions must be calculated.
- (ii) The constant CK must be changed.
- (iii) The constant FK must be changed.

(b) BOUNDARY CONDITIONS

- (i) The coefficients A(I,J) must be changed and rearranged.
- (ii) The constants D(J) must be changed and rearranged.

Discussion of Results

1. CONSISTENCY

The theoretical results given for the spherical shell enclosing an hexagonal base were obtained by employing boundary conditions (II-1) to (II-4). Often the boundary conditions (II-1) and (II-2) were replaced by the special boundary conditions (II-1*) and (II-2*) respectively as noted on the graphs.

It can be seen from FIGURES 8 to 41 that the number and location of the boundary collocation points had a relatively minor effect on the theoretical results with the exception of some irregularities close to the shell's boundary especially along the radial line, $\theta=30^\circ$, to the corner point of the shell. Reasonable agreement between the experimental and theoretical results was obtained when boundary conditions (II-1*, II-2*, II-3, II-4) were employed. The greatest number of discrepancies occurred near the shell's boundary, particularly on the radial line $\theta=30^\circ$, some evidently brought about by the stress concentration due to discontinuity in the boundary members. Better agreement could sometimes be obtained by using slightly different boundary conditions, more in concert with the shell's structure. However, the majority of discrepancies appeared to be the result of the physical shortcomings of the experimental shell.

Elimination of the horizontal normal boundary constraining force by using boundary condition (II-1) instead of (II-1*) caused increases in the normal displacement and the radial and circumferential stress couples, decreases in the radial stress resultant, especially on the radial lines $\theta = 0^\circ$ and $\theta = 10^\circ$, and some changes in the circumferential stress resultant at the boundary only.

Confining the boundary to be fully constrained against rotation by imposing the boundary condition (II-2) instead of (II-2*) caused some reduction in the normal displacement as well as some changes in the radial and circumferential stress resultants and stress couples in the vicinity of the boundary as was to be expected.

2. ACCURACY OF THE THEORETICAL SOLUTION

Logically the accuracy of the theoretical solution by the collocation method should increase with increasing numbers of boundary collocation points. In order to verify this reasoning, normal displacements were calculated at the shell's boundary for solutions using three and seven collocation points both of which satisfied the boundary equations (II-1*), (II-2*), (II-3) and (II-4) (see FIGURES 42 and 43).

Since all the computations were done to 17 figure accuracy, boundary condition (II-3),(i.e. $u_n = 0$),would be "perfectly" satisfied when the magnitude of the normal displacement was approximately of the order 10^{-17} inches for the entire boundary of the shell.

FIGURES 42 and 43 reveal that an increase in the number of boundary collocation points produces a better average satisfaction of the boundary condition (II-3). The maximum deviation of the normal displacement at the boundary from the theoretical boundary condition for three collocation points was about -5×10^{-4} inches, while for seven collocation points it was about 2×10^{-4} inches. However, the scales of these graphs do not permit to show that the minimum deviation of the normal displacement at the boundary from the theoretical boundary condition for three collocation points was of the order of 10^{-16} inches while for seven collocation points it was of the order 10^{-6} inches. This indicates that an increase in the number of collocation points gives better satisfaction of the prescribed edge conditions over the complete shell boundary as long as the resulting increase in numerical computations does not reduce the number of significant figures in the computer calculations below a "safe" level. For seven collocation points, there appears to be only six figure accuracy in the calculations, which would certainly constitute a minimum requirement. The accuracy of the theoretical solution for this shell would probably not be increased by using more than seven collocation points when double precision (17 figure) accuracy is used for all computations. It is possible, however, that in this case the accuracy might even decrease.

VECTOR DIAGRAM of SHELL ELEMENT SHOWING SECTIONAL RESULTANTS

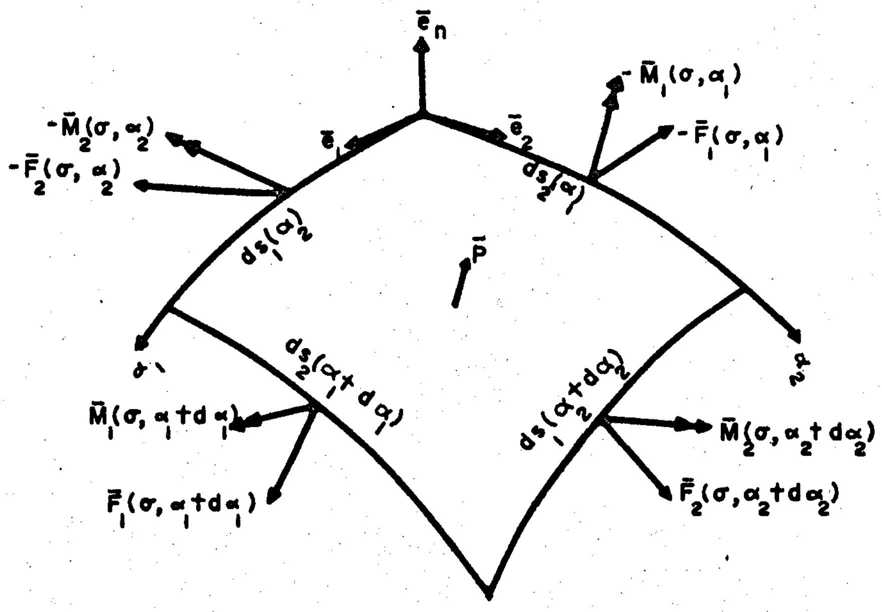

$$\bar{F}_1(\sigma) = F_{11}(\sigma)\bar{e}_1 + F_{12}(\sigma)\bar{e}_2 + F_{1n}(\sigma)\bar{e}_n$$
$$\bar{F}_2(\sigma) = F_{21}(\sigma)\bar{e}_1 + F_{22}(\sigma)\bar{e}_2 + F_{2n}(\sigma)\bar{e}_n$$
$$\bar{M}_1(\sigma) = M_{11}(\sigma)\bar{e}_1 + M_{12}(\sigma)\bar{e}_2$$
$$\bar{M}_2(\sigma) = M_{21}(\sigma)\bar{e}_1 + M_{22}(\sigma)\bar{e}_2$$
$$\bar{p} = p_1\bar{e}_1 + p_2\bar{e}_2 + p_n\bar{e}_n$$

FIGURE 1

EXPERIMENTAL SHELL ON
EDGE ROLLERS

FIGURE 2

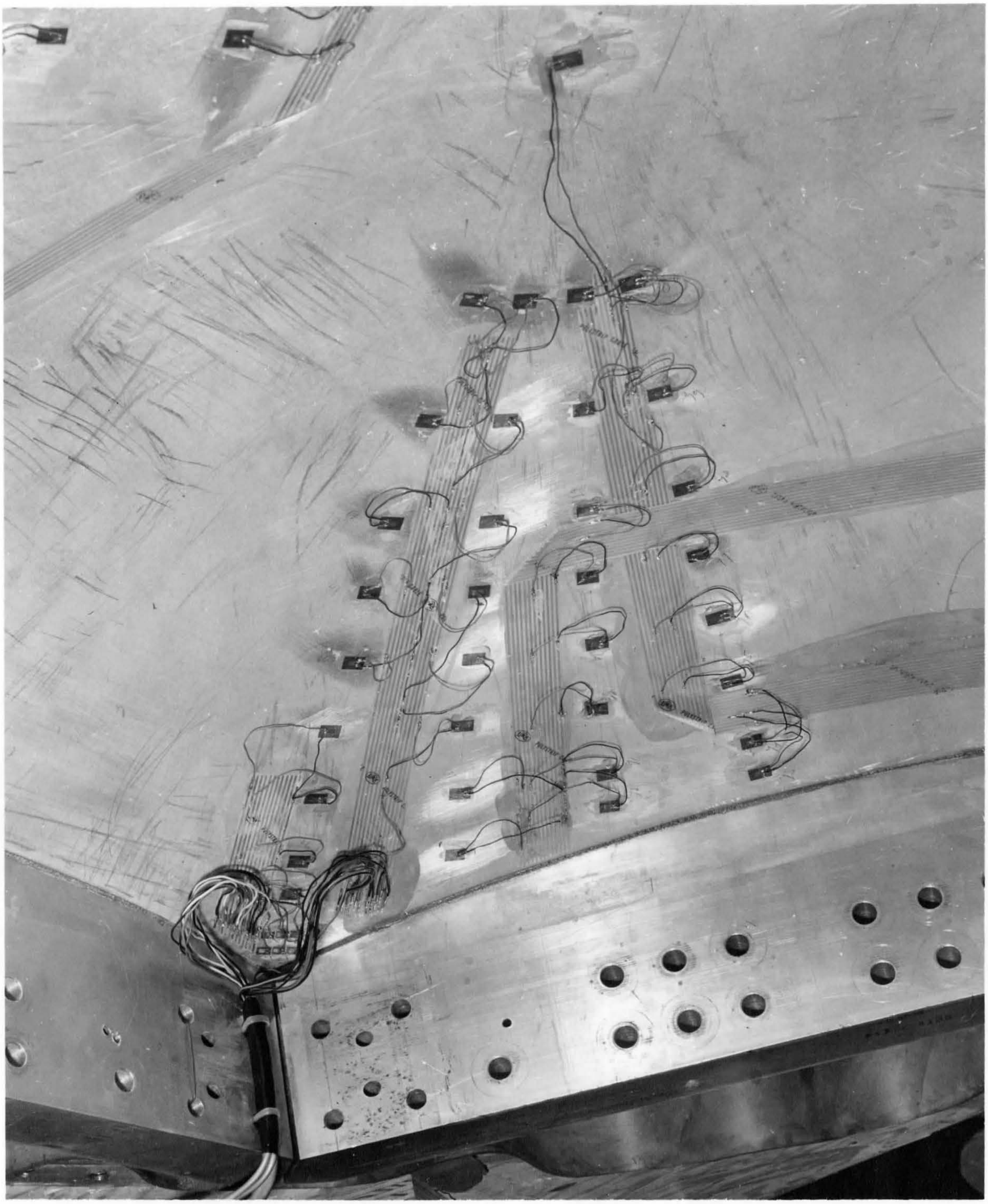

DETAIL OF SLIT CORNER SHOWING CIRCUMFERENTIAL STRAIN GAUGES

FIGURE 3

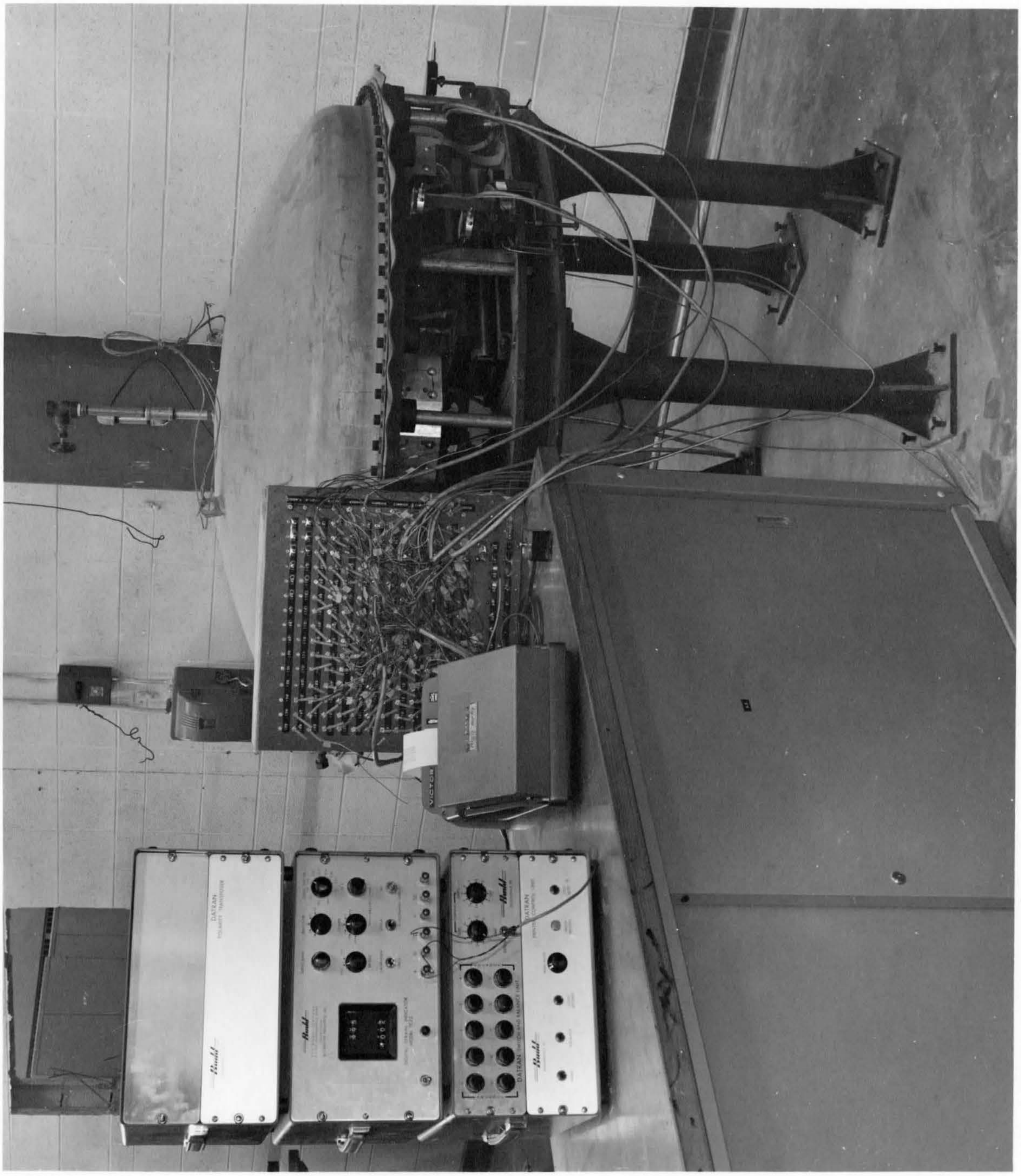

SHELL ASSEMBLY WITH DIGITAL STRAIN INDICATOR, PRINT-OUT RECORDER AND SWITCHING UNIT

FIGURE 4

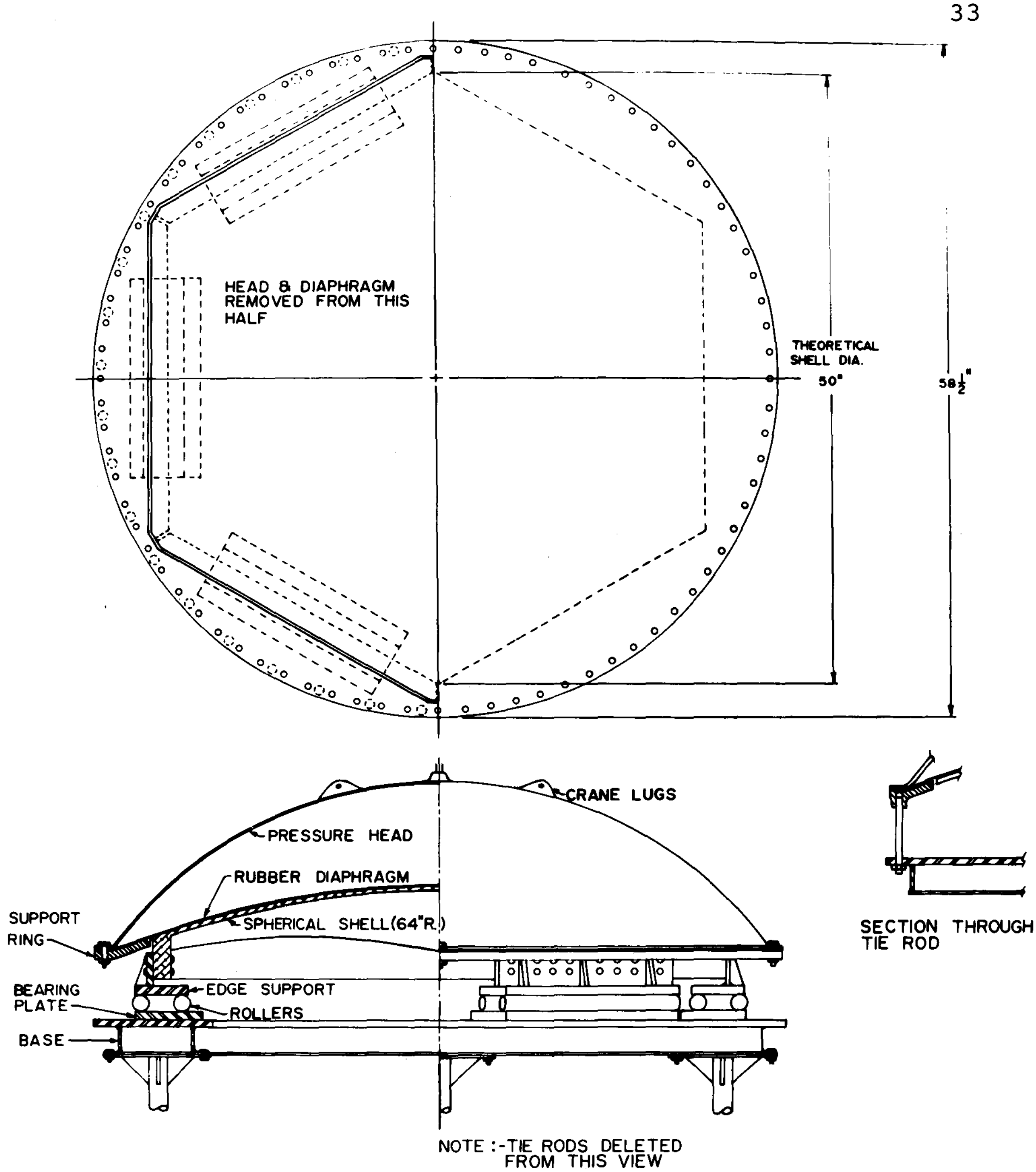

SHELL TEST ASSEMBLY

FIGURE 5

PLAN VIEW of SHELL on HEXAGONAL BASE SHOWING LOCATION of RADIAL LINES for which SECTIONAL RESULTANTS are CALCULATED

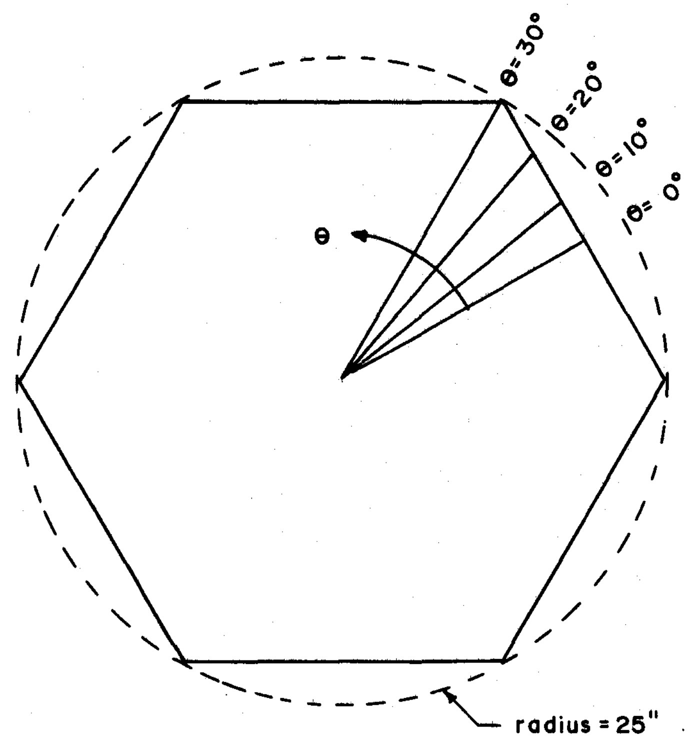

FIGURE 6

LOCATION of BOUNDARY COLLOCATION POINTS for SHELL on HEXAGONAL BASE

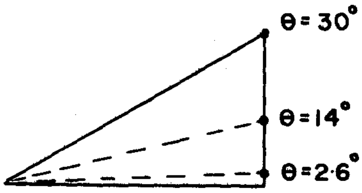

3 COLLOCATION POINTS

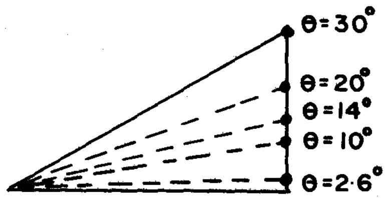

5 COLLOCATION POINTS

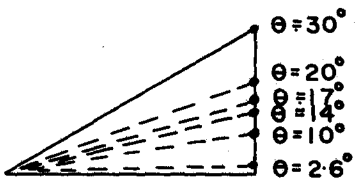

6 COLLOCATION POINTS

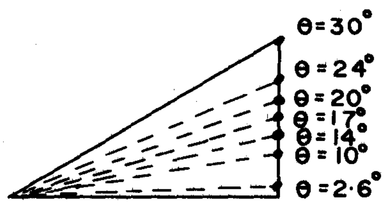

7 COLLOCATION POINTS

FIGURE 7

PLOT SHOWING THEORETICAL "U_n"
for SHELL on HEXAGONAL BASE

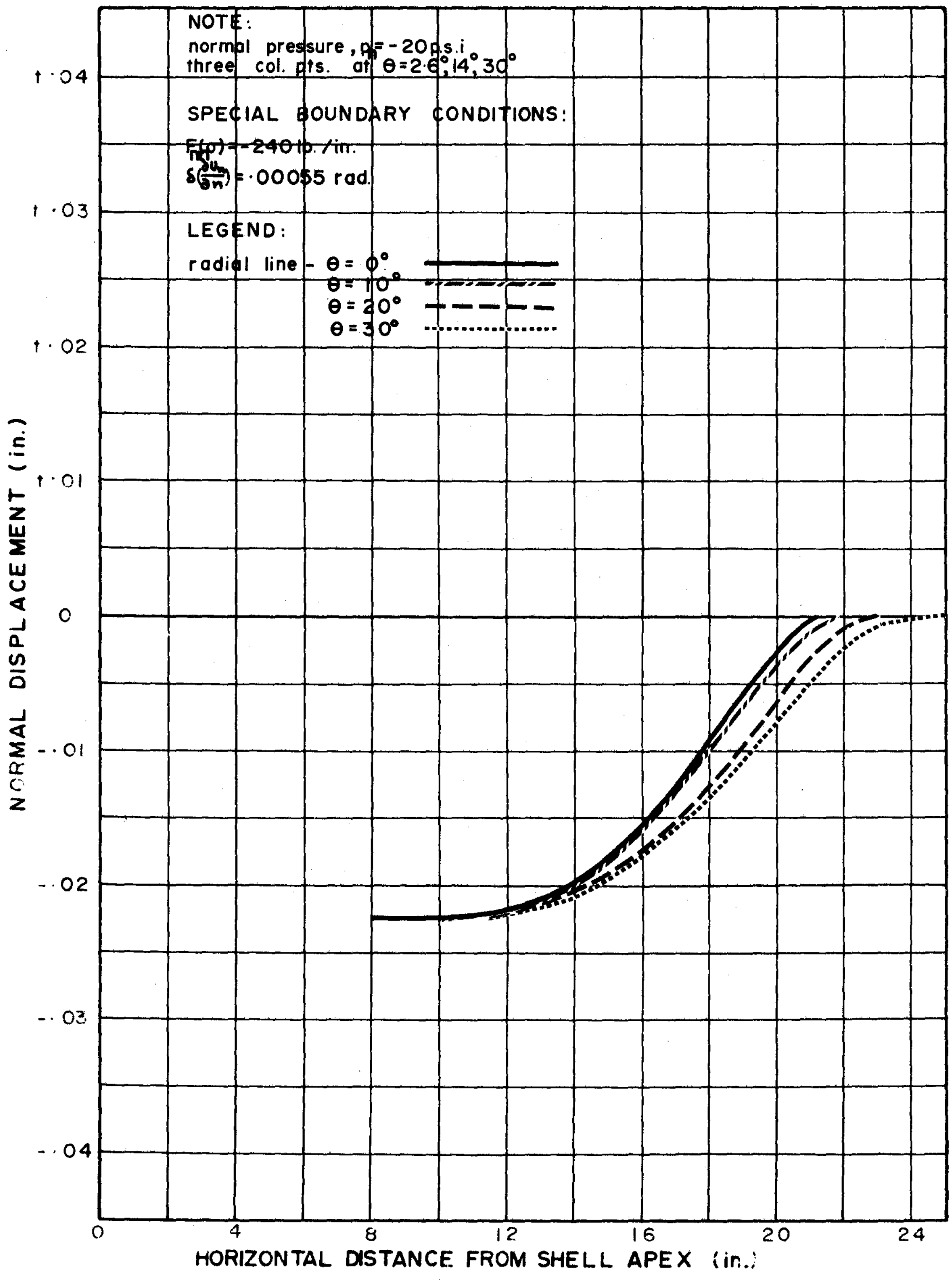

FIGURE 8

PLOT SHOWING THEORETICAL "U_n"
for SHELL on HEXAGONAL BASE

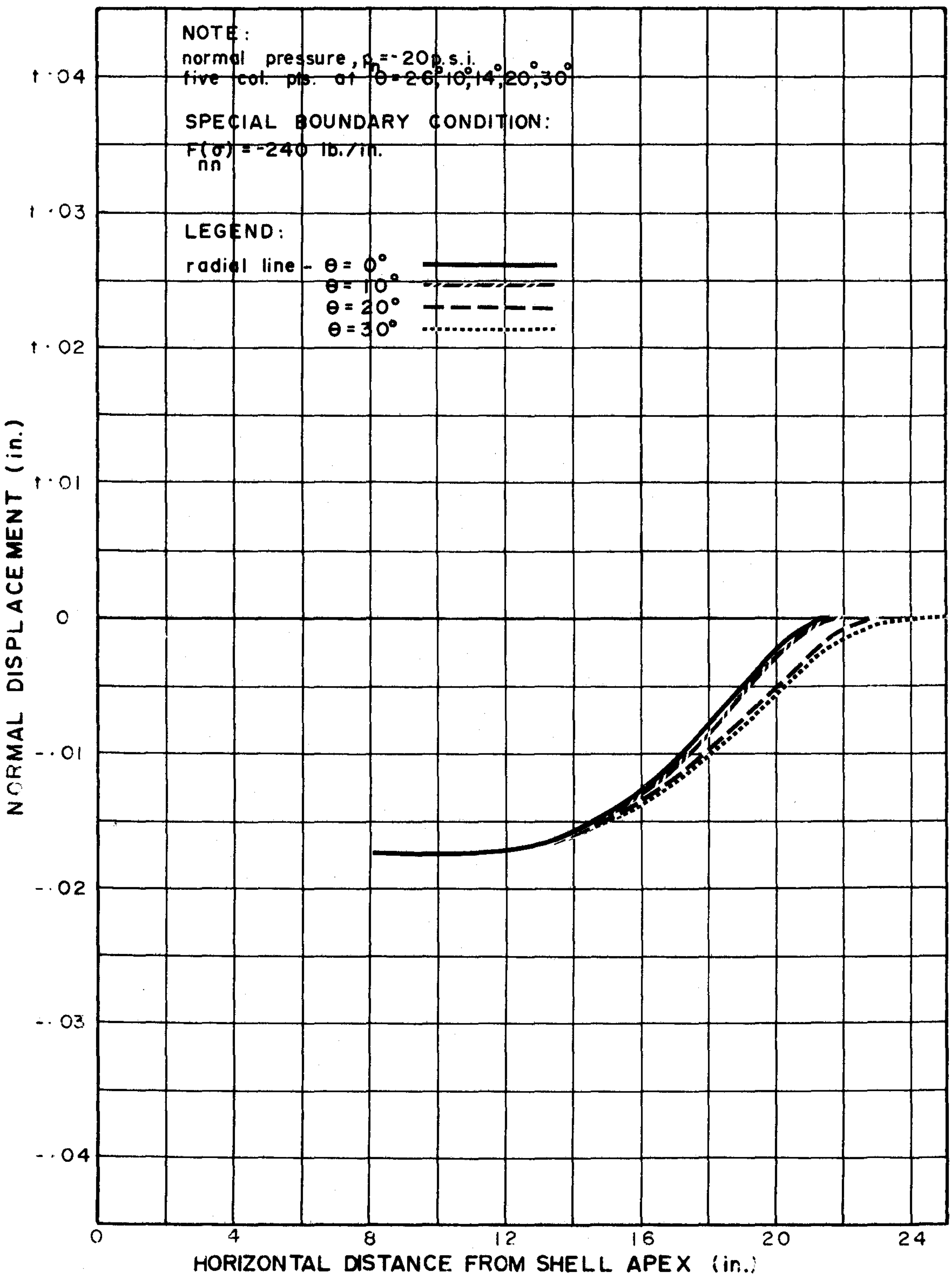

FIGURE 9

PLOT SHOWING THEORETICAL "U_n" for SHELL on HEXAGONAL BASE

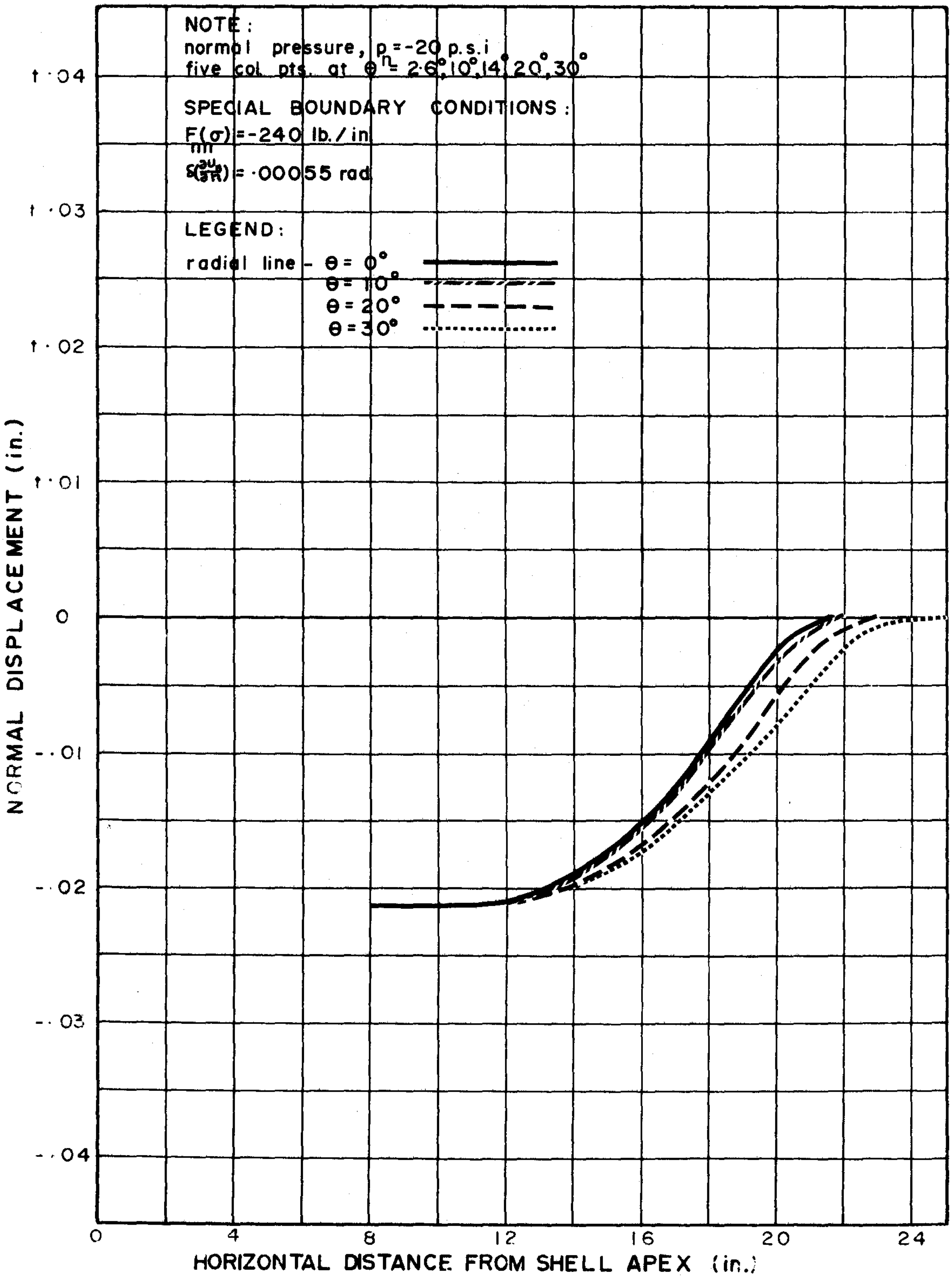

FIGURE 10

PLOT SHOWING THEORETICAL "U_n"
for SHELL on HEXAGONAL BASE

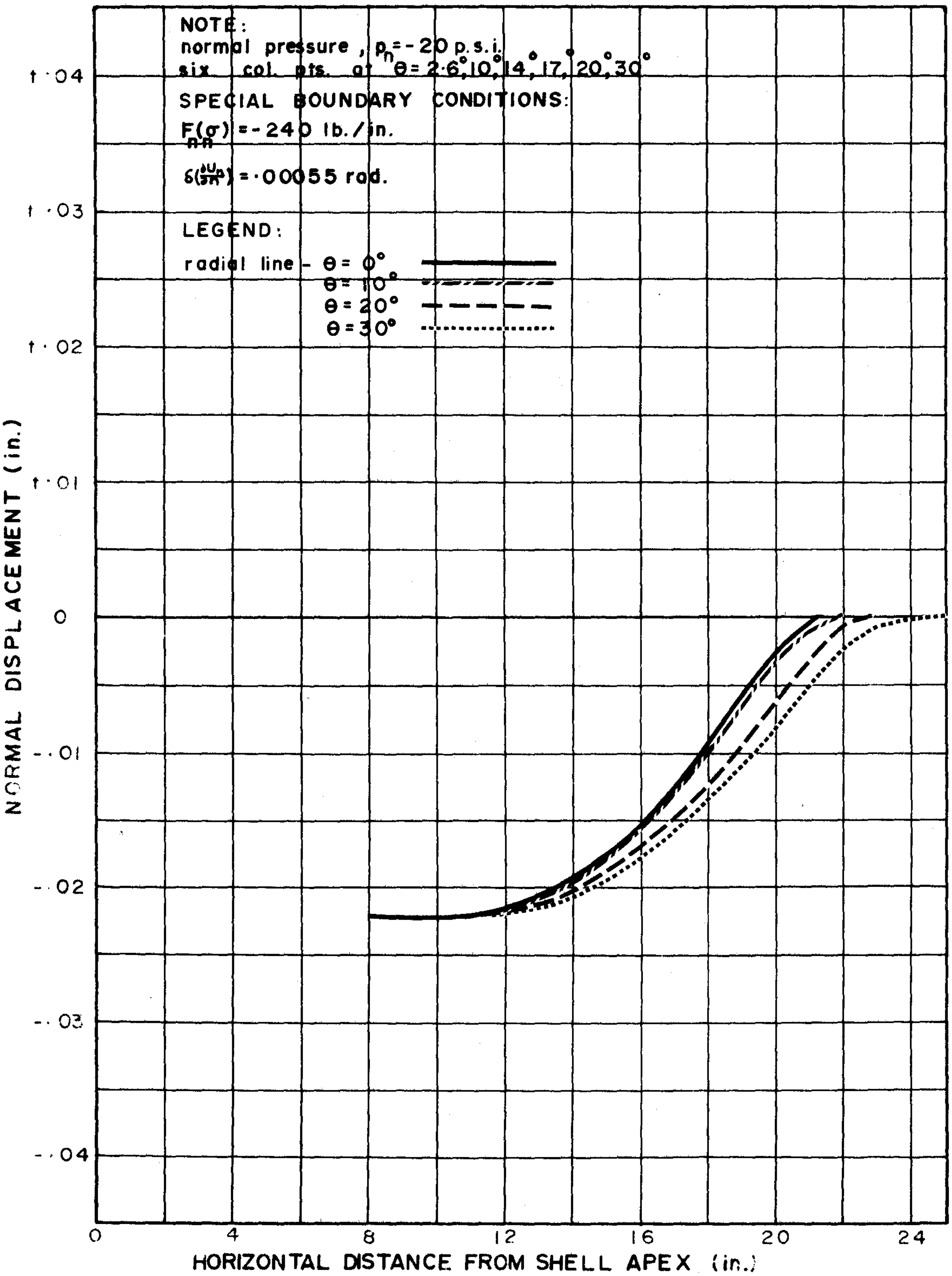

FIGURE 11

PLOT SHOWING THEORETICAL "U_n"
for SHELL on HEXAGONAL BASE

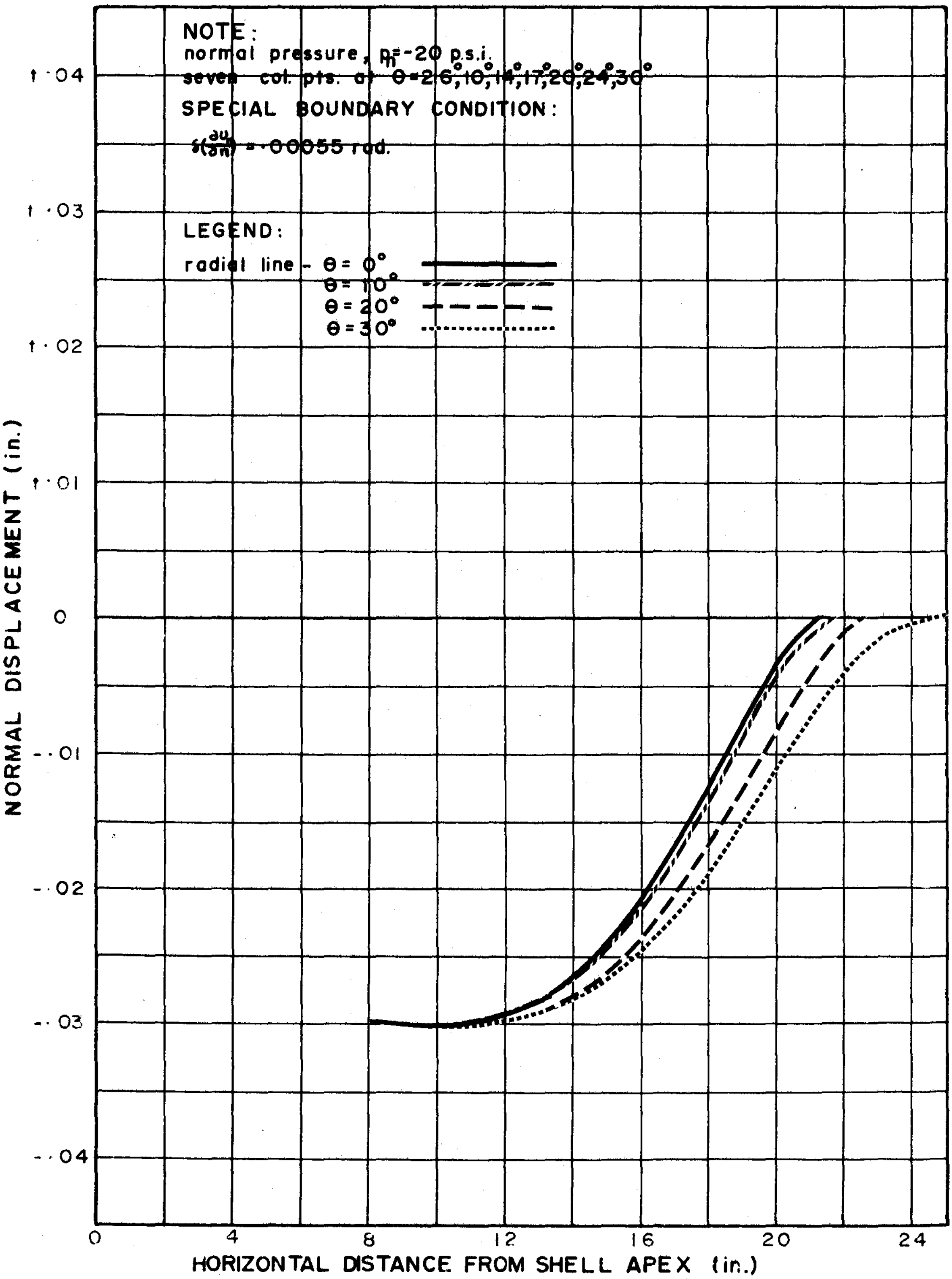

FIGURE 12

PLOT SHOWING THEORETICAL "U_n"
for SHELL on HEXAGONAL BASE

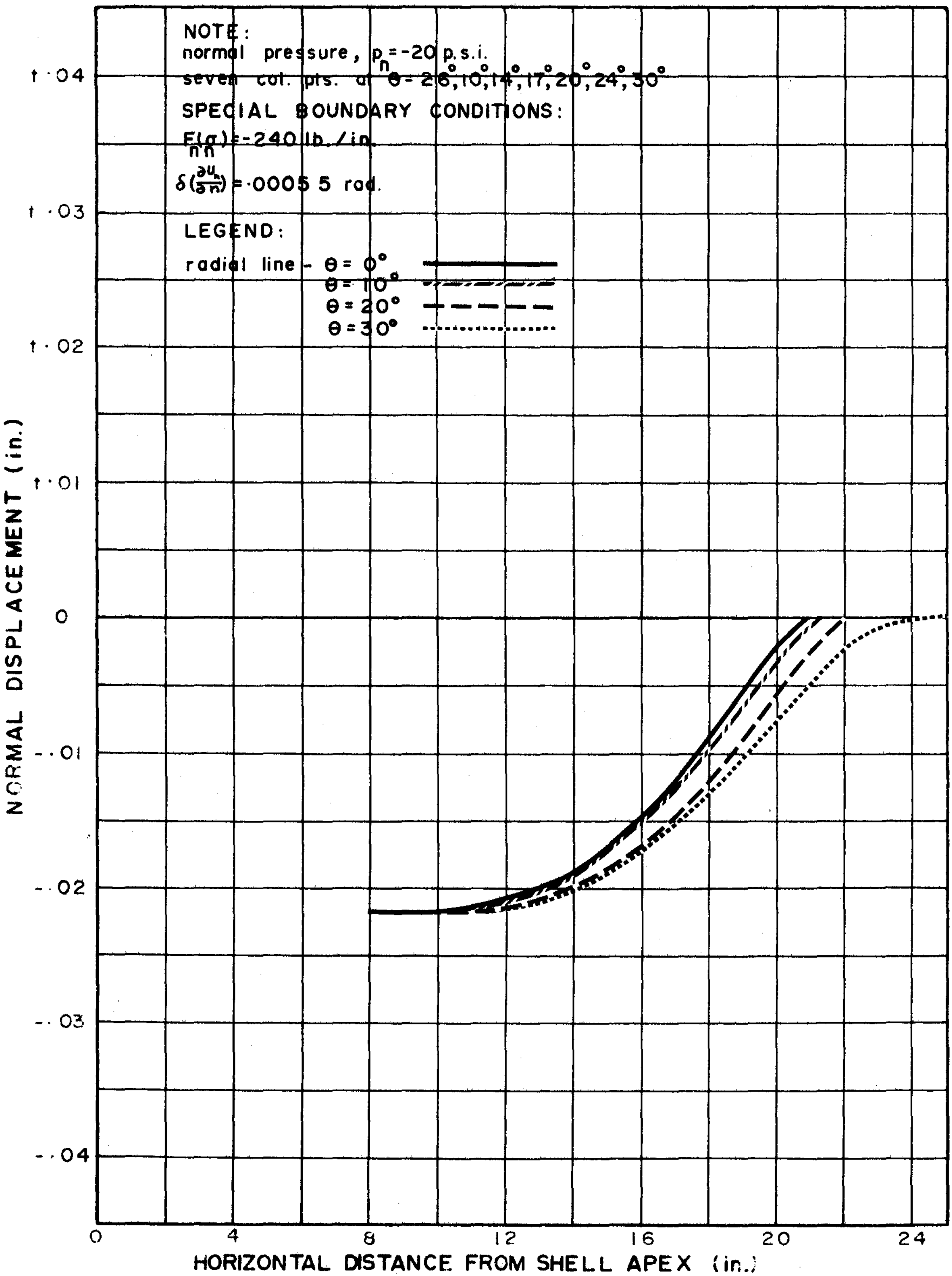

FIGURE 13

PLOT SHOWING EXPERIMENTAL "$F_{rr}(\sigma)$"
for SHELL on HEXAGONAL BASE

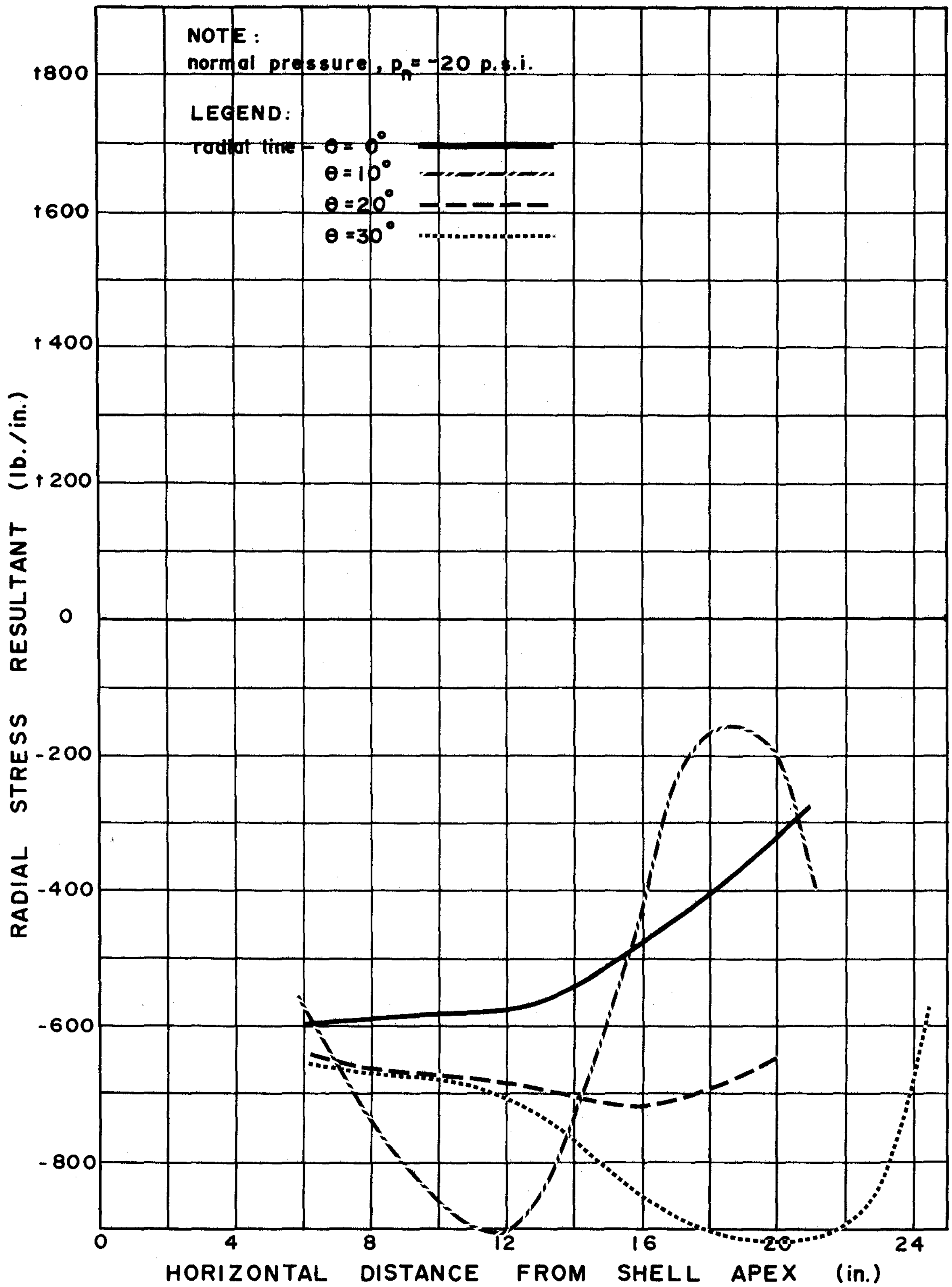

FIGURE 14

PLOT SHOWING THEORETICAL "$F_{rr}(\sigma)$"
for SHELL on HEXAGONAL BASE

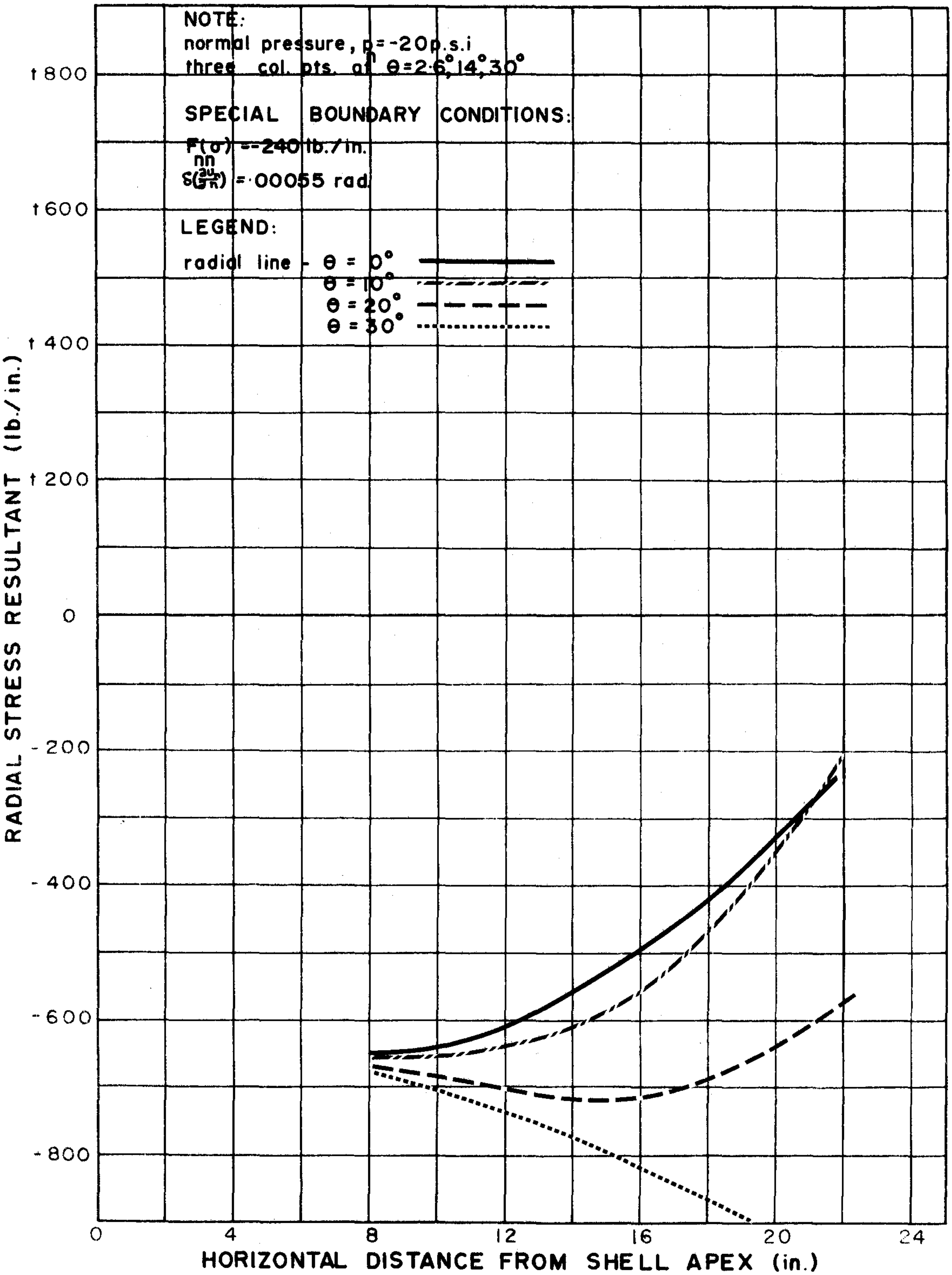

FIGURE 15

PLOT SHOWING THEORETICAL "$F_{rr}(\sigma)$"
for SHELL on HEXAGONAL BASE

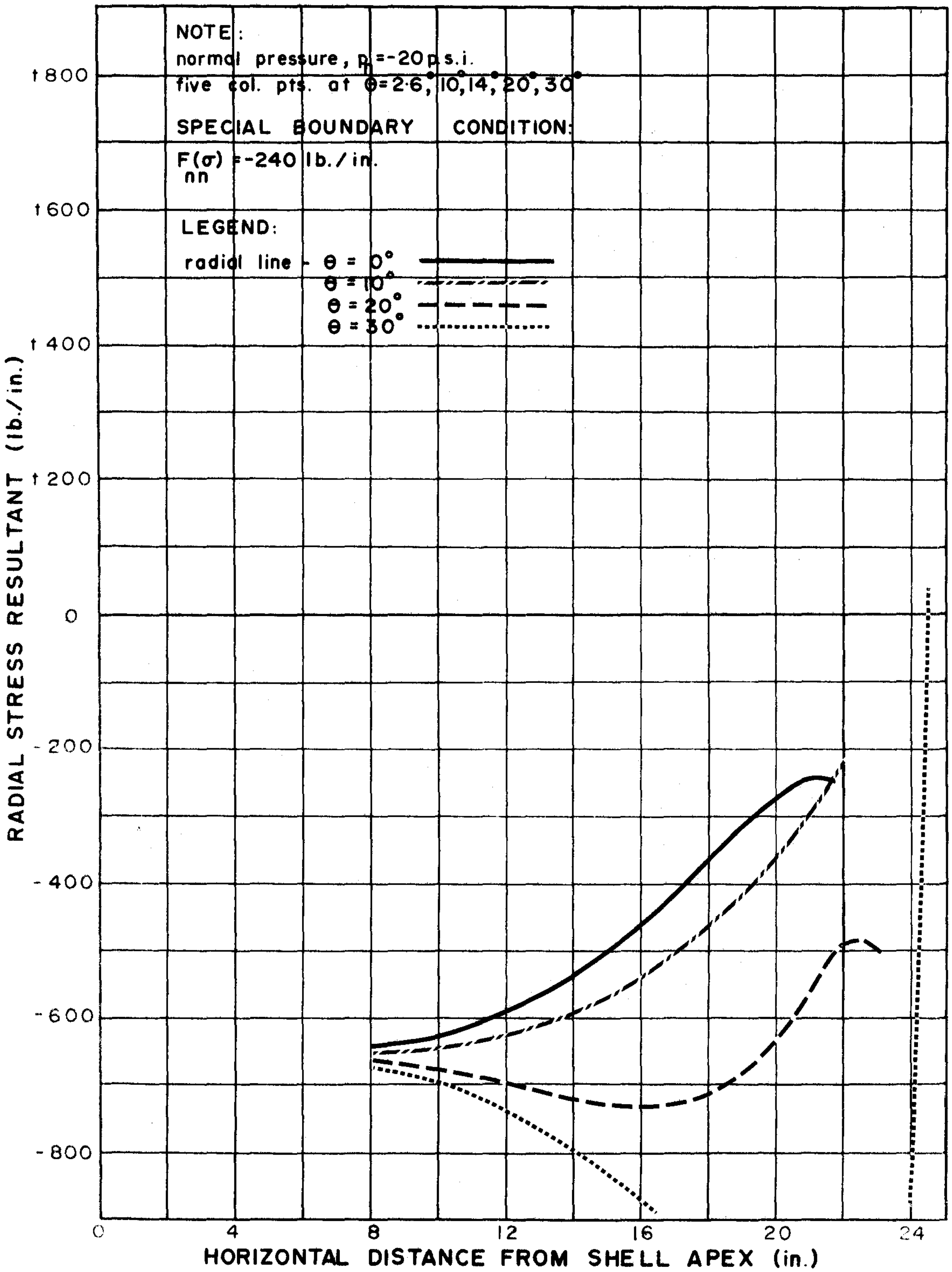

FIGURE 16

PLOT SHOWING THEORETICAL "$F_{rr}(\sigma)$"
for SHELL on HEXAGONAL BASE

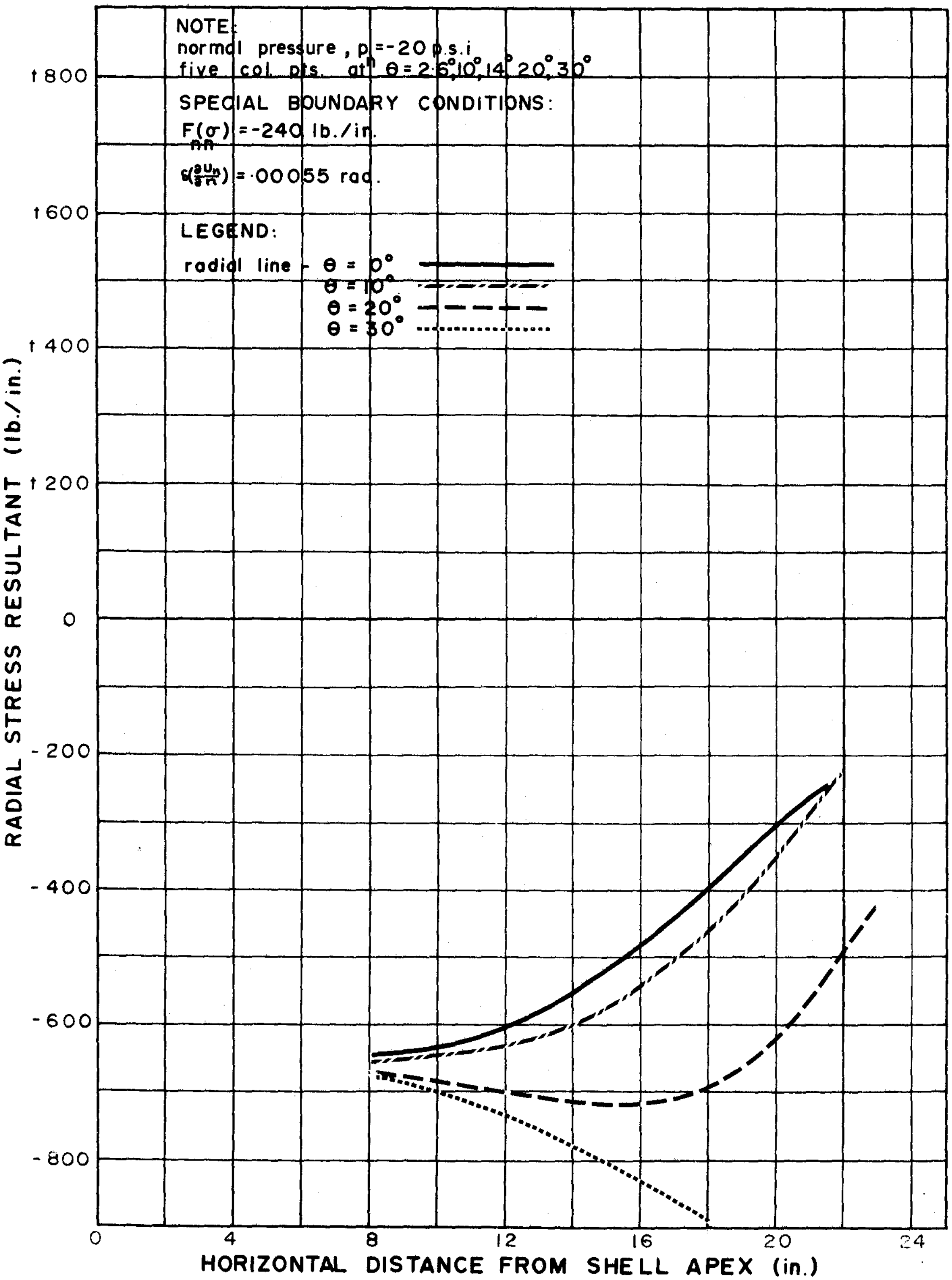

FIGURE 17

PLOT SHOWING THEORETICAL "$F_{rr}(\sigma)$"
for SHELL on HEXAGONAL BASE

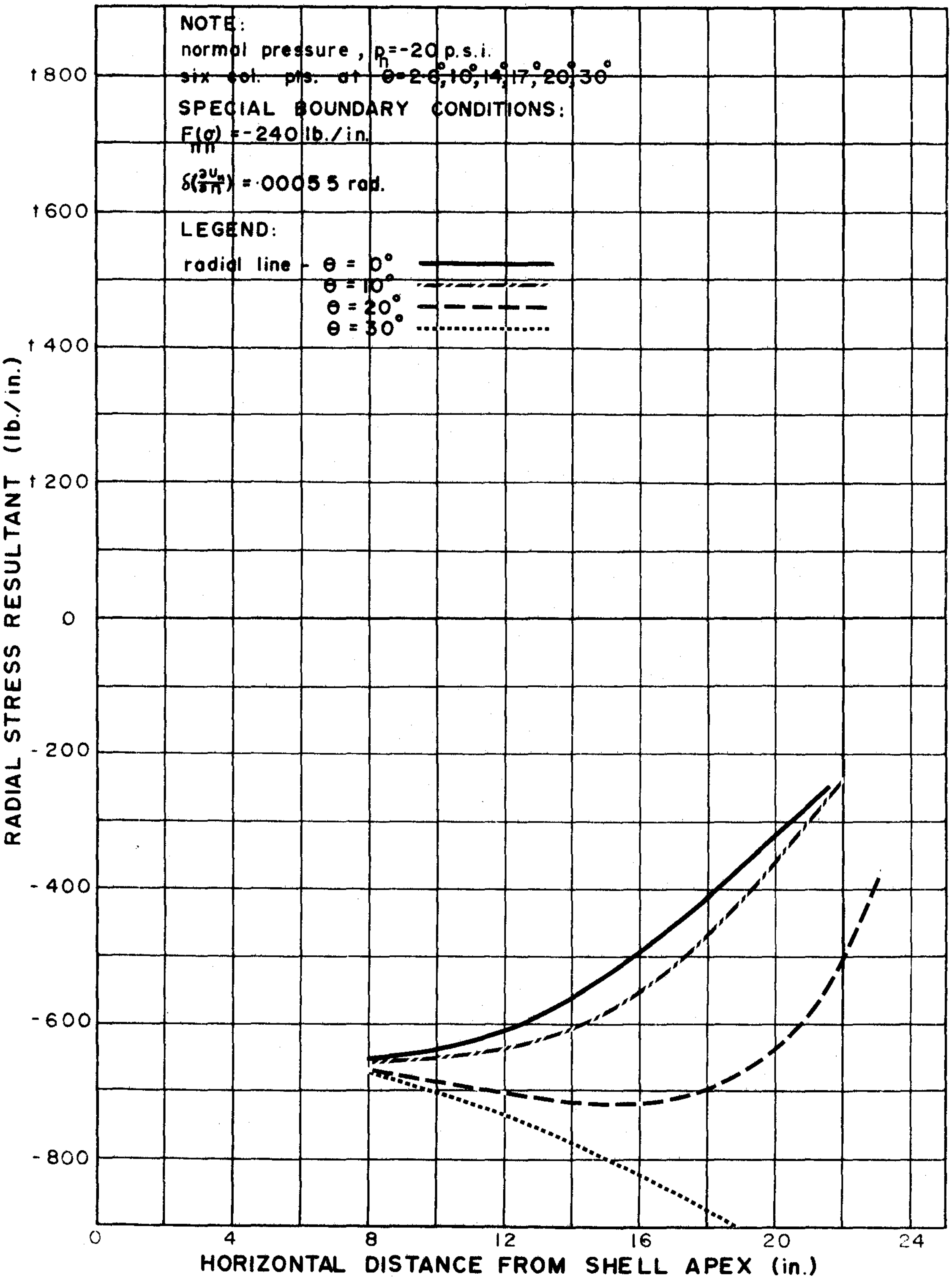

FIGURE 18

PLOT SHOWING THEORETICAL "$F_{rr}(\sigma)$"
for SHELL on HEXAGONAL BASE

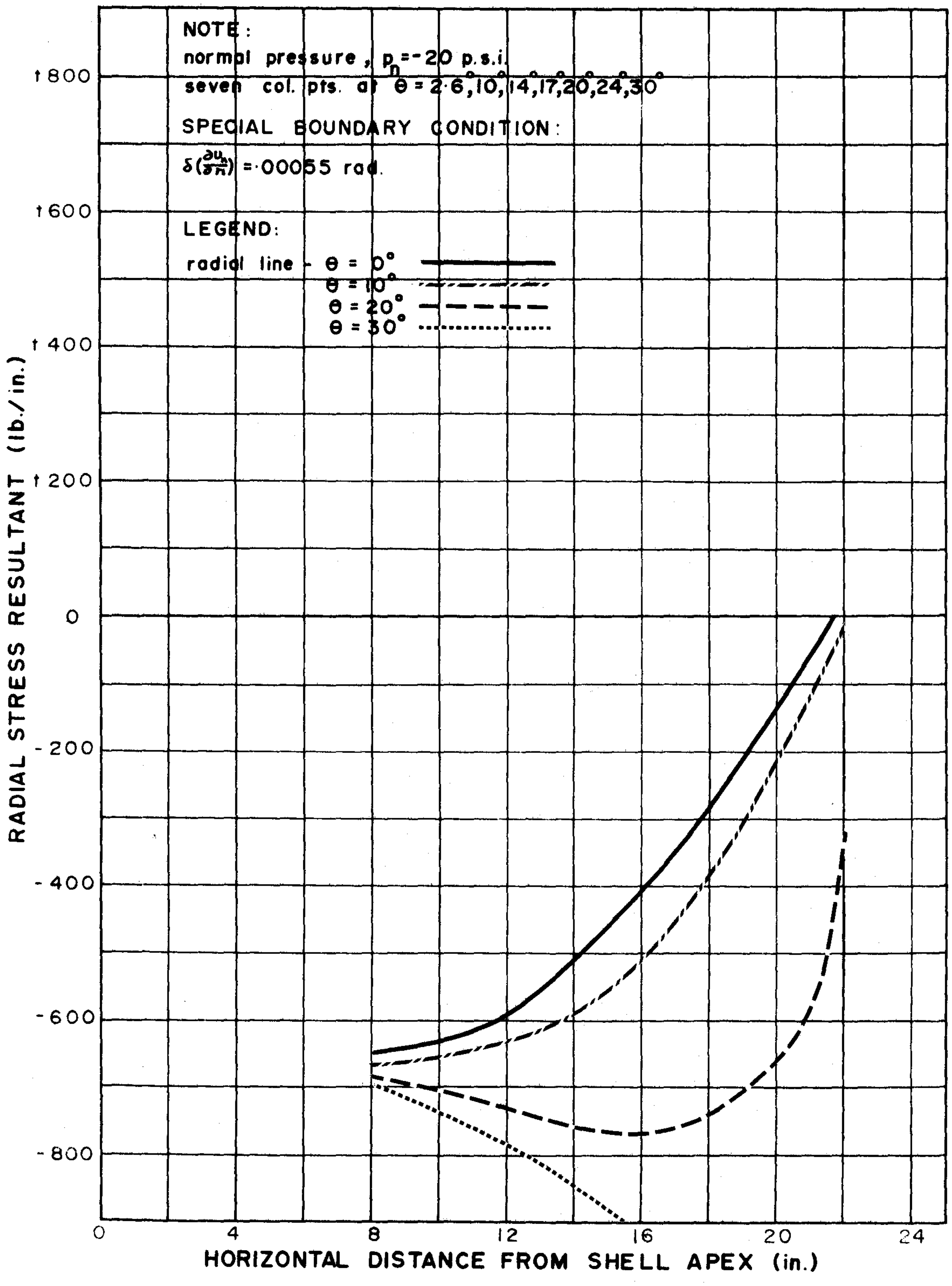

FIGURE 19

PLOT SHOWING THEORETICAL "$F_{rr}(\sigma)$"
for SHELL on HEXAGONAL BASE

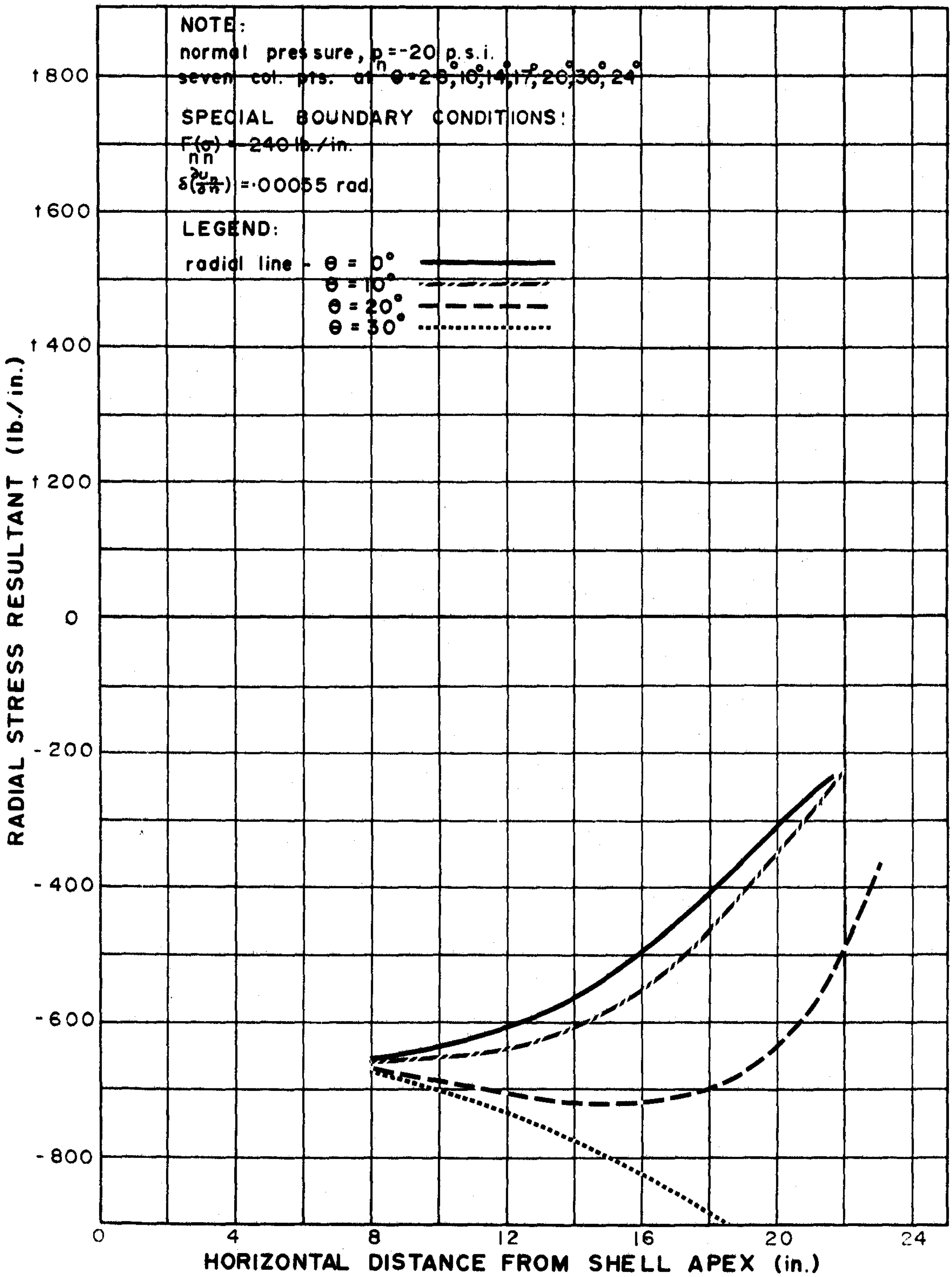

FIGURE 20

PLOT SHOWING EXPERIMENTAL "$F_{\theta\theta}(\sigma)$"
for SHELL on HEXAGONAL BASE

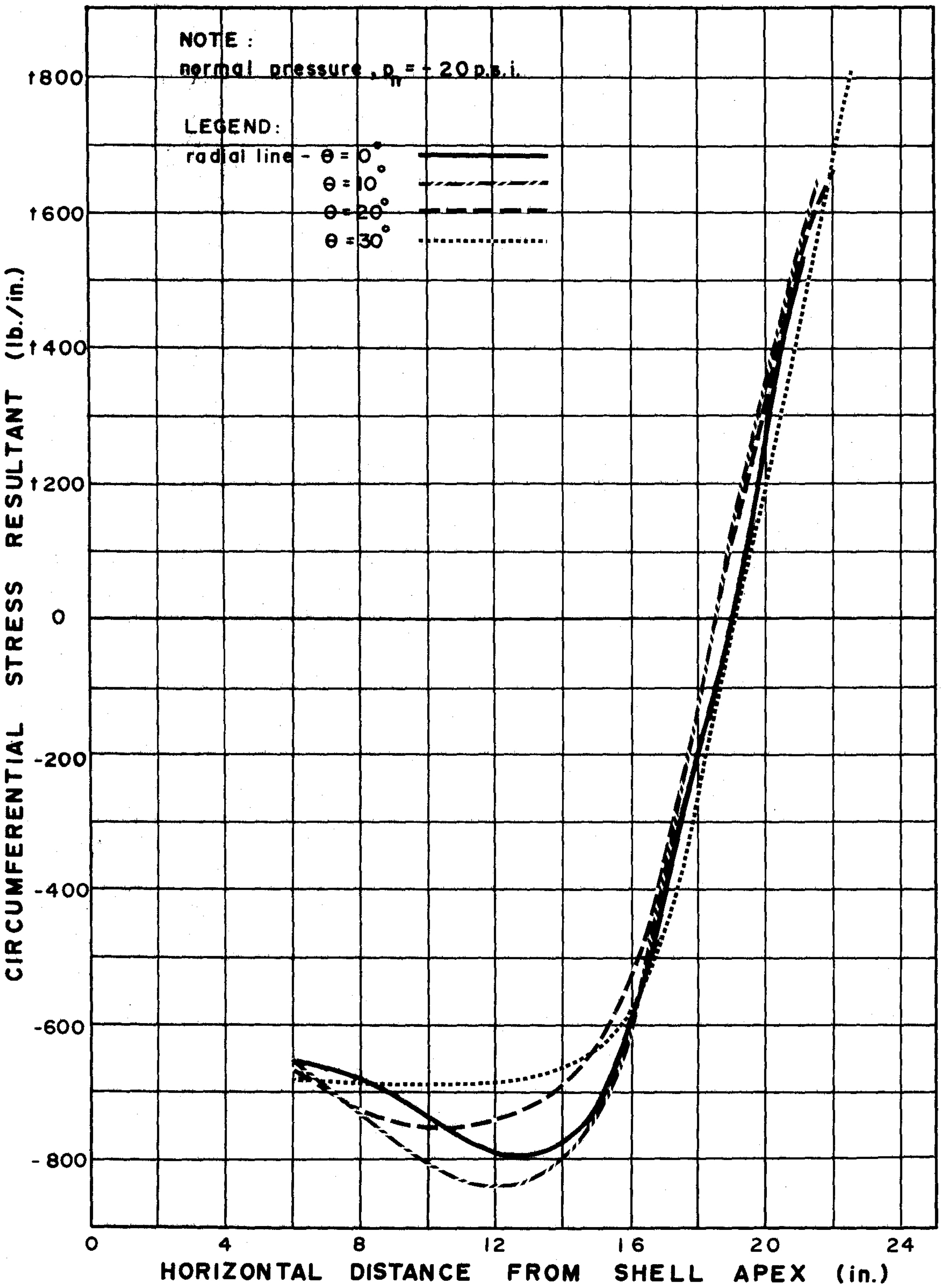

FIGURE 21

PLOT SHOWING THEORETICAL "$F_{\theta\theta}(\sigma)$"
for SHELL on HEXAGONAL BASE

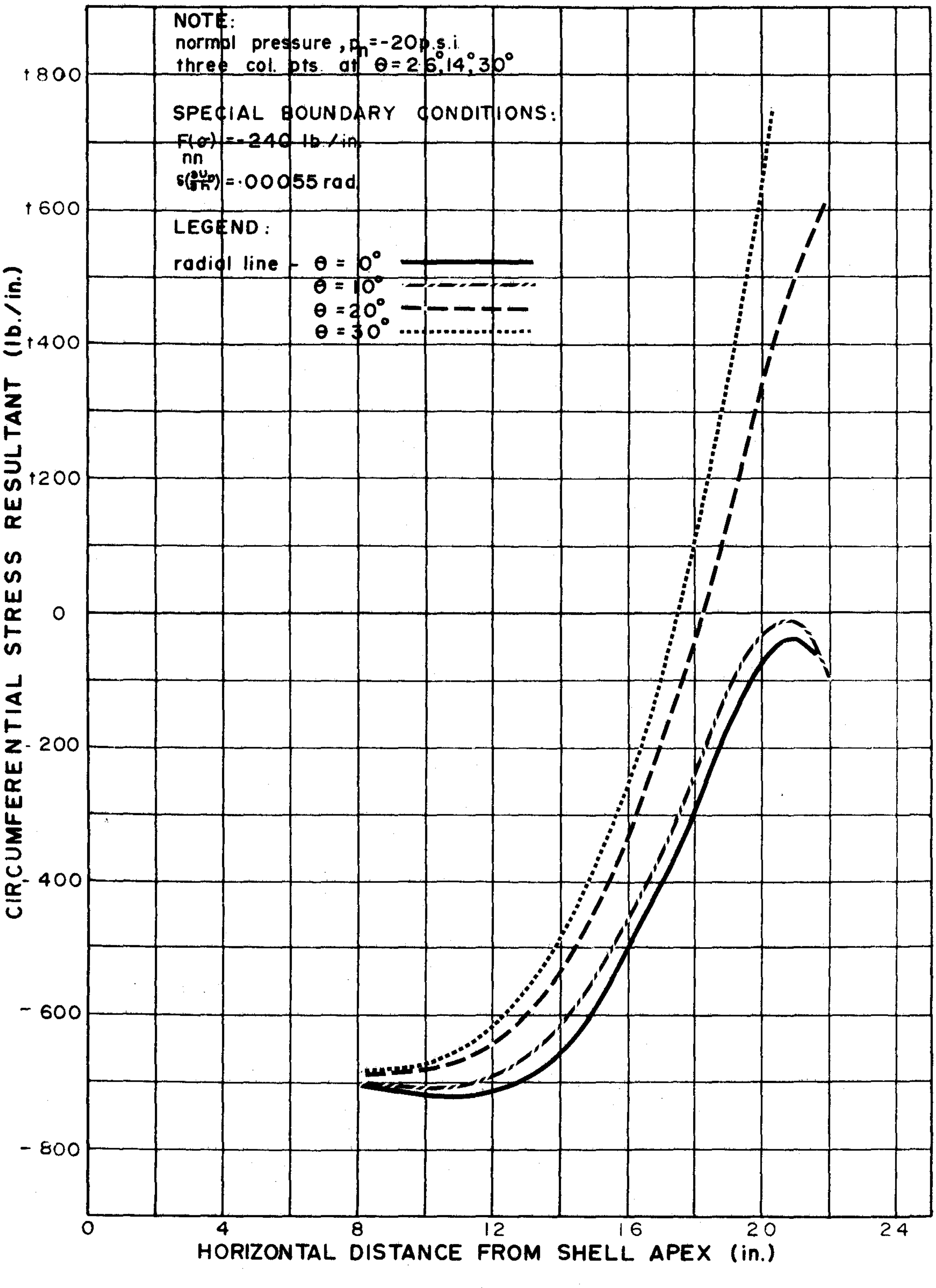

FIGURE 22

PLOT SHOWING THEORETICAL "$F(\sigma)_{\theta\theta}$"
for SHELL on HEXAGONAL BASE

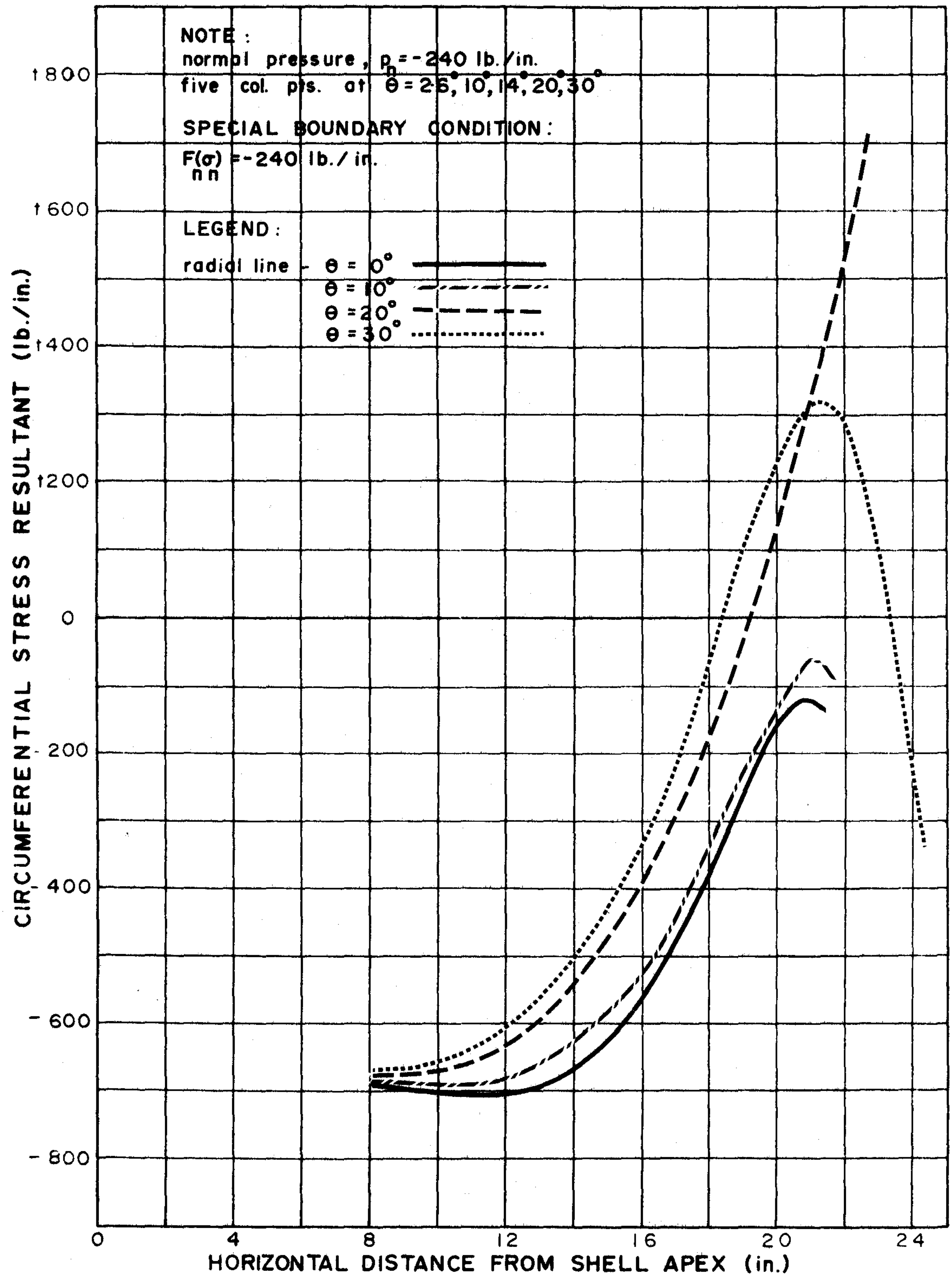

FIGURE 23

PLOT SHOWING THEORETICAL "$F_{\theta\theta}(\sigma)$"
for SHELL on HEXAGONAL BASE

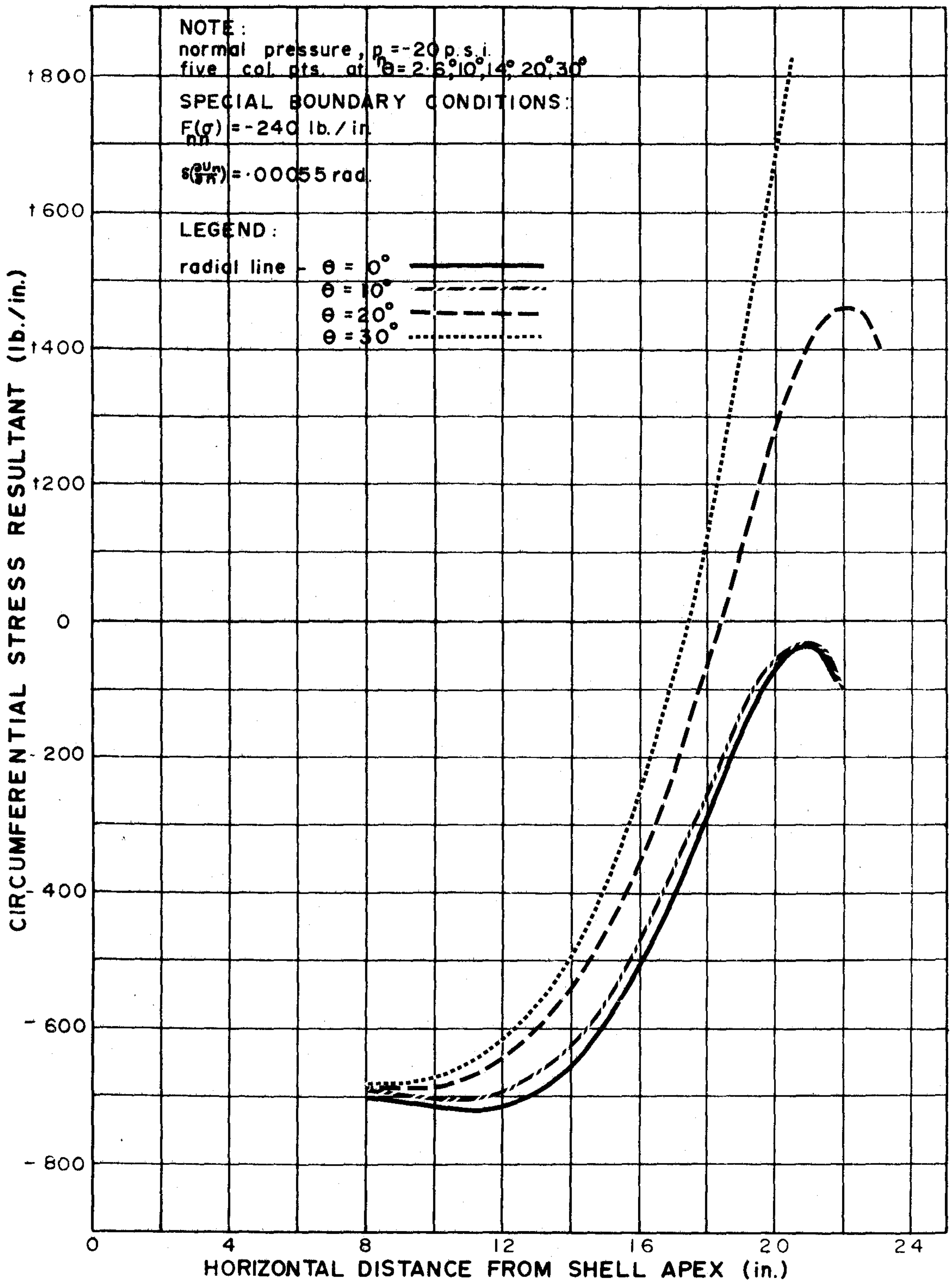

FIGURE 24

PLOT SHOWING THEORETICAL "$F_{\theta\theta}(\sigma)$"
for SHELL on HEXAGONAL BASE

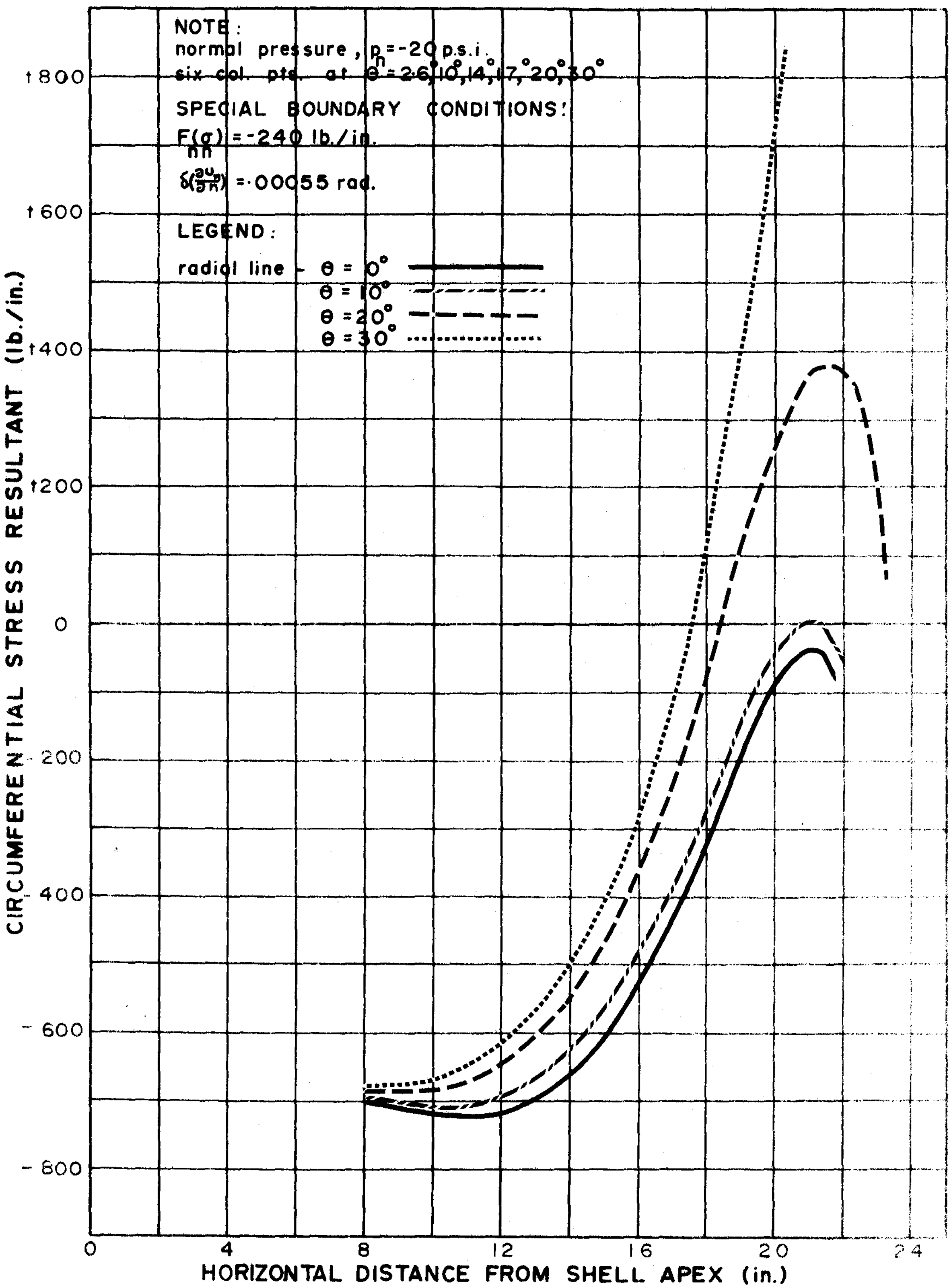

FIGURE 25

PLOT SHOWING THEORETICAL "$F_{\theta\theta}(\sigma)$" for SHELL on HEXAGONAL BASE

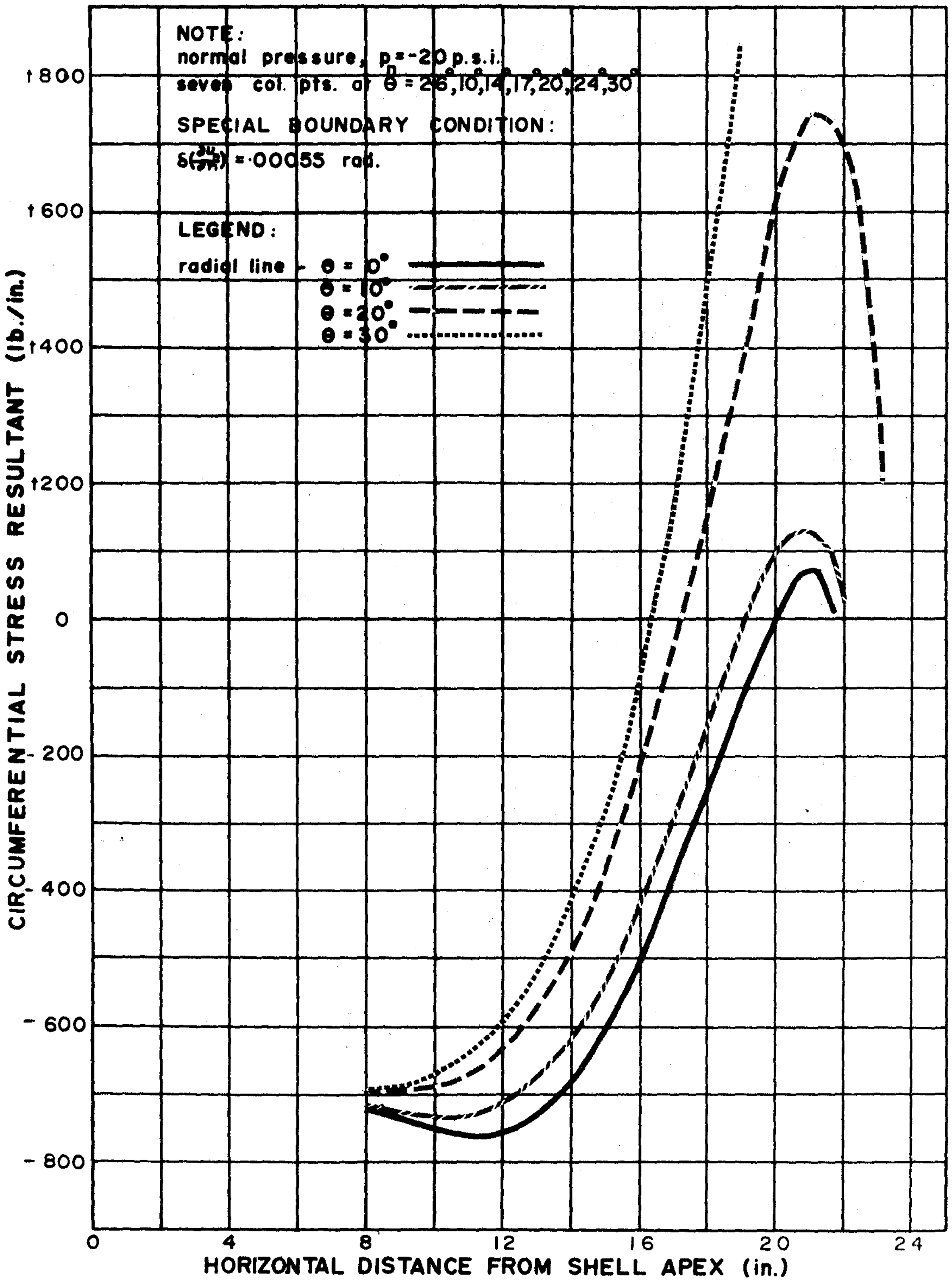

FIGURE 26

PLOT SHOWING THEORETICAL "$F_{\theta\theta}(\sigma)$" for SHELL on HEXAGONAL BASE

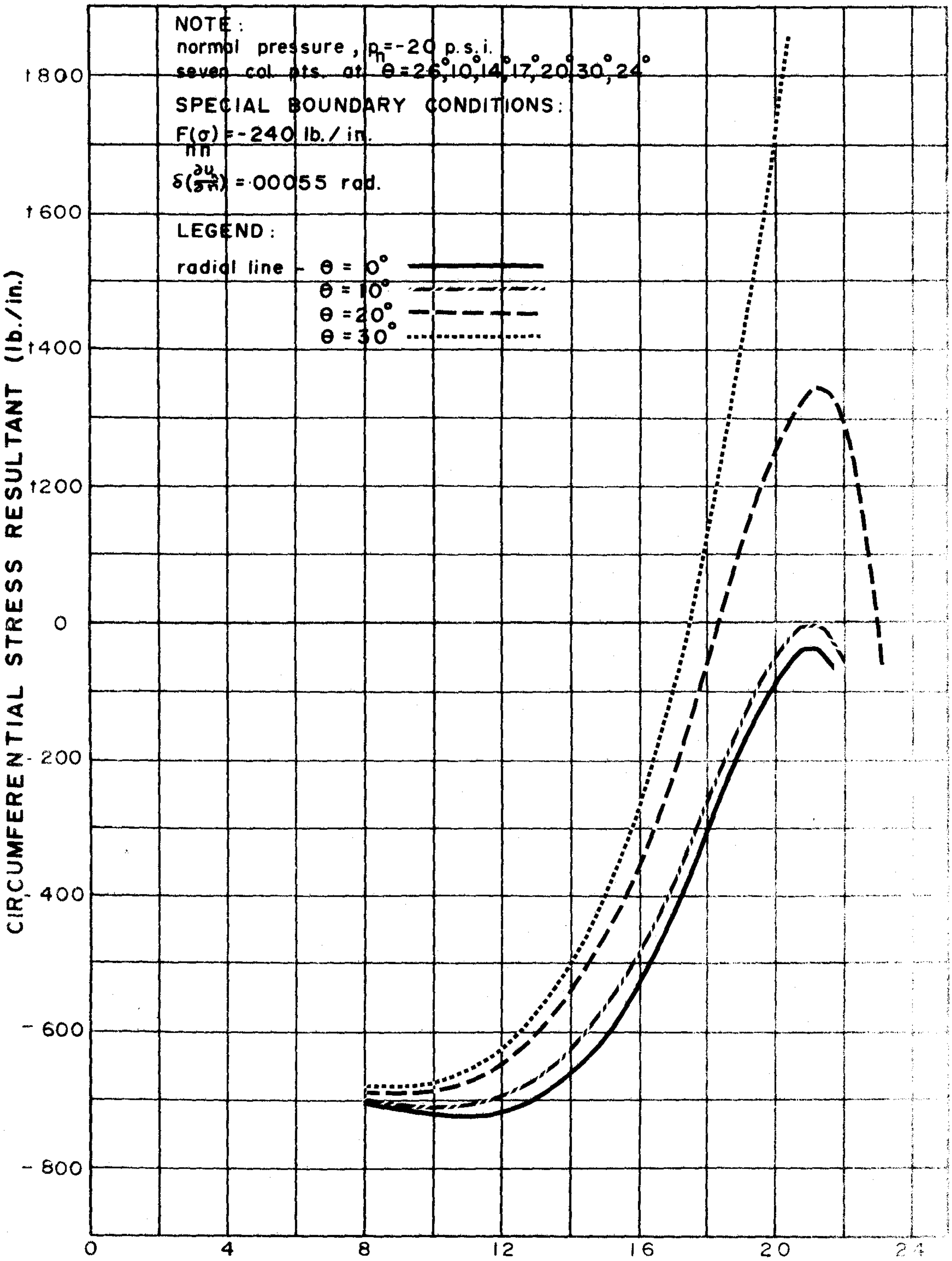

FIGURE 27

PLOT SHOWING EXPERIMENTAL "$M_{r\theta}(\sigma)$"
for SHELL on HEXAGONAL BASE

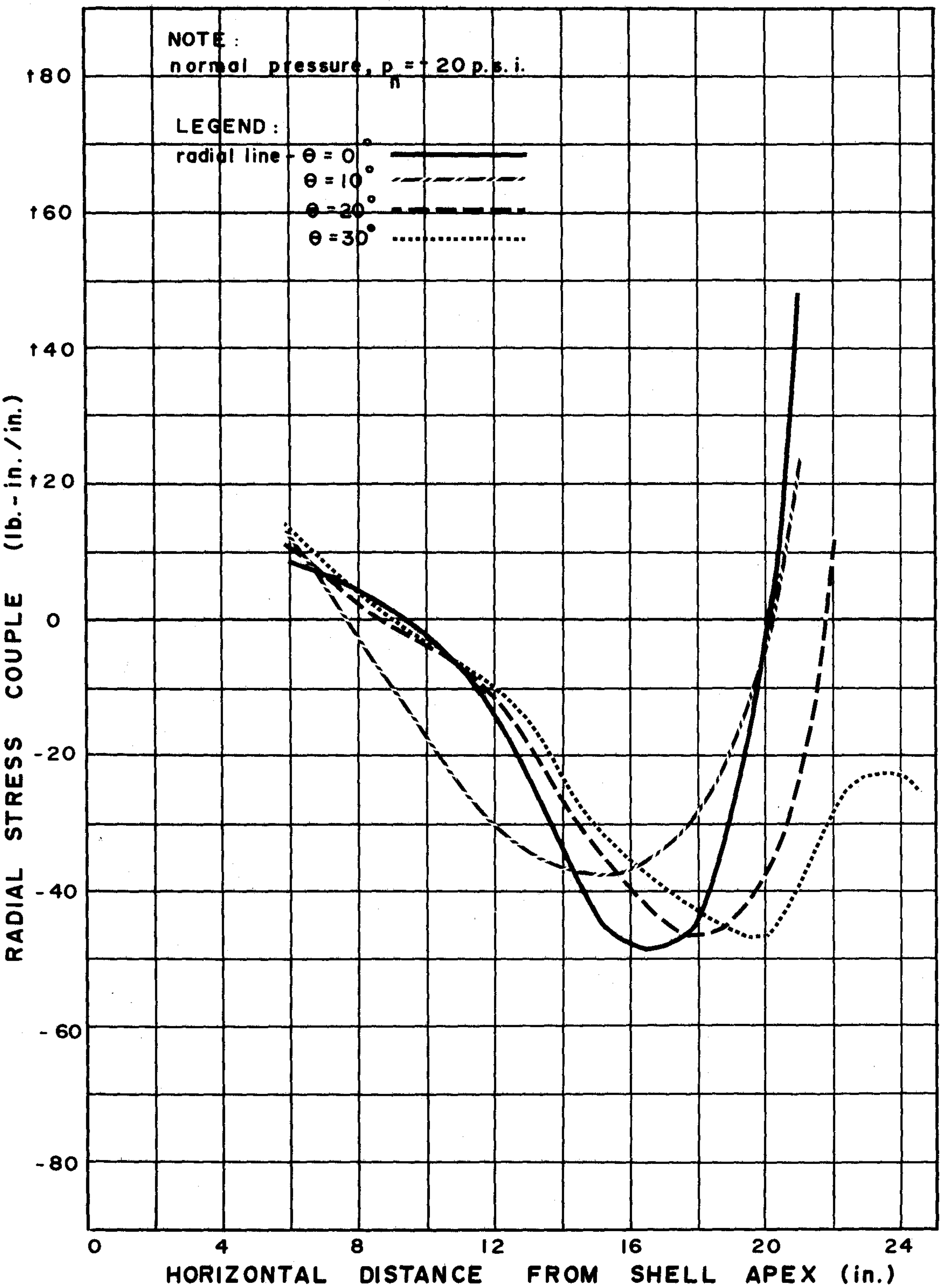

FIGURE 28

PLOT SHOWING THEORETICAL "$M_{r\theta}(\sigma)$"
for SHELL on HEXAGONAL BASE

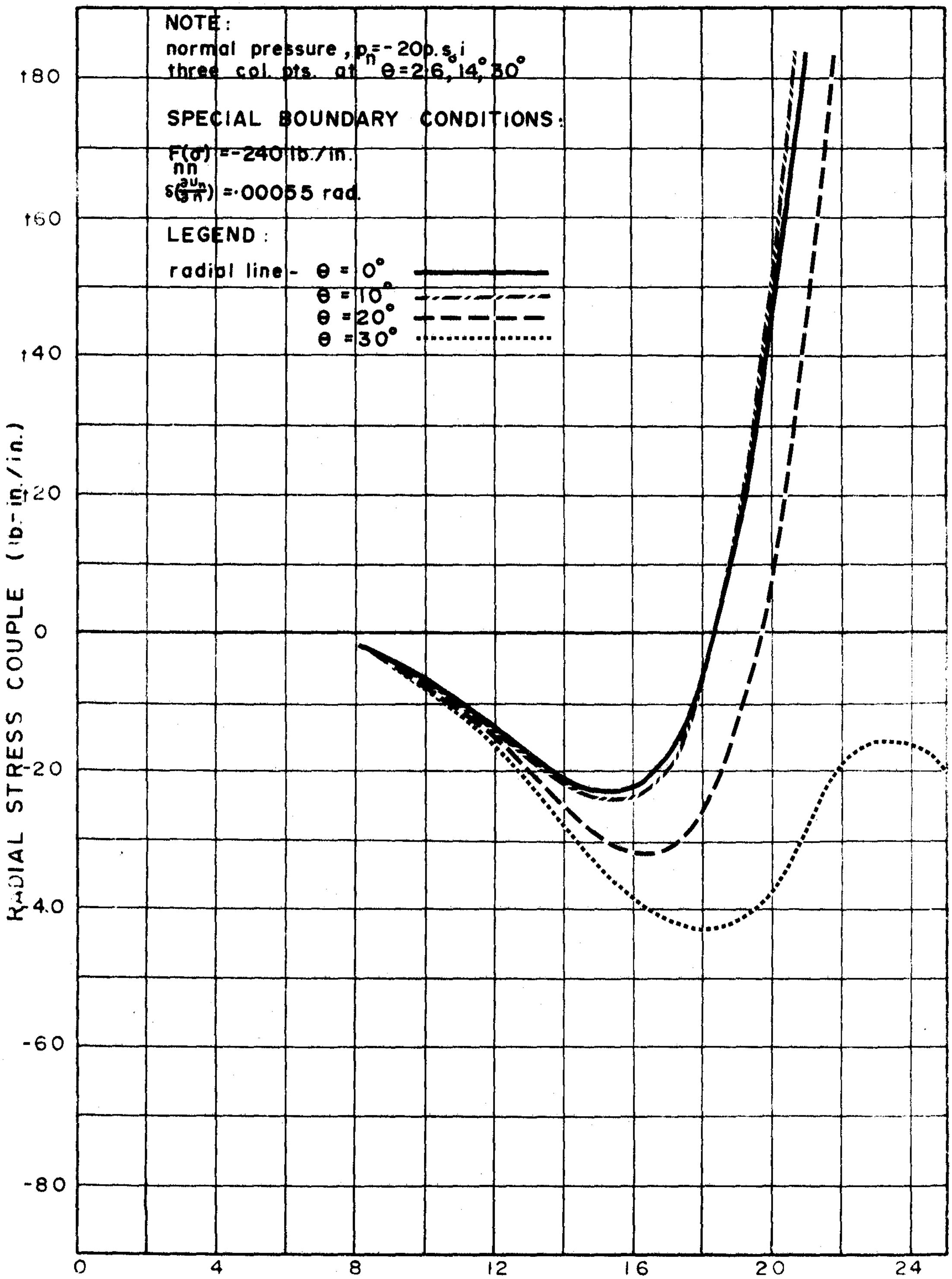

FIGURE 29

PLOT SHOWING THEORETICAL "$M_{r\theta}(\sigma)$" for SHELL on HEXAGONAL BASE

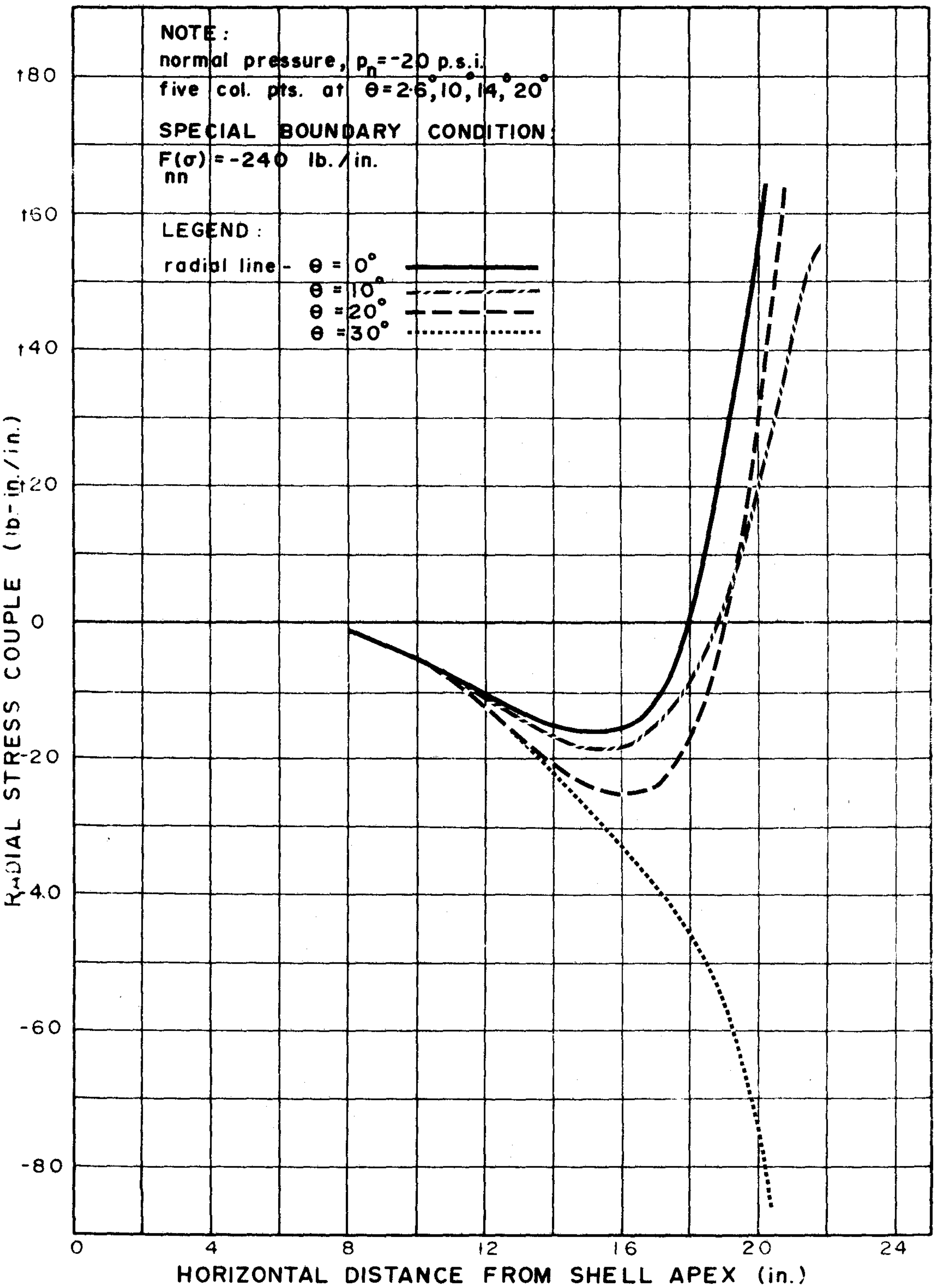

FIGURE 30

PLOT SHOWING THEORETICAL "$M_{r\theta}(\sigma)$"
for SHELL on HEXAGONAL BASE

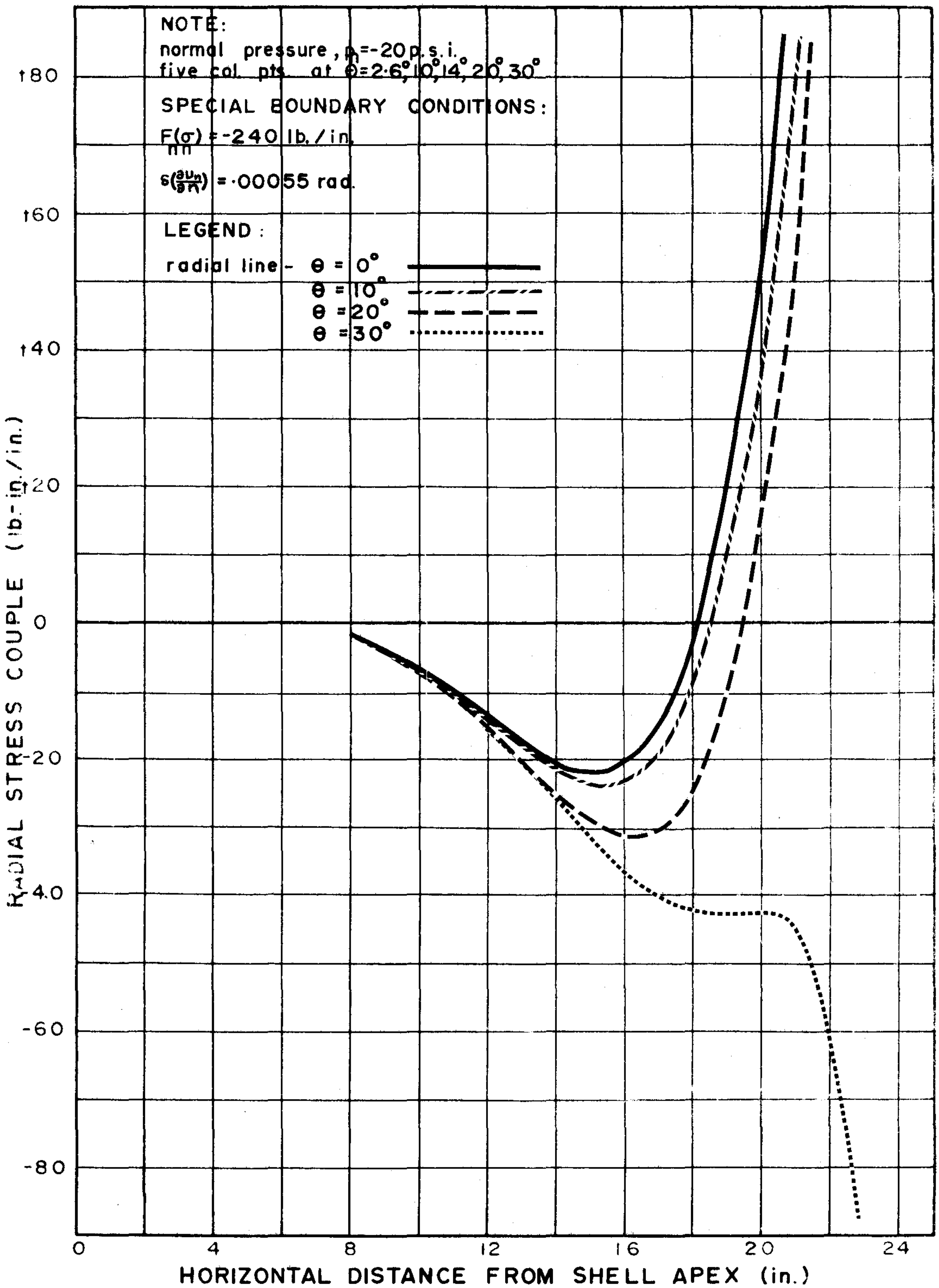

FIGURE 31

PLOT SHOWING THEORETICAL "$M_{r\theta}(\sigma)$"
for SHELL on HEXAGONAL BASE

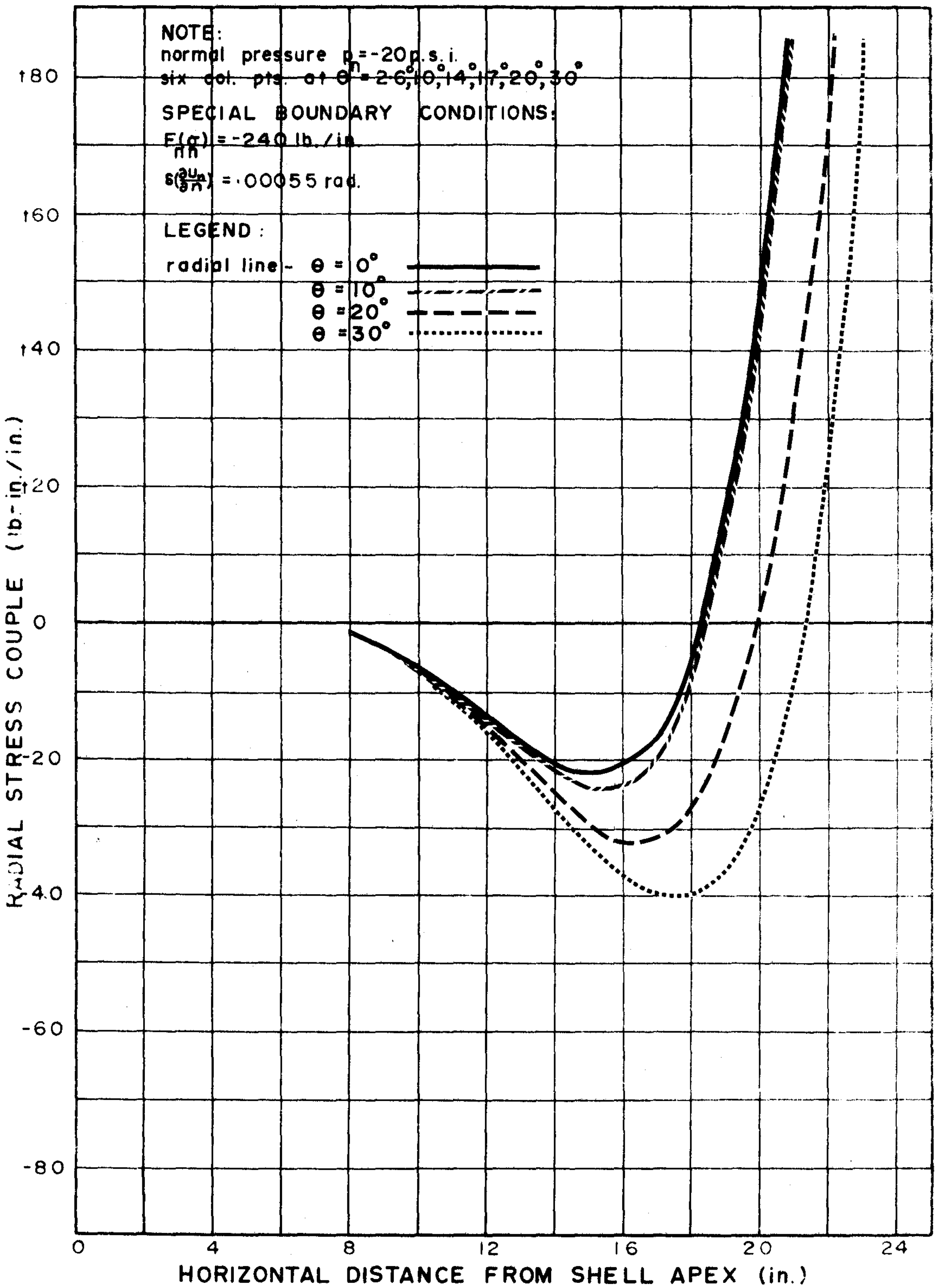

FIGURE 32

PLOT SHOWING THEORETICAL "$M_{r\theta}(\sigma)$"
for SHELL on HEXAGONAL BASE

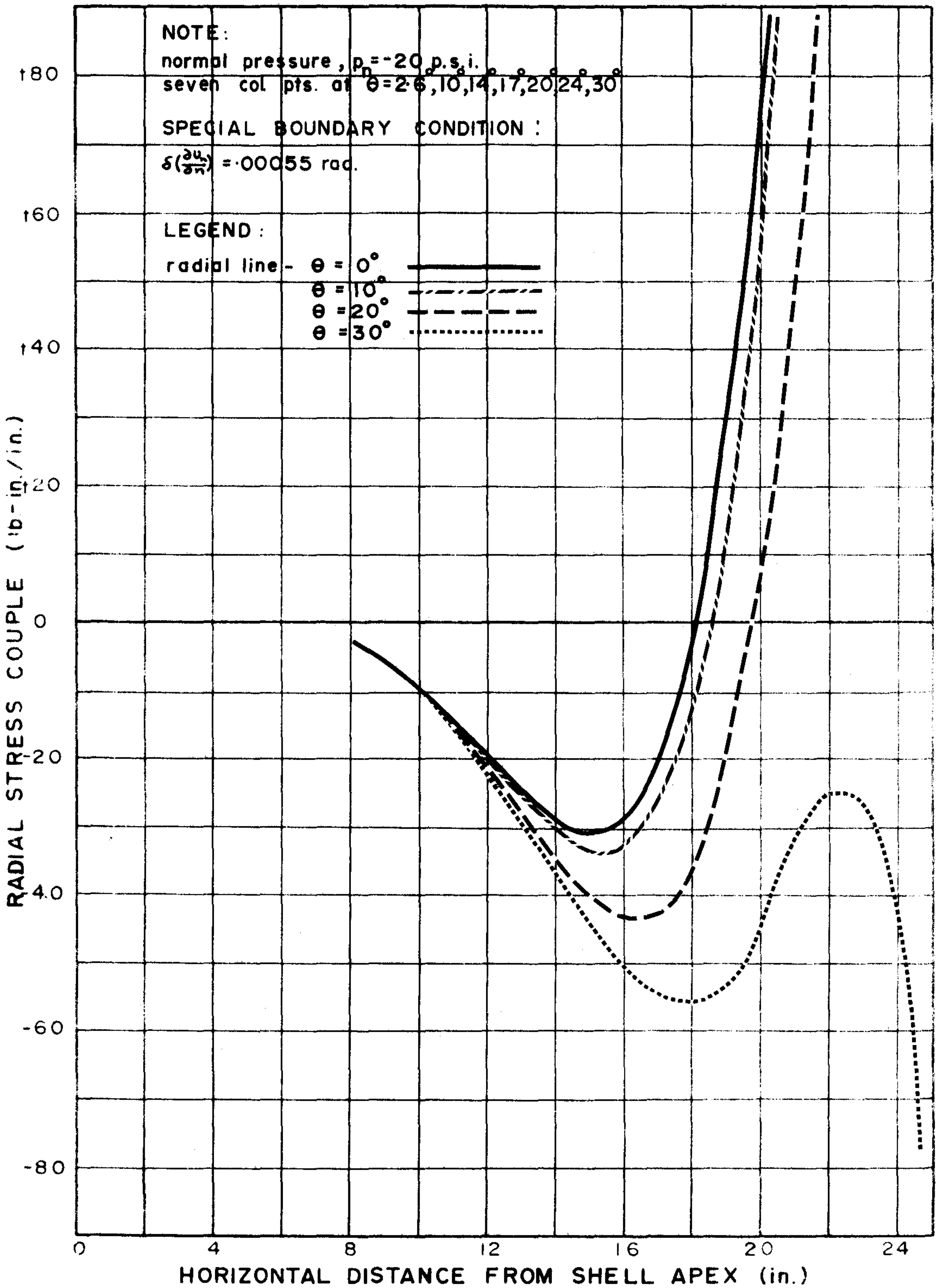

FIGURE 33

PLOT SHOWING THEORETICAL "$M_{r\theta}(\sigma)$"
for SHELL on HEXAGONAL BASE

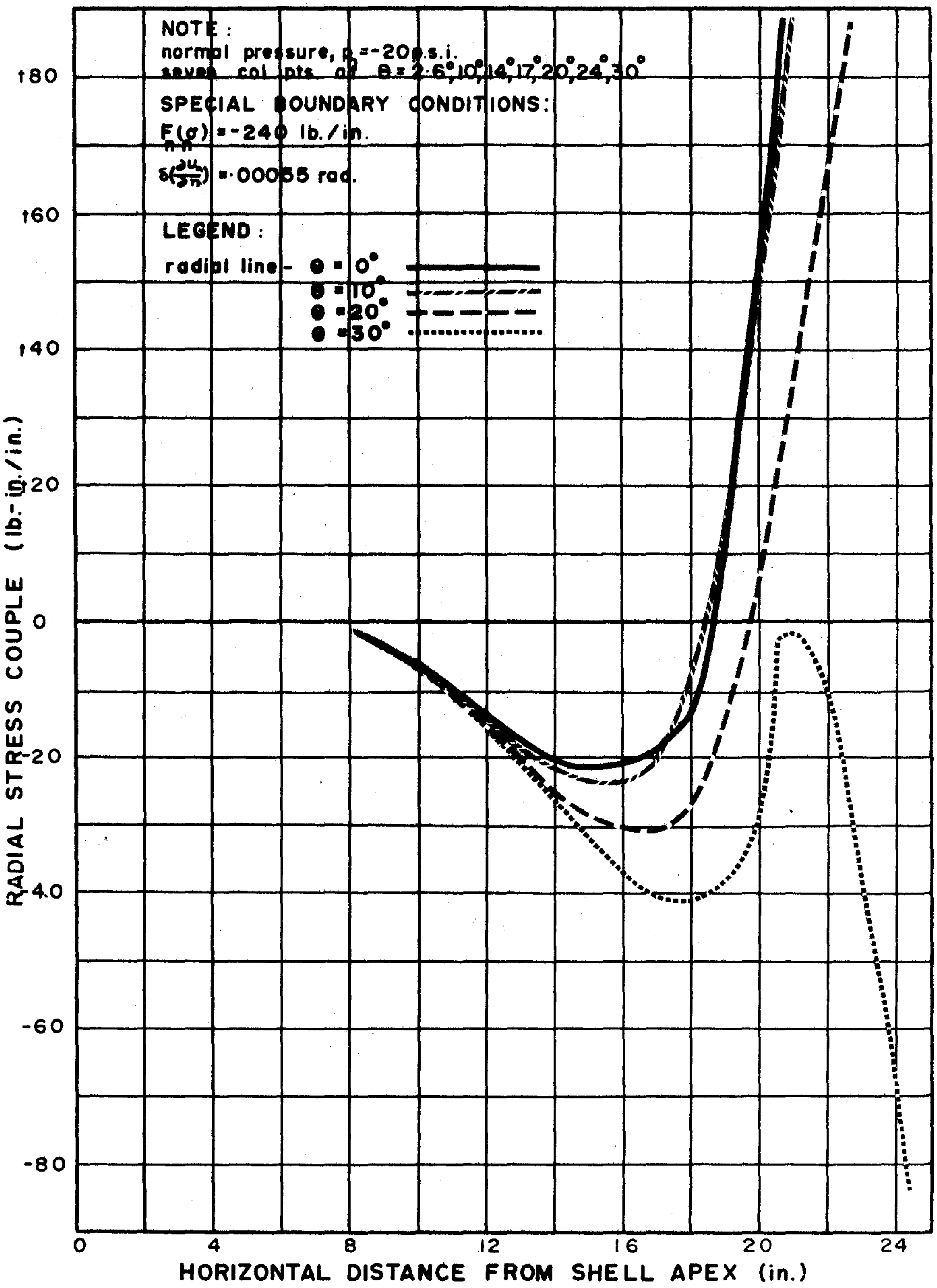

FIGURE 34

PLOT SHOWING EXPERIMENTAL "$M(\sigma)_{\theta r}$"
for SHELL on HEXAGONAL BASE

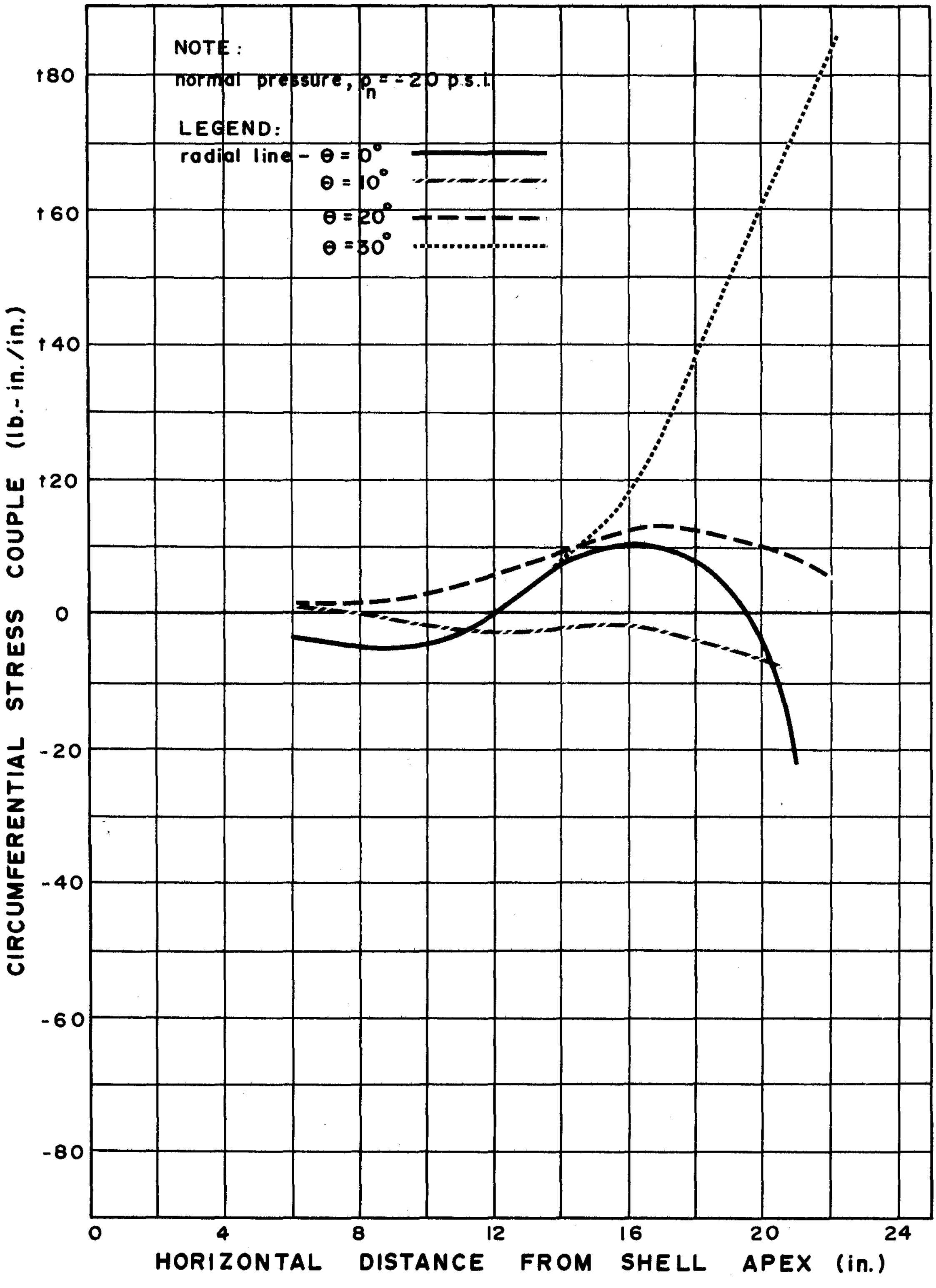

FIGURE 35

PLOT SHOWING THEORETICAL "$M_{\theta r}(\sigma)$" for SHELL on HEXAGONAL BASE

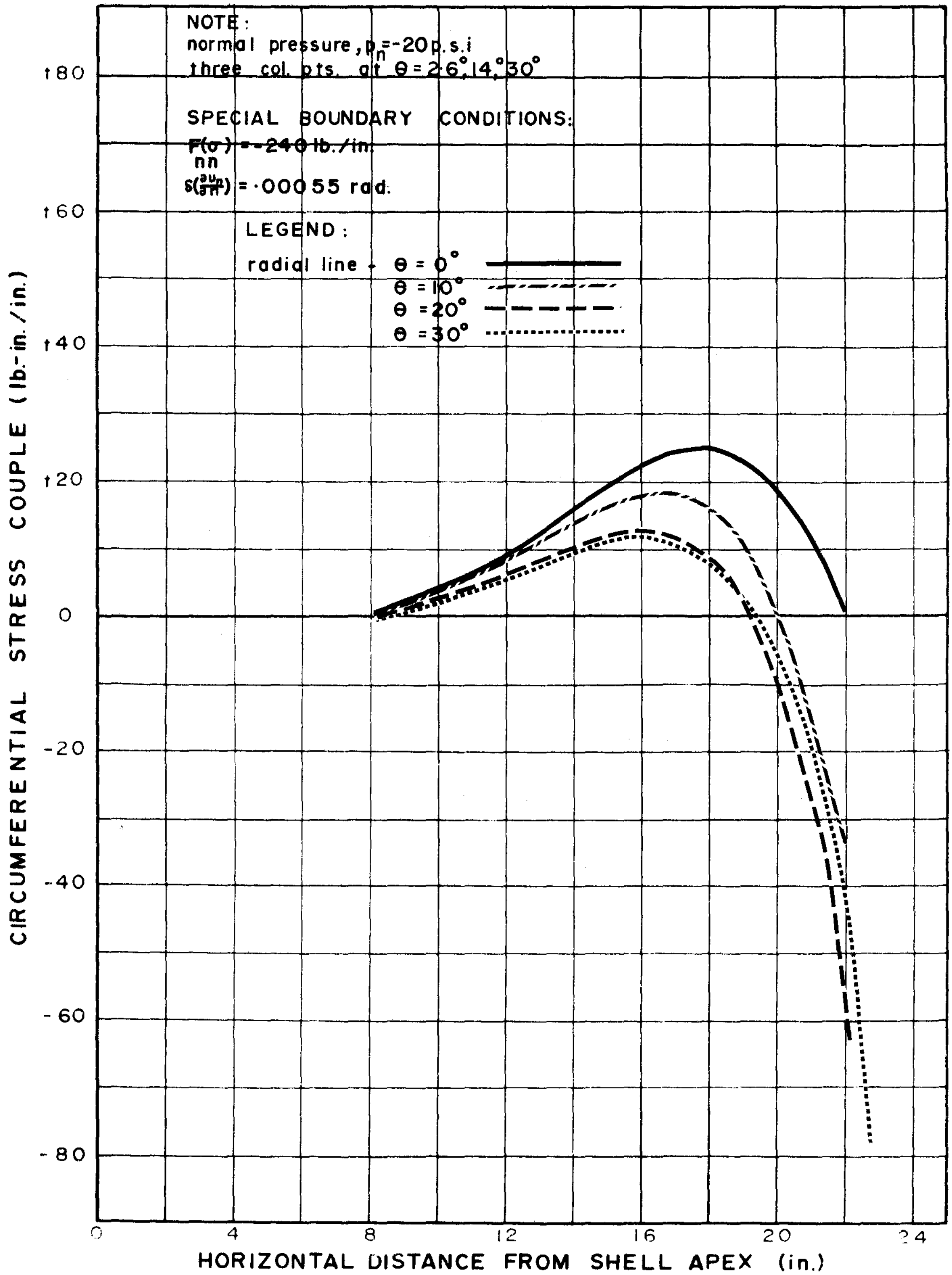

FIGURE 36

PLOT SHOWING THEORETICAL "$M(\sigma)_{\theta r}$" for SHELL on HEXAGONAL BASE

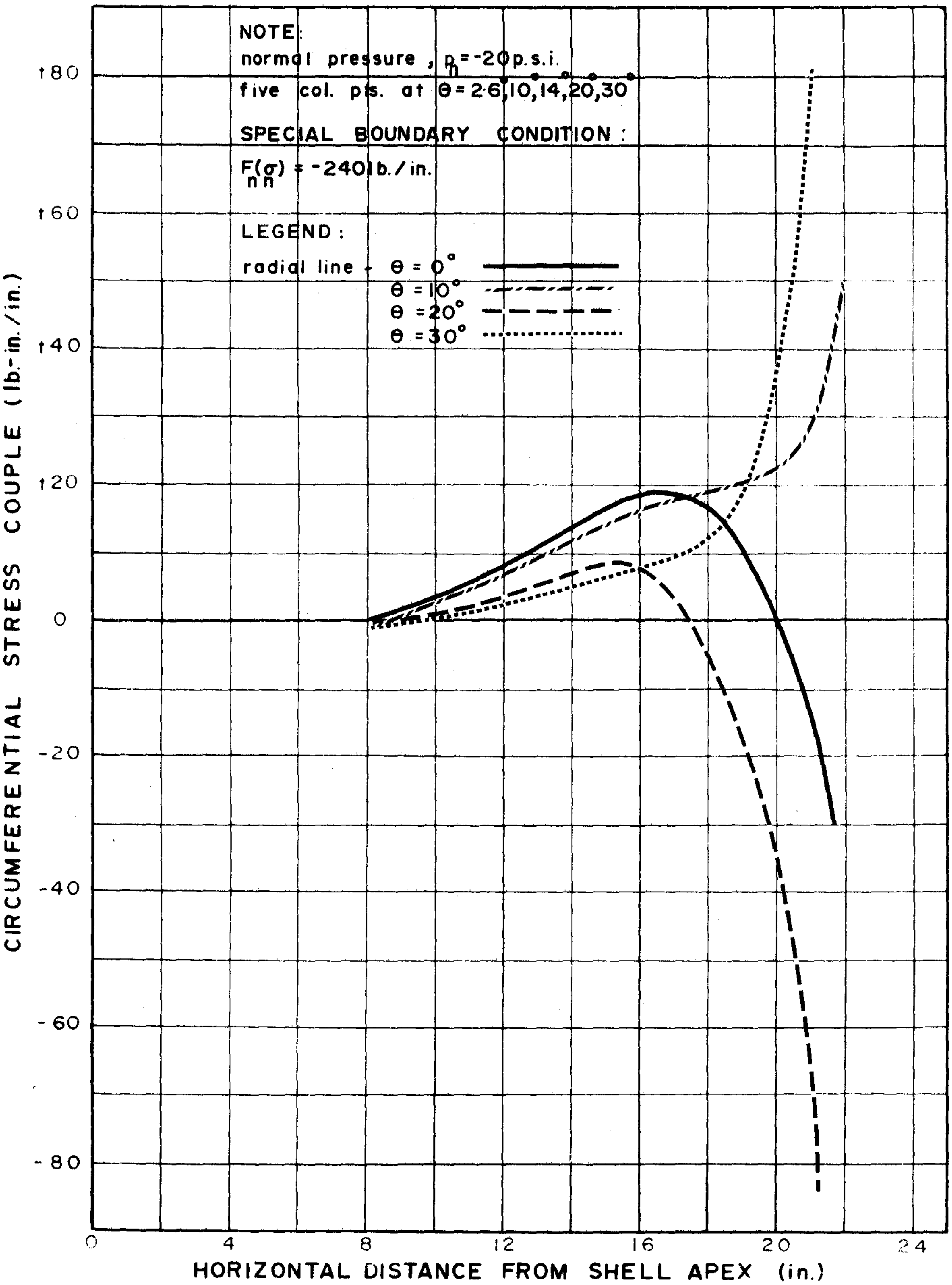

FIGURE 37

PLOT SHOWING THEORETICAL "$M_{(\sigma)}$" for SHELL on HEXAGONAL BASE

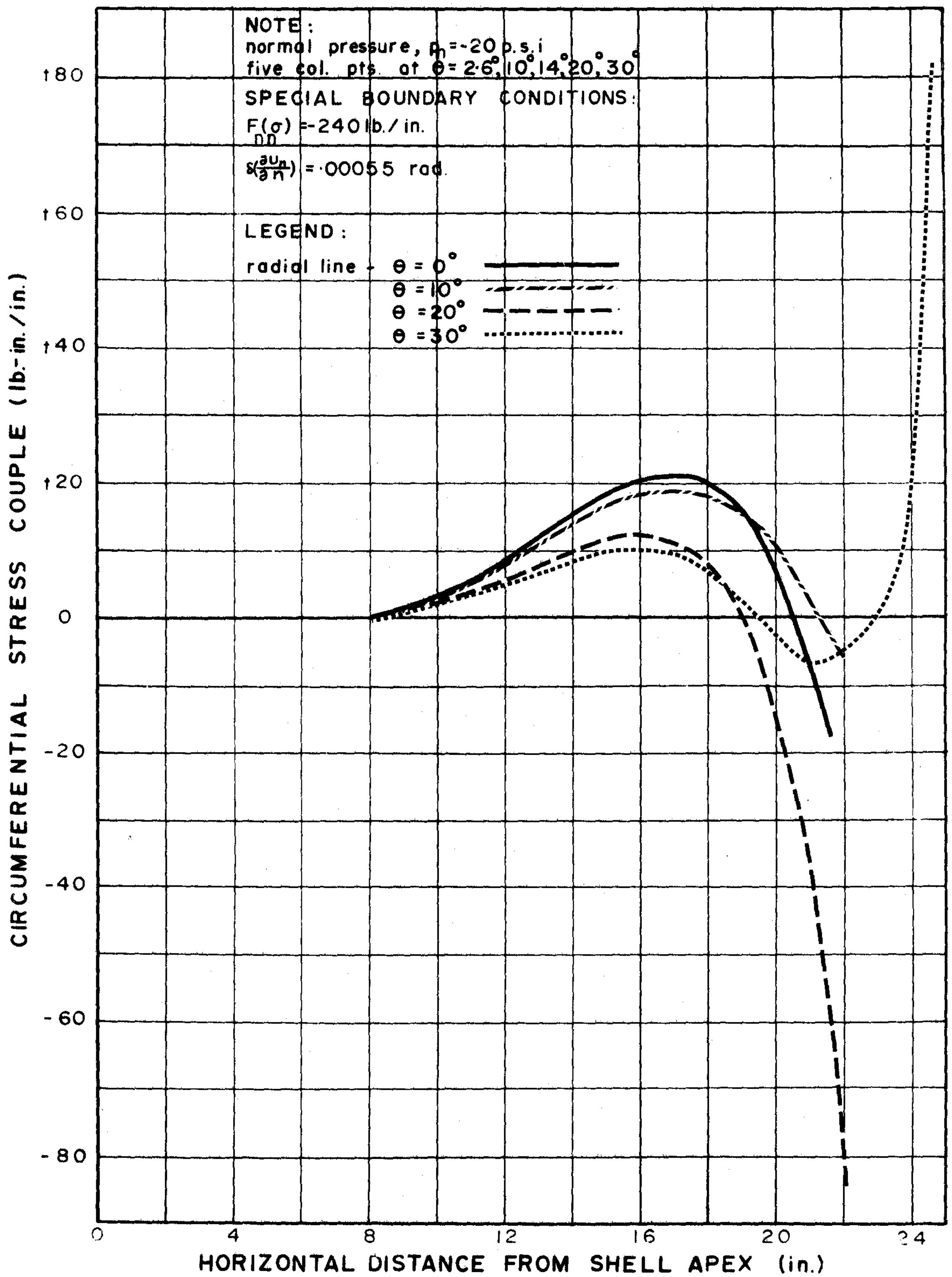

FIGURE 38

PLOT SHOWING THEORETICAL "$M_{(\sigma)\theta r}$" for SHELL on HEXAGONAL BASE

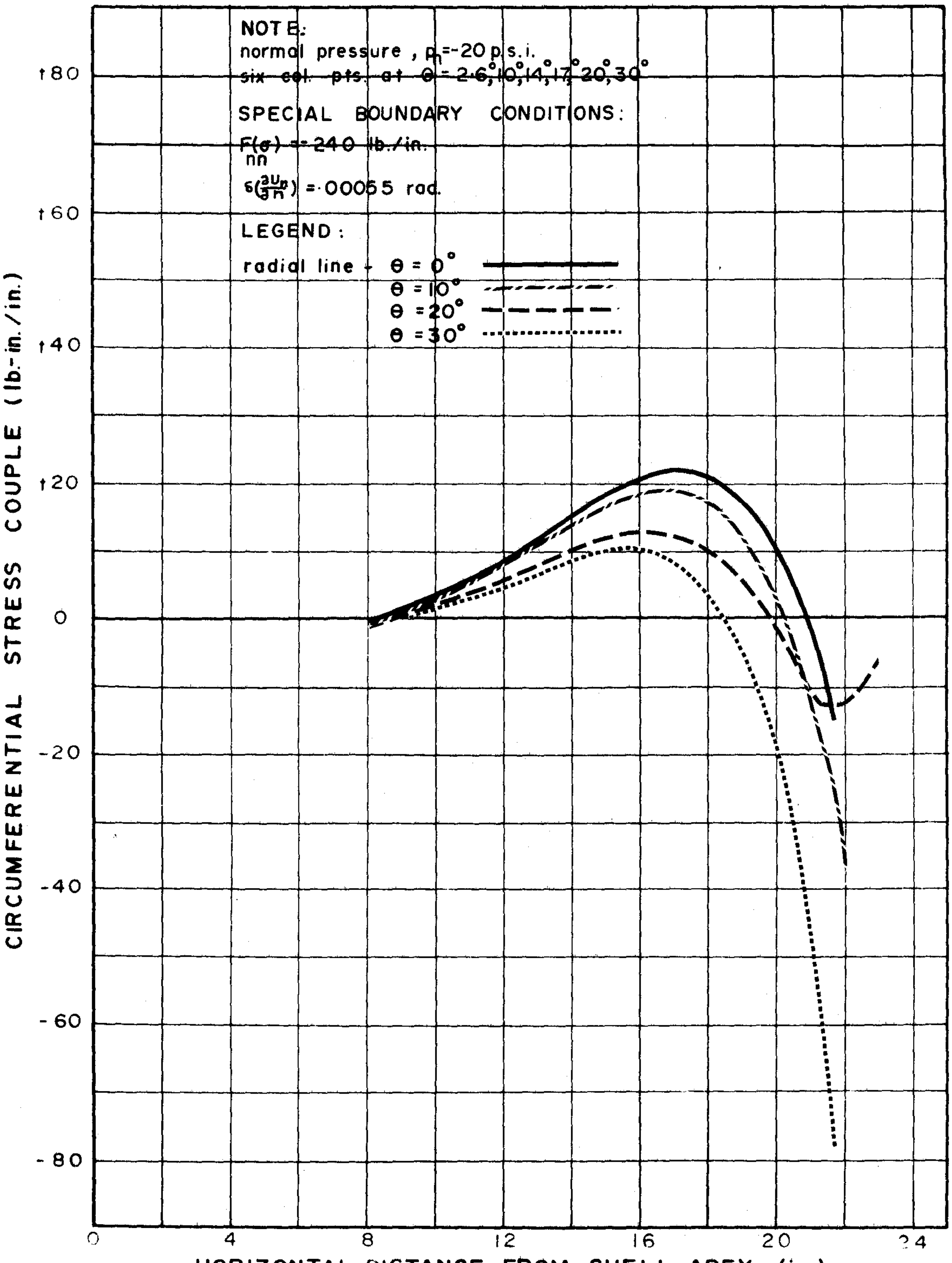

FIGURE 39

PLOT SHOWING THEORETICAL "$M_{\theta r}(\sigma)$"
for SHELL on HEXAGONAL BASE

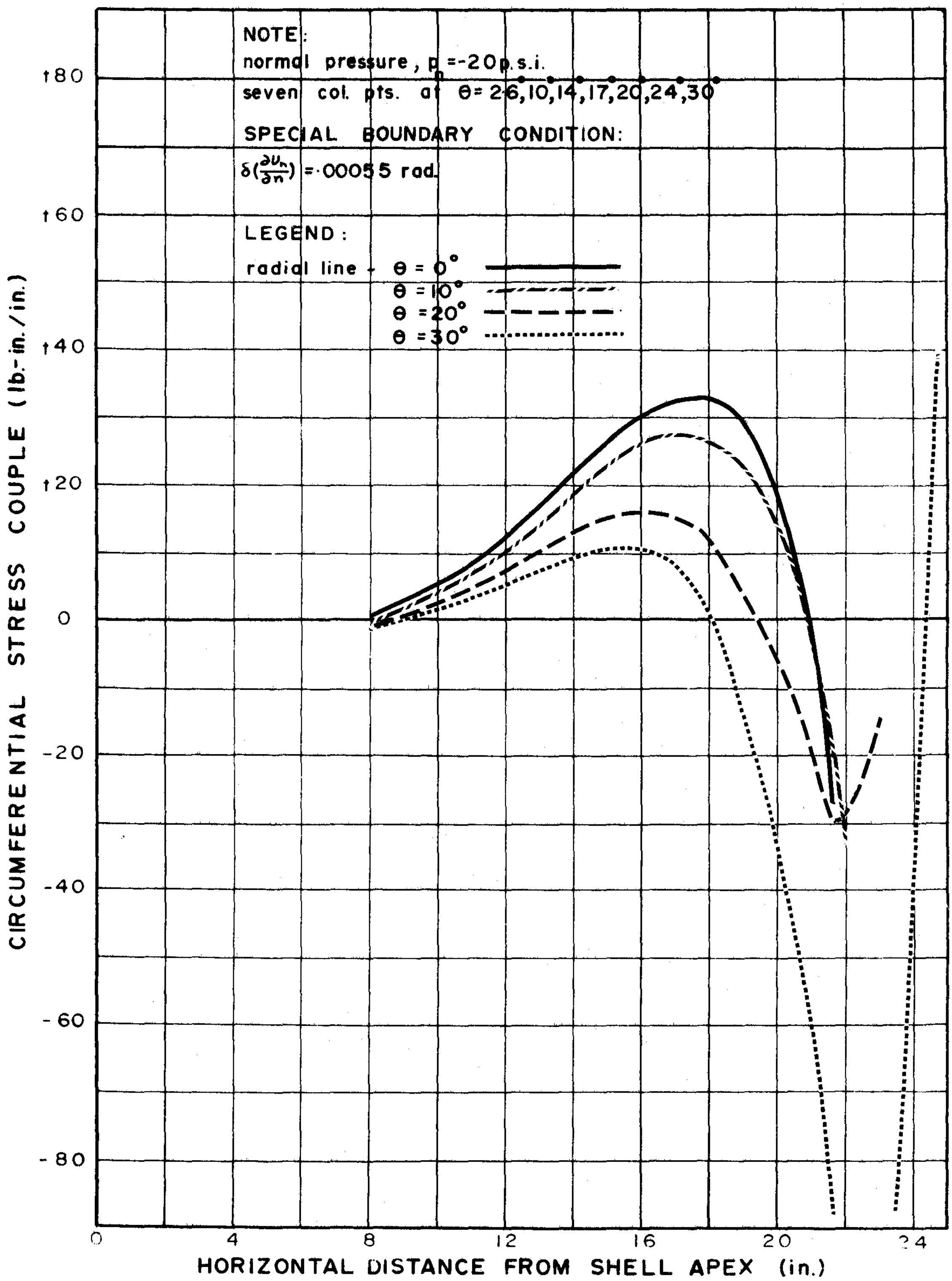

FIGURE 40

PLOT SHOWING THEORETICAL "$M_{\sigma r}(\sigma)$"
for SHELL on HEXAGONAL BASE

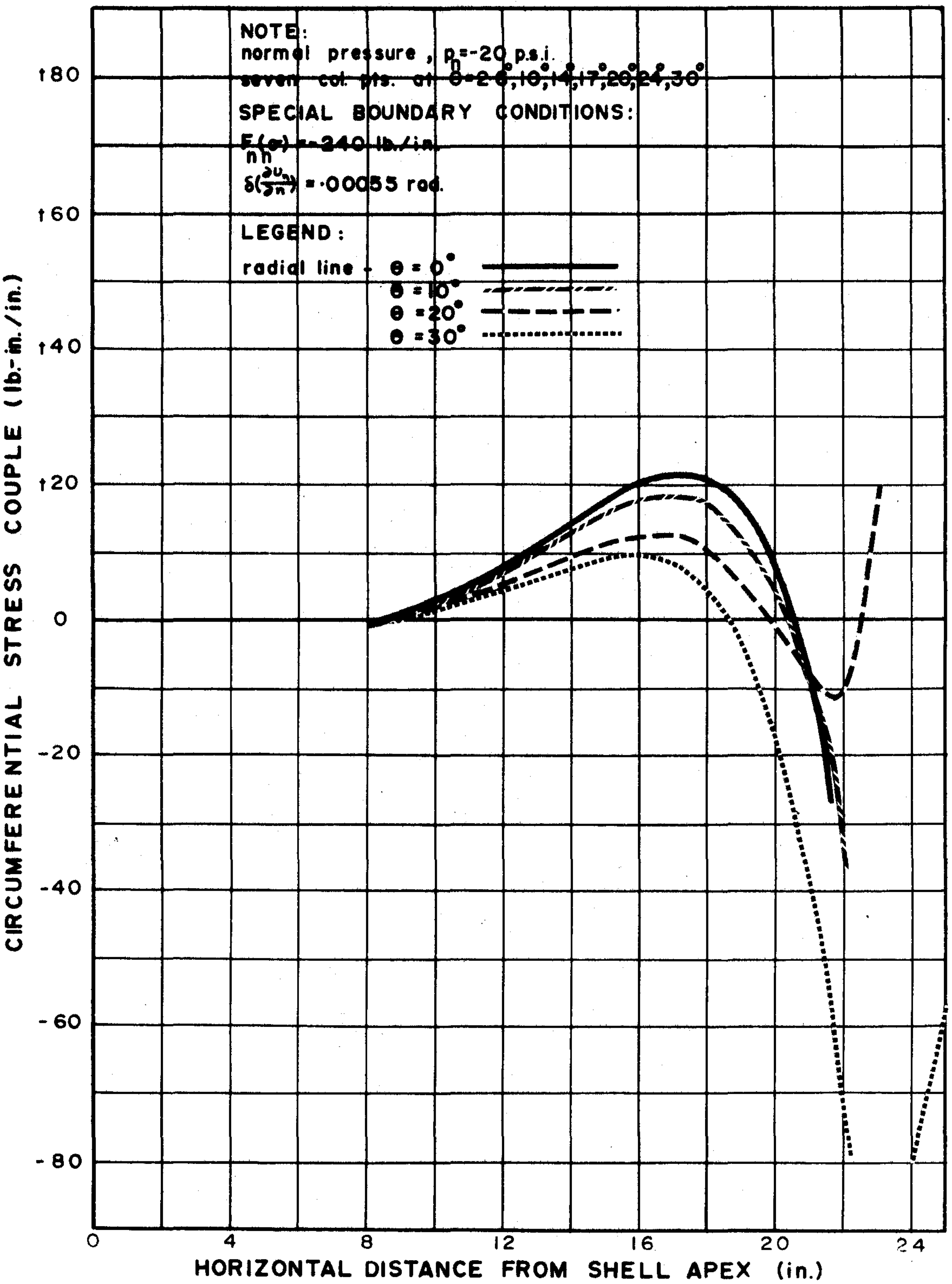

FIGURE 41

VARIATION of "U_n" on the BOUNDARY of SHELL on HEXAGONAL BASE for THREE COLLOCATION POINTS

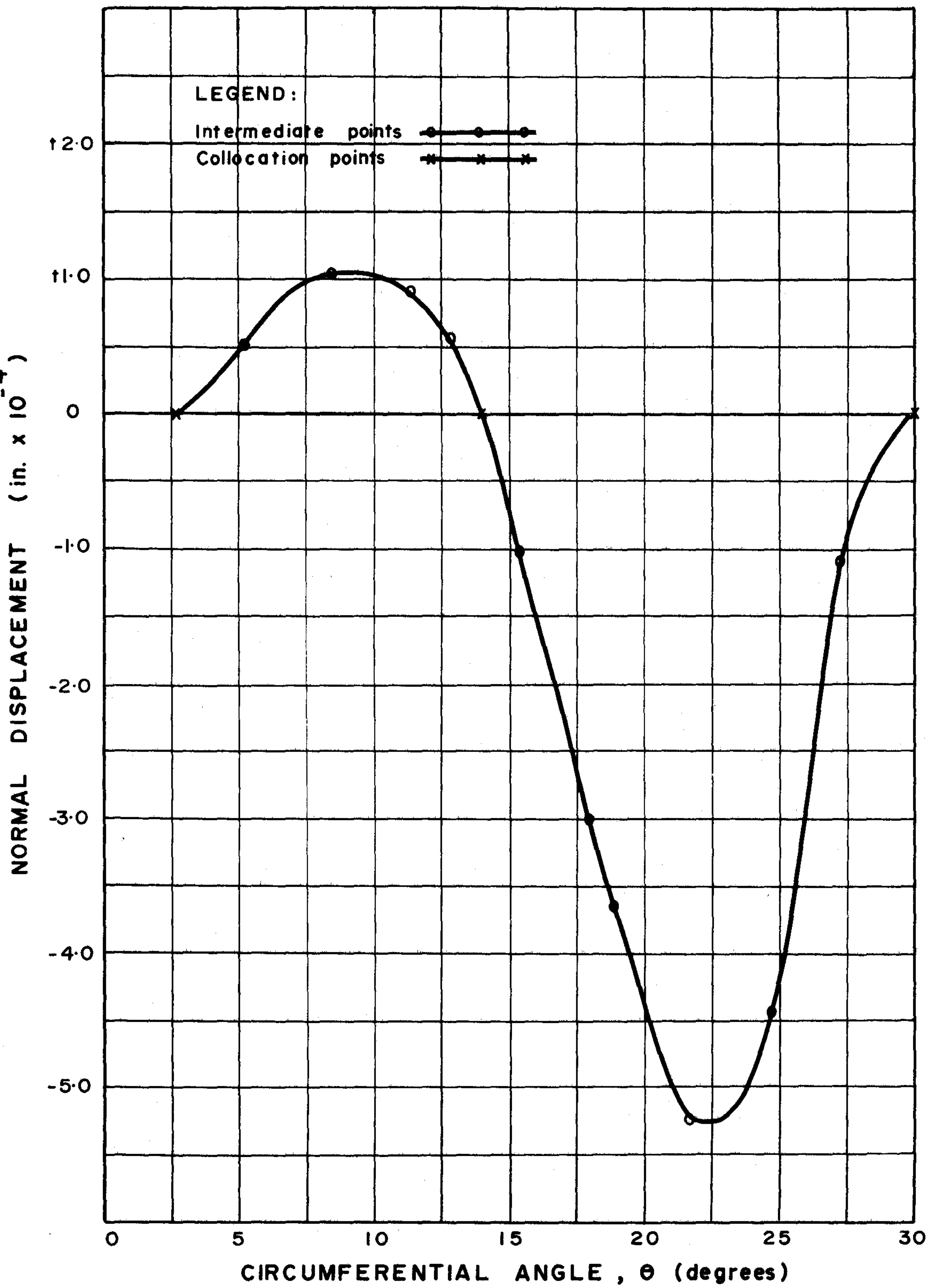

FIGURE 42

VARIATION of "U_n" on the BOUNDARY of SHELL on HEXAGONAL BASE for SEVEN COLLOCATION POINTS

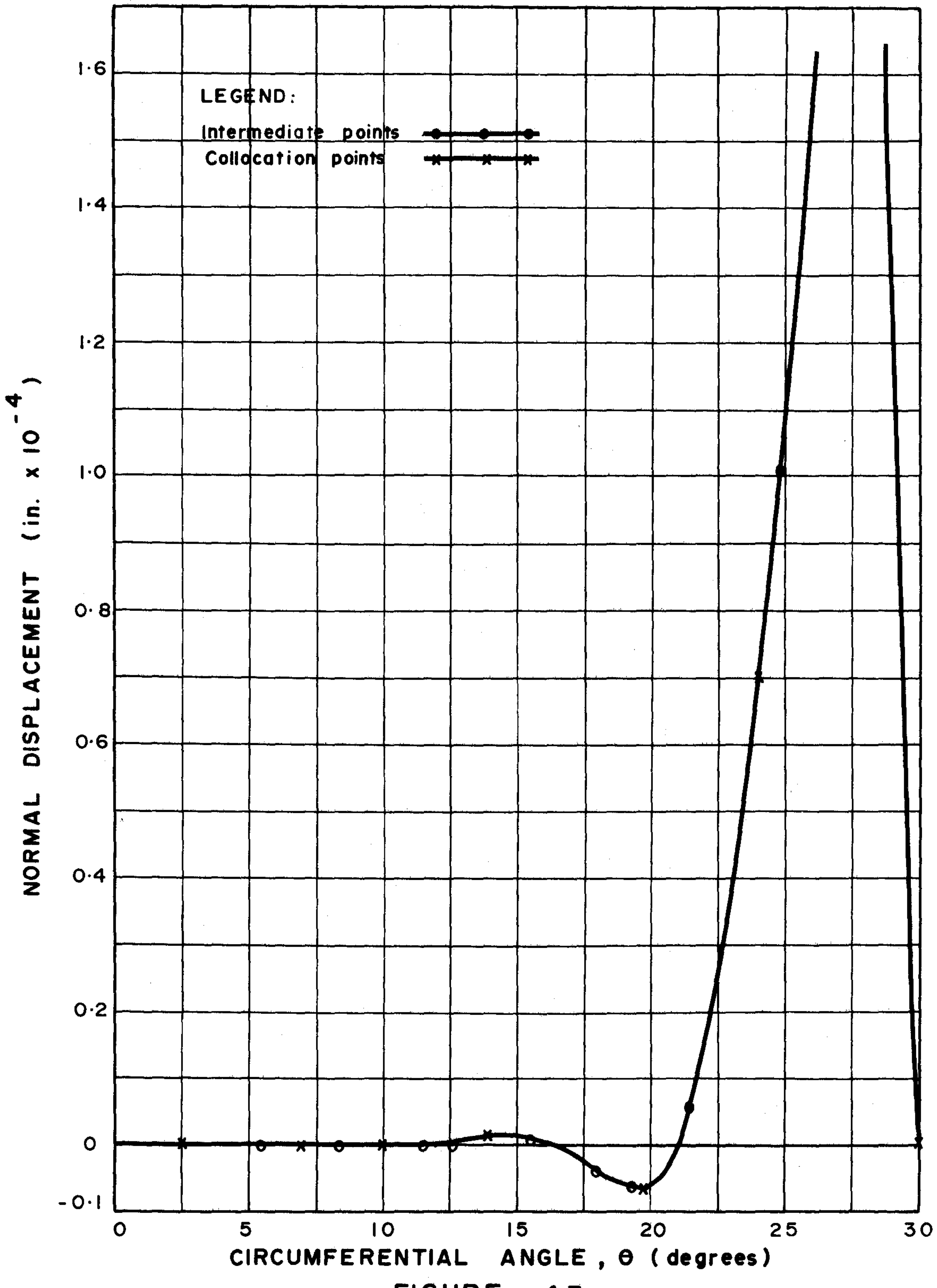

FIGURE 43

CHAPTER III

SHELL ENCLOSING RECTANGULAR BASE

DIKOVICH in 1960 gave a solution for a rotational parabolic shell enclosing a rectangular base and subjected to a uniform normal pressure. This solution also employs the fundamental shallow shell equations which were derived by MUSHTARI in 1938 and VLASOV in 1949 and are given in APPENDIX A as (A-1) and (A-2). However, DIKOVICH obtained one fourth order differential equation in normal displacement from (A-1) and (A-2) which are fourth order differential equations containing both the normal displacement and the stress function. This equation was modified for a shell with rotationally symmetric parabolic middle surface. BERNOULLI's Semi-Direct solution was applied and normal displacement was assumed to be given by a trigonometric cosine series. The homogeneous solution for the normal displacement was coupled with the particular solution and the result was simplified for rectangular symmetry. This solution for the normal displacement was substituted in the MUSHTARI-VLASOV equations to give a solution for the stress function which also was assumed to be given by a trigonometric cosine series.

Consequently DIKOVICH's solution does not neglect the transverse bending stiffness of the shell as do membrane solutions given by a plethora of authors. However, her solution does limit the combinations of boundary conditions which can be applied to lateral sides of the shell, since both the normal displacement and the stress function are assumed to have trigonometric cosine series solutions. For example, if the normal displacement is assumed to vanish at the shell's boundary, then the radial and circumferential stress couples which contain only second derivatives of normal displacement, must also vanish.

ORAVAS gave a similar solution in 1957 (2) by means of WEBB complex dependent variable technique for rotationally symmetric, parabolic shells which may be considered to be shells of translation as a special case.

In this chapter a comparison of normal displacements and sectional resultants, computed by DIKOVICH's solution and by the collocation solution for the radial line $\theta = 0^{\circ}$, is made for a pair of shells of similar middle surface which enclose identical rectangular bases and are subjected to the same normal pressure.

The geometry of the shell for which DIKOVICH's solution applied is described by the parameters

$$\varkappa = \sqrt{\frac{f}{\delta}} = 2.0$$

$$a = 25.0 \cos \frac{\pi}{4} = 17.66 \text{ in.}$$

where

2f represents the height of the apex above the shell's base, 5.085 in.,

2a represents the horizontal length of each of the shell's four boundaries,

and δ represents the shell's thickness, 0.432 in.

The shell for which the collocation solution applied also had boundaries of the same horizontal length, 2a, whose corners touched a base circle of the same diameter, 50 inches; it had the same shell thickness and its spherical middle surface had a radius of 64 inches so that the apex was the same distance, 5.085 inches, above the shell's base.

Geometrically the only difference between the two shells lay in the curvature of their middle surfaces. The curvature of the parabolic shell was slightly flatter near the apex and steeper near the boundaries than was the curvature of the spherical shell.

The boundary conditions which the two solutions satisfied were, however, not quite identical.

DIKOVICH's solution satisfied the boundary conditions :

$$
\begin{aligned}
u_n &= 0 \\
M(\sigma)_{ns} &= 0 \\
F(\sigma)_{nn} &= 0
\end{aligned}
\qquad \text{(III-1)}
$$

At $\theta = 0^\circ$ these boundary conditions become :

$$
\begin{aligned}
u_n &= 0 \\
F(\sigma)_{rr} &= F(\sigma)_{\theta\theta} = 0 \\
M(\sigma)_{r\theta} &= M(\sigma)_{\theta r} = 0
\end{aligned}
\qquad \text{(III-1*)}
$$

The collocation solution satisfied the boundary conditions :

$$
\begin{aligned}
u_n &= 0 \\
M(\sigma)_{ns} &= 0 \\
F(\sigma)_{nn} &= 0 \\
\epsilon_{ss} &= 0
\end{aligned}
\qquad \text{(III-2)}
$$

at all seven collocation points except at the corner for $\theta = 45^\circ$, where the strain was not assumed to vanish. At $\theta = 0^\circ$ these boundary conditions become :

$$
\begin{aligned}
u_n &= 0 \\
F(\sigma)_{rr} &= F(\sigma)_{\theta\theta} = 0 \\
M(\sigma)_{r\theta} &= 0 \\
\epsilon_{ss} &= 0
\end{aligned}
\qquad \text{(III-2*)}
$$

Comparison of the boundary conditions (III-1*) and (III-2*) shows that the collocation solution replaces the boundary condition $M_{\theta r}(\sigma) = 0$ at $\theta = 0^{\circ}$, used in DIKOVICH's solution, by $\epsilon_{ss} = 0$.

The normal displacements and sectional resultants calculated by both solutions are graphically depicted in FIGURES 46 to 50. It can be seen that while the radial and circumferential stress resultants concur for both solutions, the normal displacement and the radial and circumferential stress couples have significantly larger values for the collocation solution.

The dissimilarities between the normal displacements and the radial and circumferential stress couples as calculated by the two methods are probably aggravated by the incongruity of some of the boundary conditions.

However, the stress resultant boundary conditions in (III-1*) and (III-2*) were identical and consequently the radial and circumferential stress resultants of both solutions are quite similar. This indicates that comparable results can be obtained by either method of solution provided that their boundary conditions can be made completely compatible.

PLAN VIEW of SHELL on RECTANGULAR BASE SHOWING LOCATION of RADIAL LINES for which SECTIONAL RESULTANTS are CALCULATED

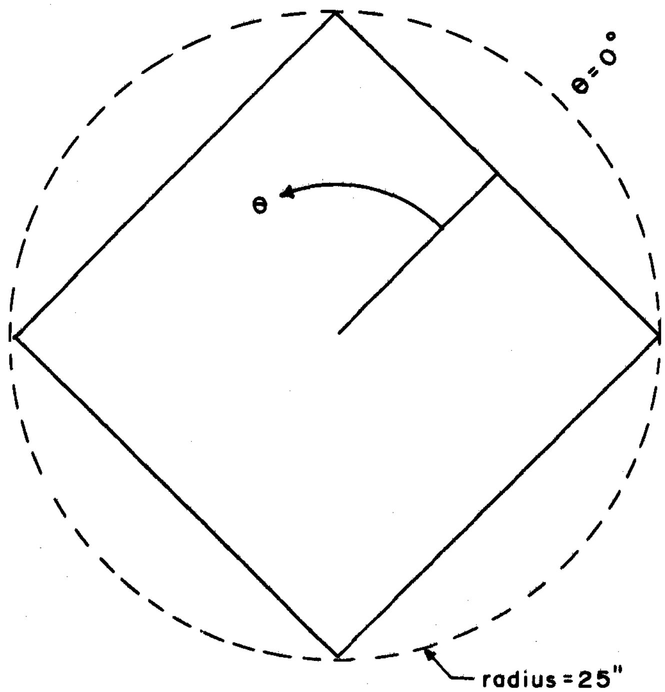

FIGURE 44

LOCATION of BOUNDARY COLLOCATION POINTS for SHELL on RECTANGULAR BASE

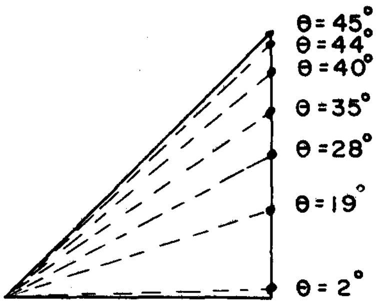

7 COLLOCATION POINTS

FIGURE 45

PLOT SHOWING THEORETICAL "U_n"
for SHELL on RECTANGULAR BASE

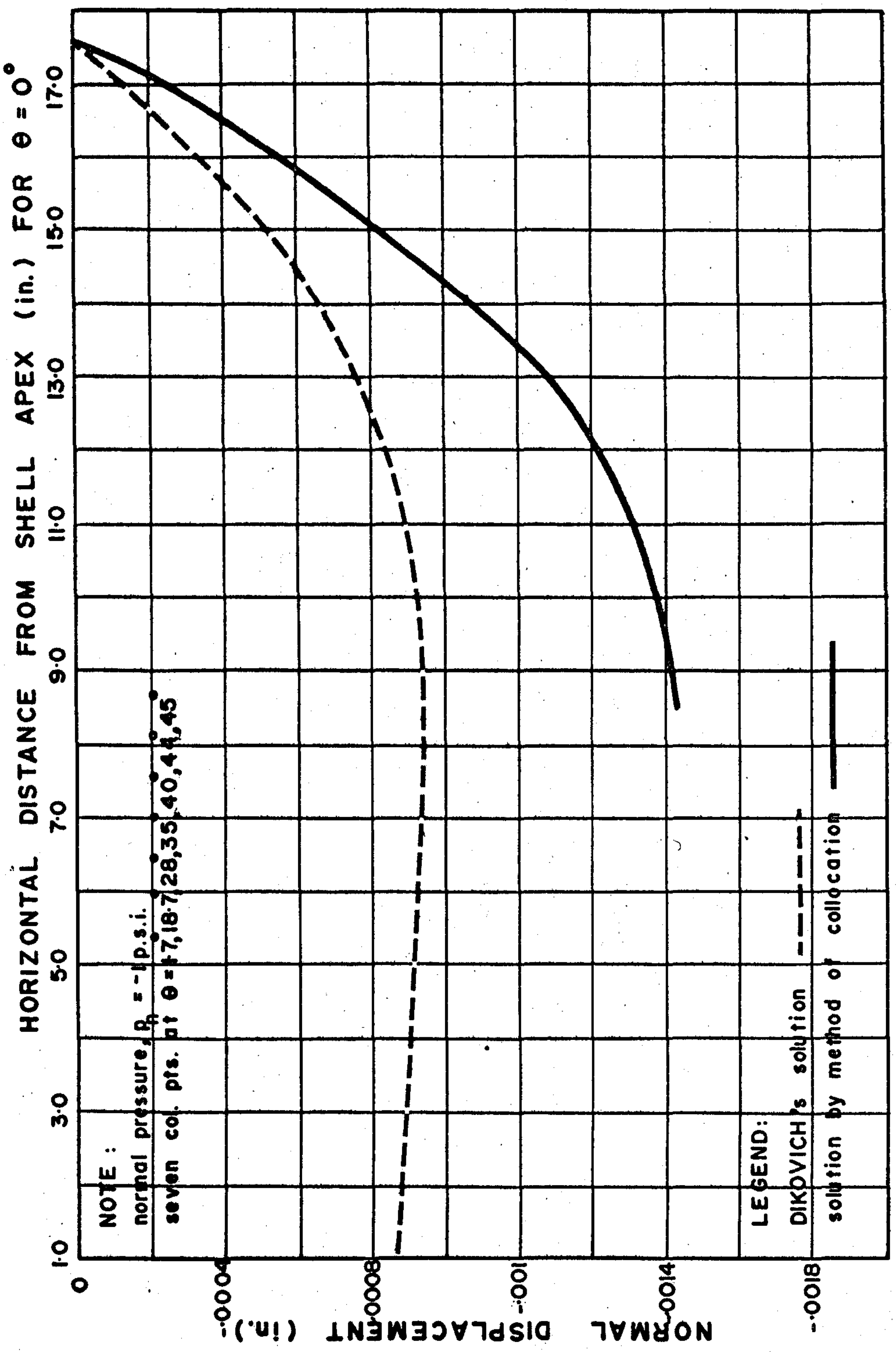

FIGURE 46

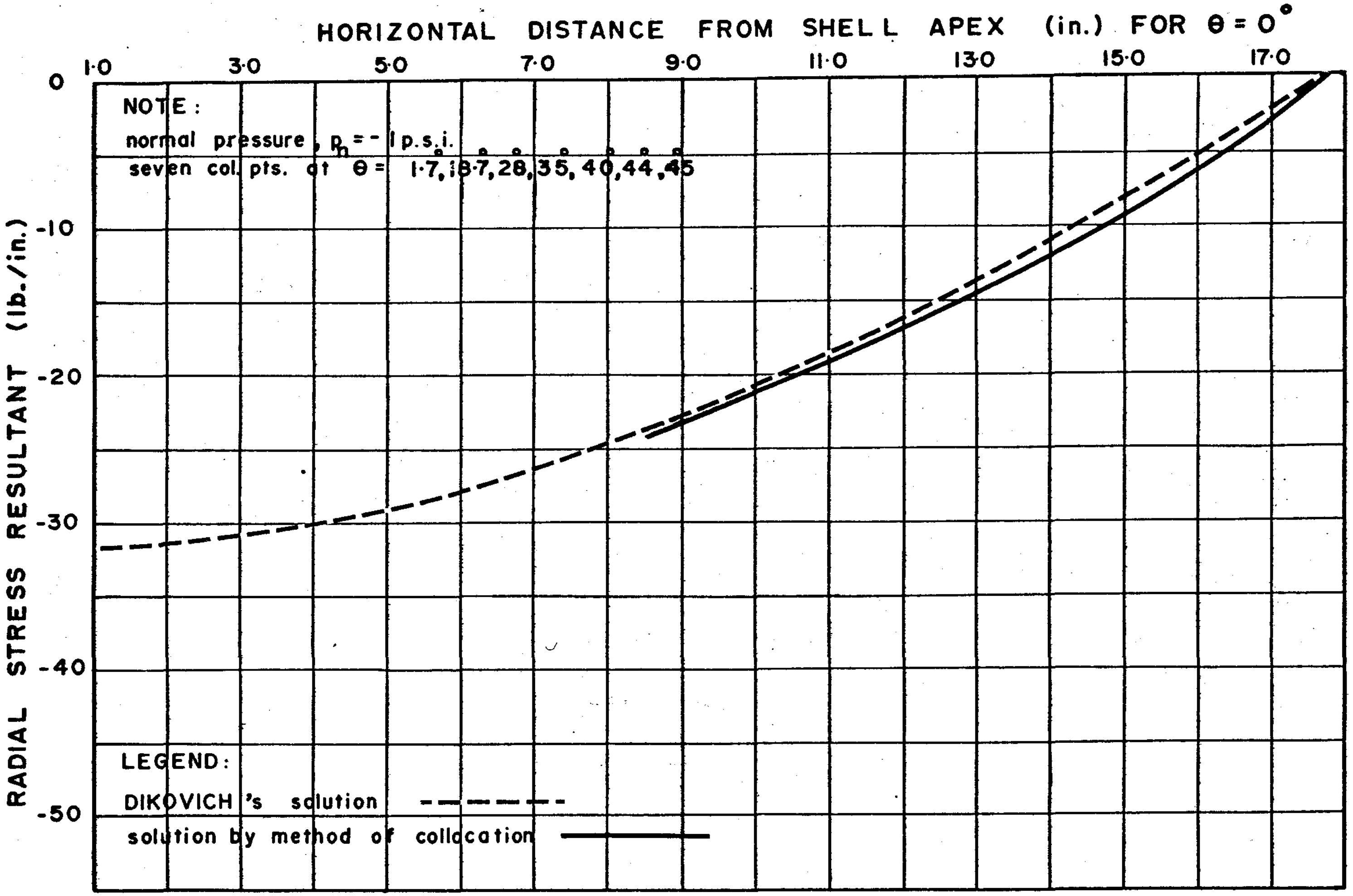

FIGURE 47

PLOT SHOWING THEORETICAL "$F_{rr}(\sigma)$" for SHELL on RECTANGULAR BASE

PLOT SHOWING THEORETICAL "$F(\sigma)_{\theta\theta}$"
for SHELL on RECTANGULAR BASE

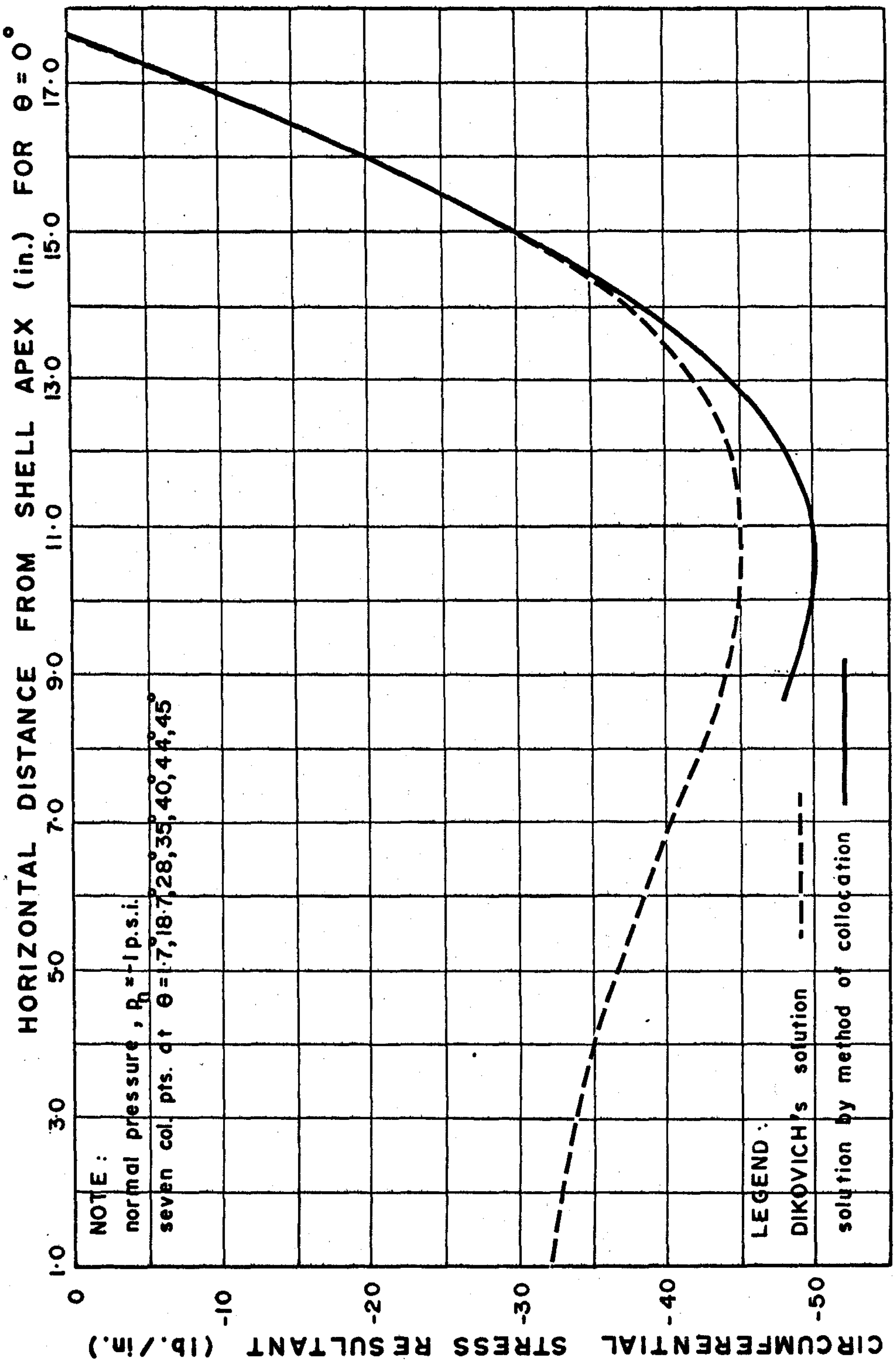

FIGURE 48

PLOT SHOWING THEORETICAL "$M_{r\theta}(\sigma)$"
for SHELL on RECTANGULAR BASE

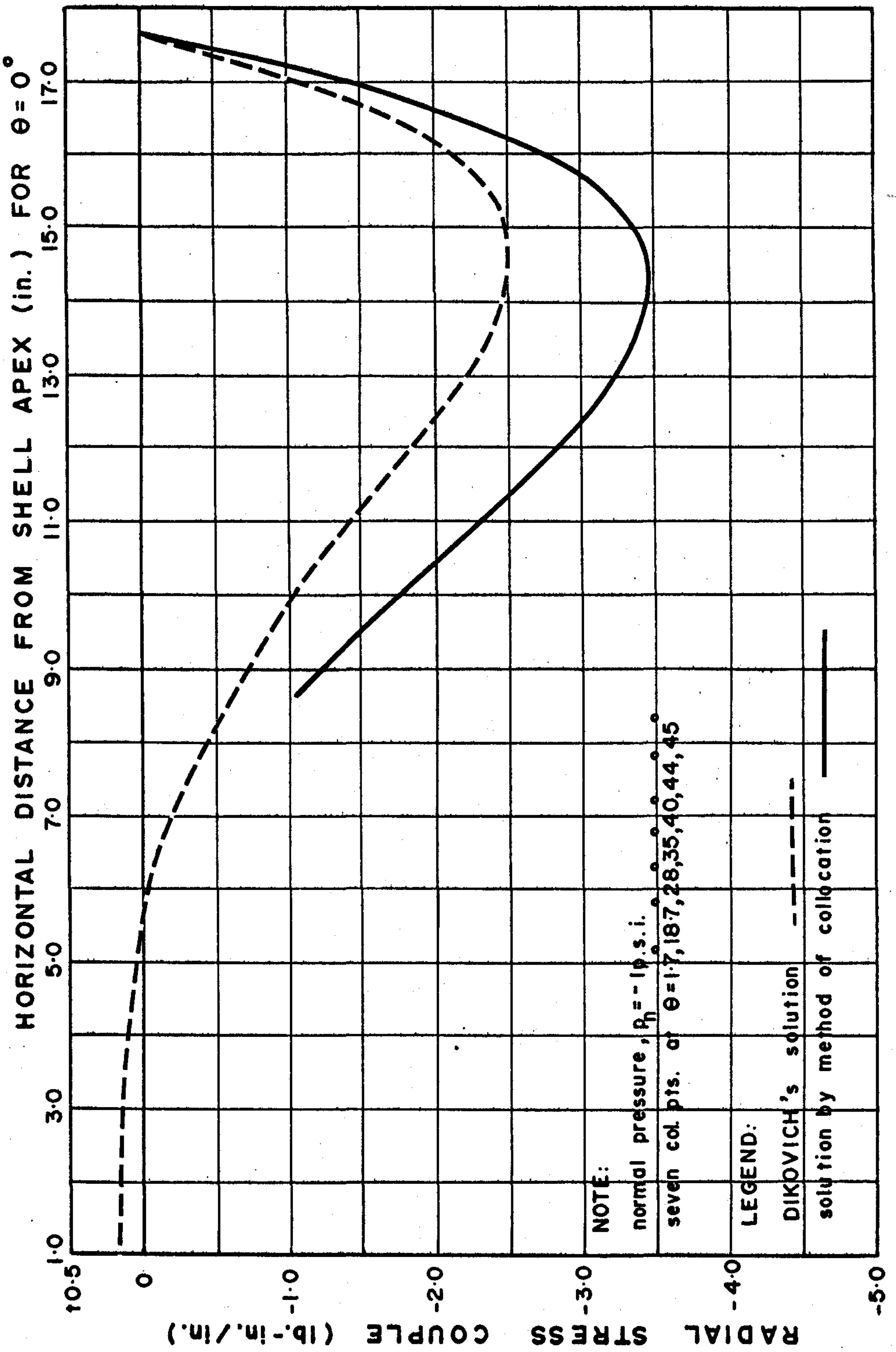

FIGURE 49

FIGURE 50

PLOT SHOWING THEORETICAL "$M_{\theta r}(\sigma)$" for SHELL on RECTANGULAR BASE

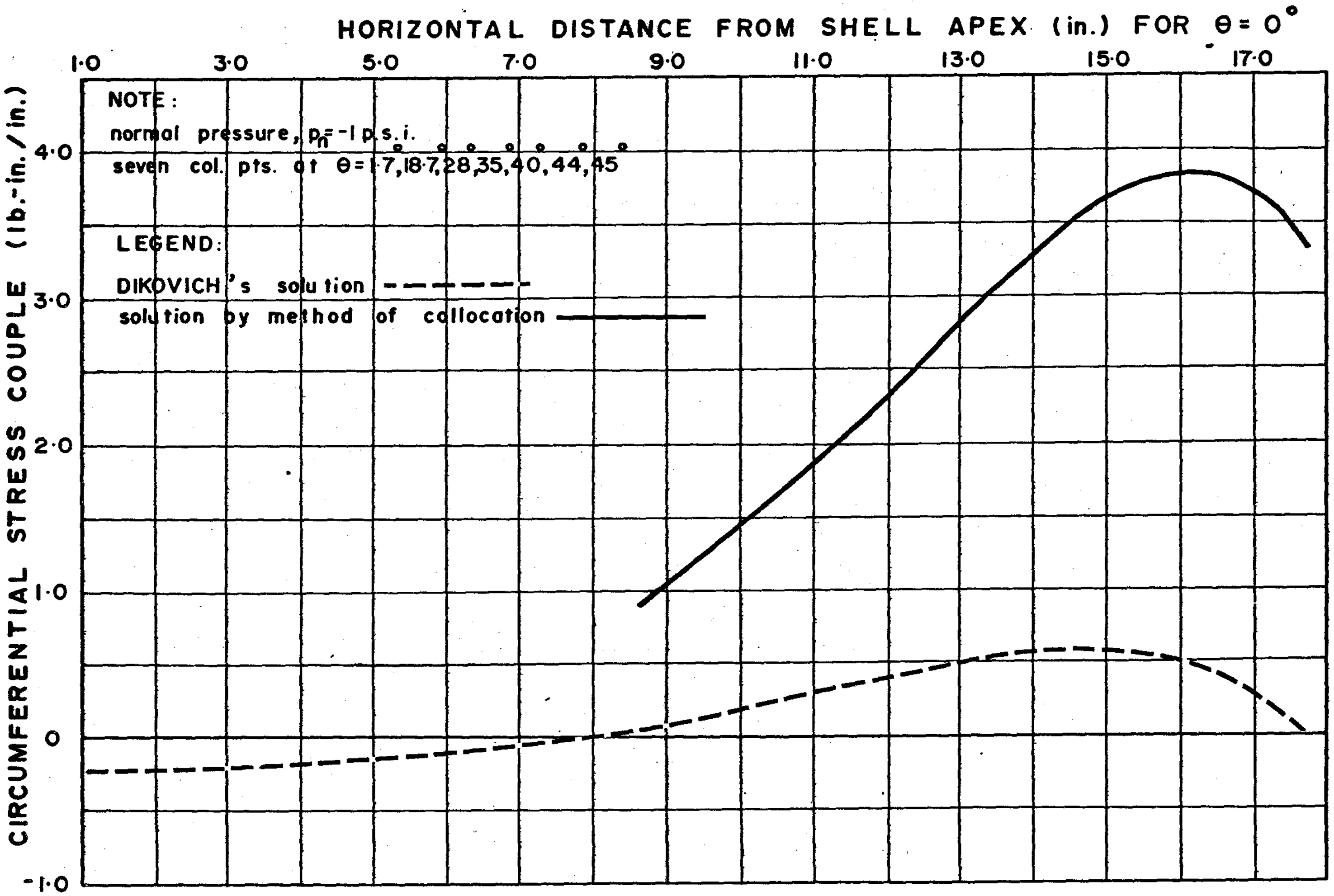

CHAPTER IV

SHELL ENCLOSING TRIANGULAR BASE

A solution by the collocation method is given for a shallow, thin, calotte shell of spherical middle surface enclosing a triangular base. Shells of this type have been constructed in practice. The shell which was solved had the same thickness, 0.375 inches, spherical middle surface radius, 64 inches, and base circle radius, 25 inches, as the shell enclosing an hexagonal base studied in CHAPTER II.

The boundary equations

$$\begin{aligned} \epsilon_{ss} &= 0 \\ M(\sigma)_{ns} &= 0 \\ u_n &= 0 \\ F(\sigma)_{nn} &= 0 \end{aligned} \qquad \text{(IV-1)}$$

were satisfied at all the collocation points except at the shell's corner where the normal boundary force, $F(\sigma)_{nn}$, was not assumed to be zero which is more in concert with the actual boundary condition of such shells. These boundary conditions would occur in practice if the shell's boundary was supported on a very narrow boundary diaphragm.

FIGURES 53 to 57 depict the values of the normal displacements and sectional resultants which were computed theoretically along the radial lines shown in FIGURE 51 by employing the seven collocation points shown in FIGURE 52.

The distributions of the normal displacements and the sectional resultants were consistent with the results given for the spherical shell enclosing an hexagonal base in FIGURES 12, 19, 26, 33 and 40 of CHAPTER II, even though the boundary conditions satisfied by both shells were not identical. The boundary condition $M(\sigma)_{ns} = 0$ used by the shell enclosing a triangular base was replaced by the condition

$$\delta\left(\frac{\partial u_n}{\partial n}\right) = 0.00055 \text{ radians}$$

for the solution of the shell enclosing an hexagonal base. Also the shell enclosing an hexagonal base assumed that it was the strain rather than the normal force which did not vanish at the corner collocation point. The magnitudes of the normal displacements and the sectional resultants became similar for both shells near their apex.

A solution for the shell enclosing a triangular base was attempted for ten boundary collocation points; however the results were inconsistent. This attempt supported the conclusion drawn in CHAPTER II which maintains that an increase in the number of boundary collocation points above seven, would likely decrease the number of significant figures in the increased number of requisite numerical computations below a "safe" level. An indication of the increase in the number of computations involved is given by the size of the N x N matrix of the boundary equation coefficients, where N=4L-1 and L represents the number of collocation points employed. For example, seven collocation points necessitate the solution of a 27 x 27 matrix while ten collocation points necessitate the solution of a 39 x 39 matrix.

In CHAPTER II a comparison of the degree of satisfaction of the boundary condition $u_n = 0$ for solutions, employing three and seven collocation points respectively, revealed a decrease in the number of significant figures in the computations from sixteen to six when double precision accuracy was used throughout. Logically then, the solution which satisfied ten boundary collocation points would require approximately 20 to 25 figure accuracy throughout its computations in order to yield reliable numerical results, provided that the same precautions outlined in CHAPTER II and APPENDIX B were taken.

Some questions were considered with regard to the reliability of the theoretical solution in which four boundary conditions must be satisfied at all the collocation points except one point where only three boundary conditions must be satisfied.

A solution for the shell enclosing a triangular base was attempted using the same seven boundary collocation points but assuming that the strain rather than the normal force did not vanish at the corner boundary point. The results, which were obtained by this solution, were almost identical to the results given in FIGURES 53 to 57, with the exception of minor variations near the boundary corner. This indicated that the non-homogeneous boundary collocation point does not affect the reliability of the solution for seven boundary collocation points. Obviously the perturbing effect of the non-homogeneous collocation point on the accuracy of the results would be greater when the solution employed fewer collocation points.

PLAN VIEW of SHELL on TRIANGULAR BASE SHOWING LOCATION of RADIAL LINES for which SECTIONAL RESULTANTS are CALCULATED

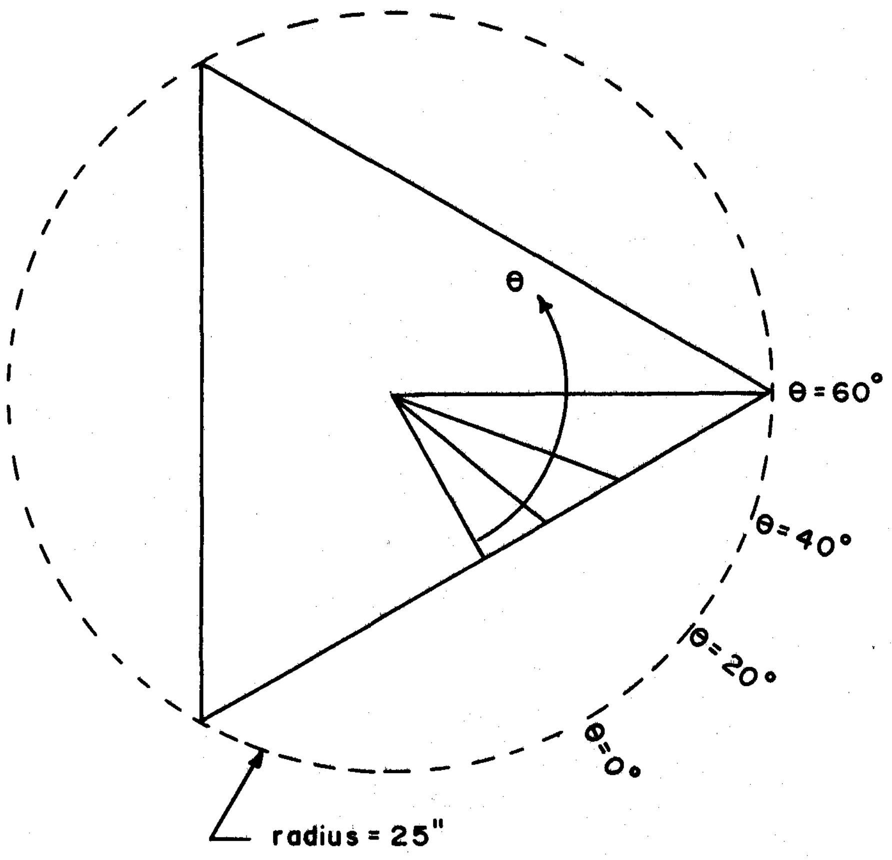

FIGURE 51

LOCATION of BOUNDARY COLLOCATION POINTS
for SHELL on TRIANGULAR BASE

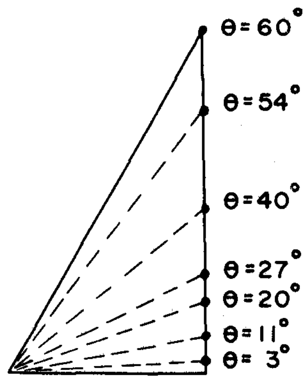

7 COLLOCATION POINTS

FIGURE 52

PLOT SHOWING THEORETICAL "U_n"
for SHELL on TRIANGULAR BASE

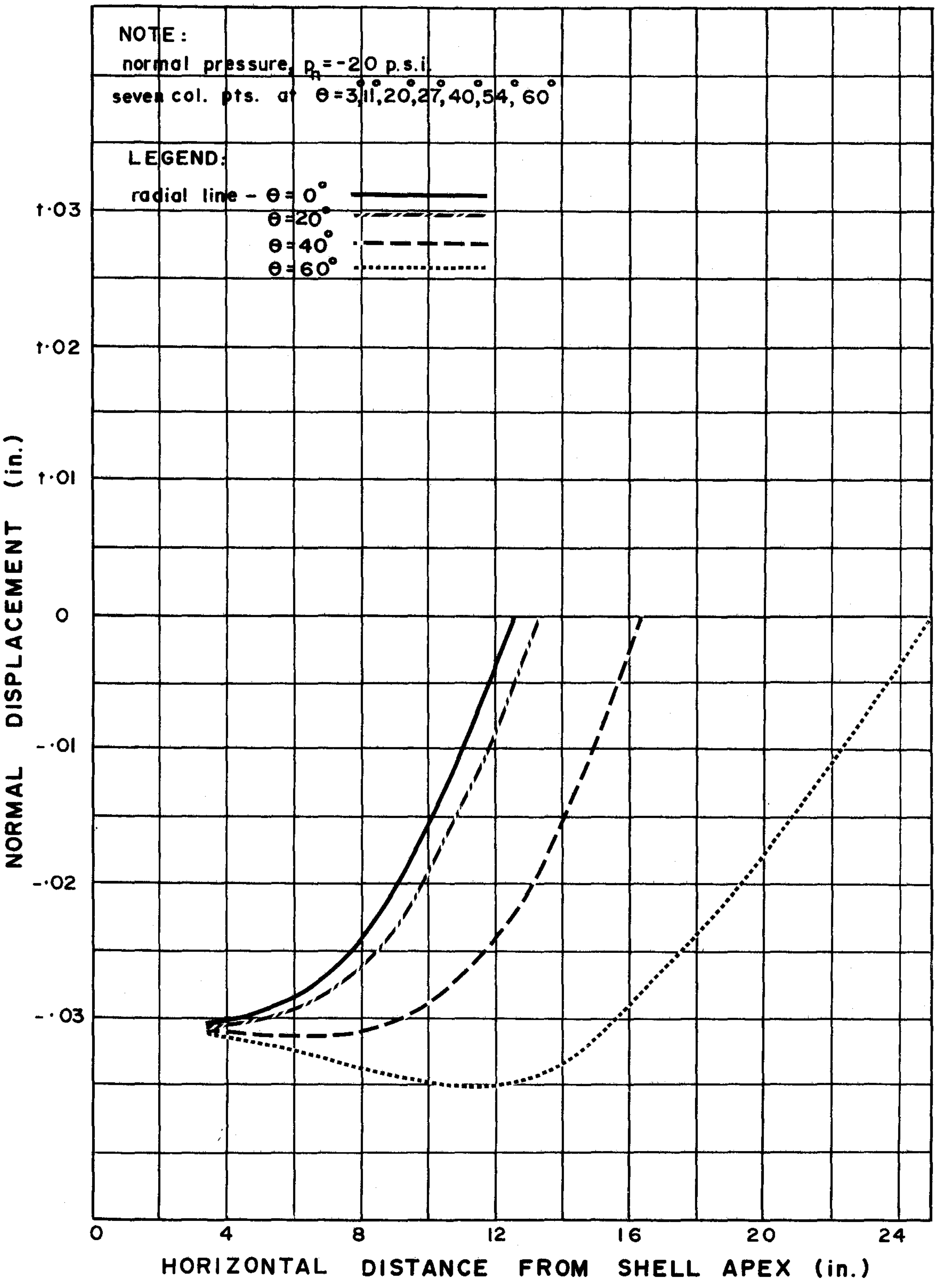

FIGURE 53

PLOT SHOWING THEORETICAL "$F_{rr}(\sigma)$" for SHELL on TRIANGULAR BASE

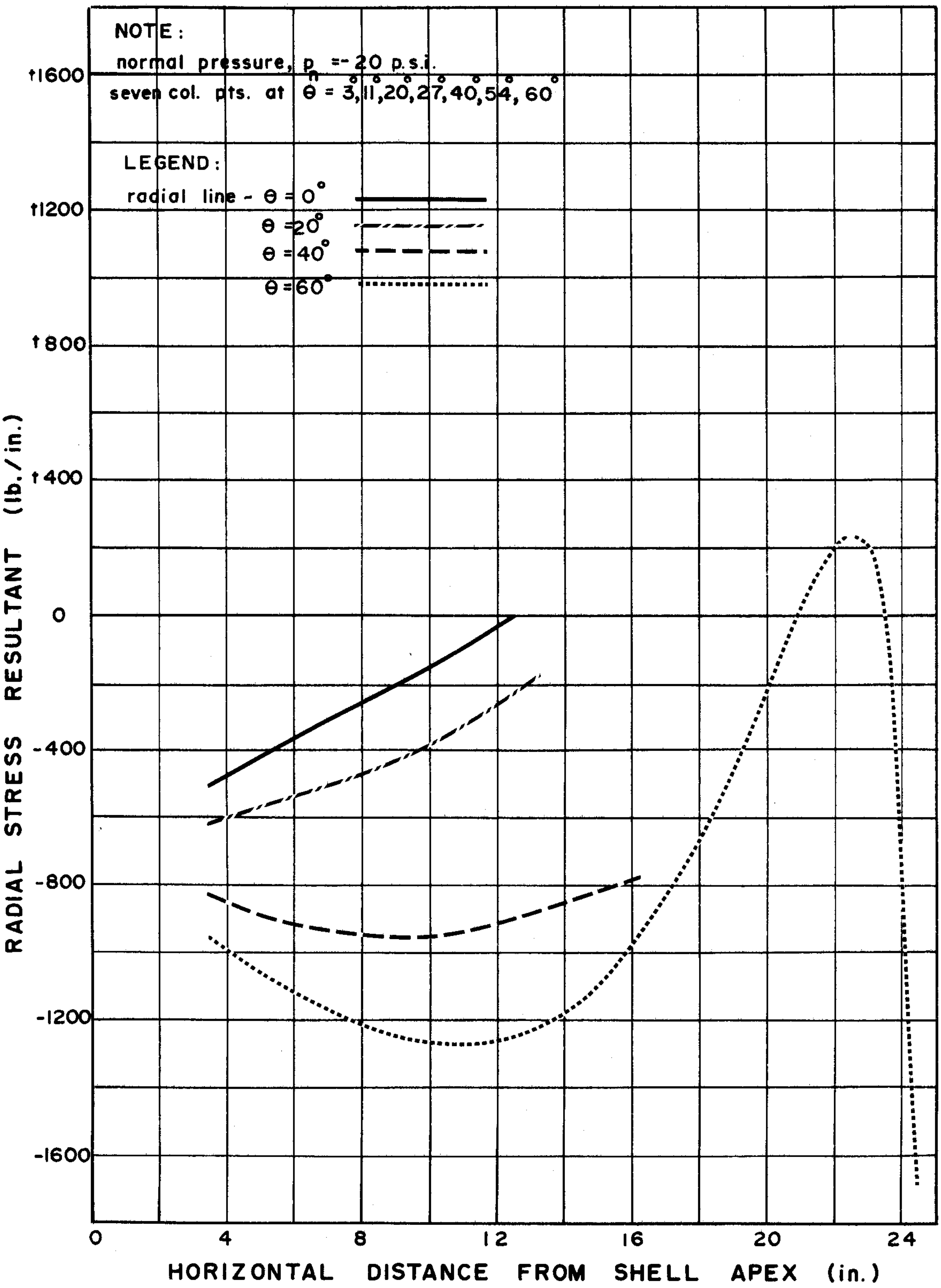

FIGURE 54

PLOT SHOWING THEORETICAL "$F_{\theta\theta}(\sigma)$"
for SHELL on TRIANGULAR BASE

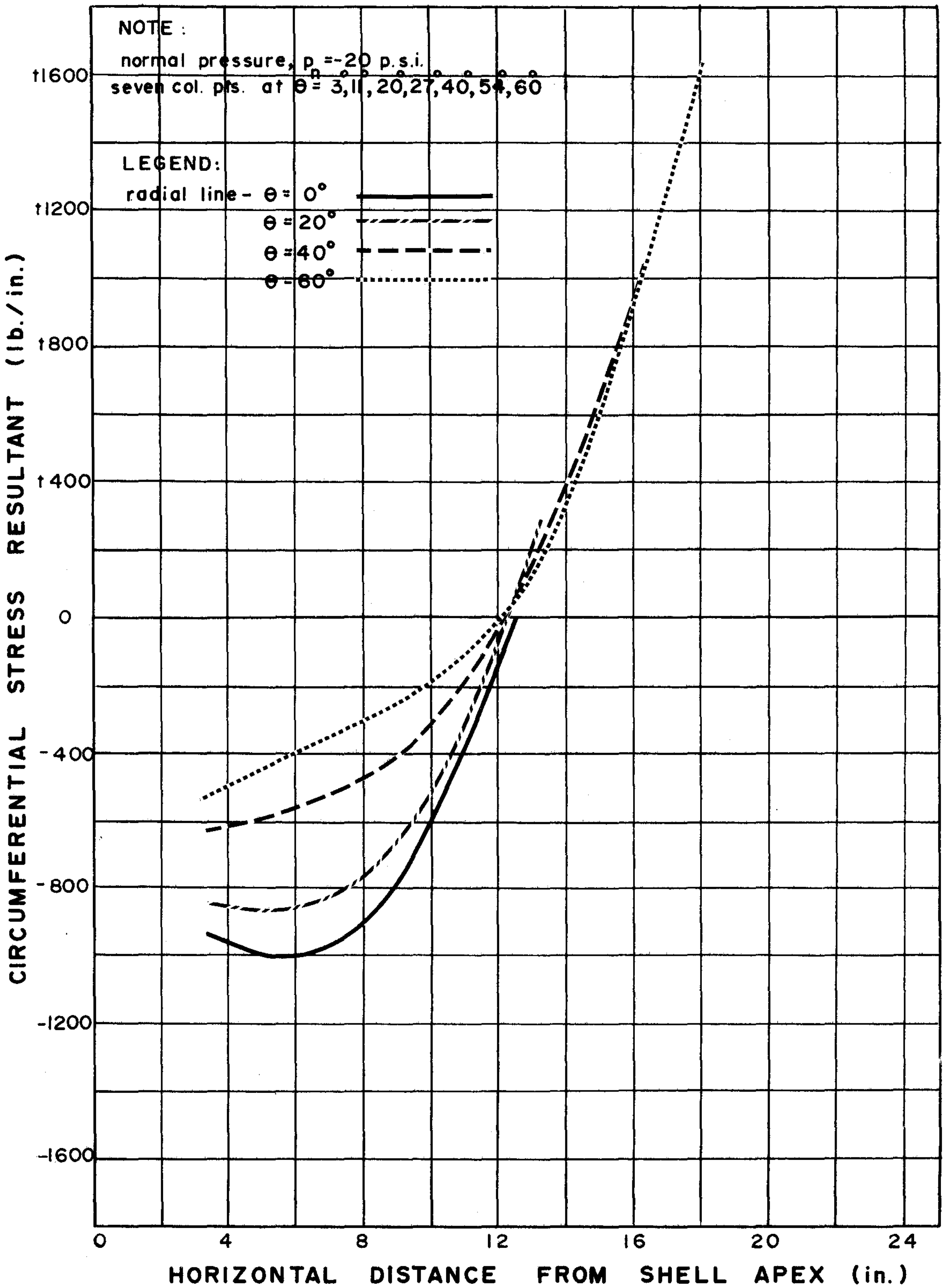

FIGURE 55

PLOT SHOWING THEORETICAL "$M_{r\theta}(\sigma)$"
for SHELL on TRIANGULAR BASE

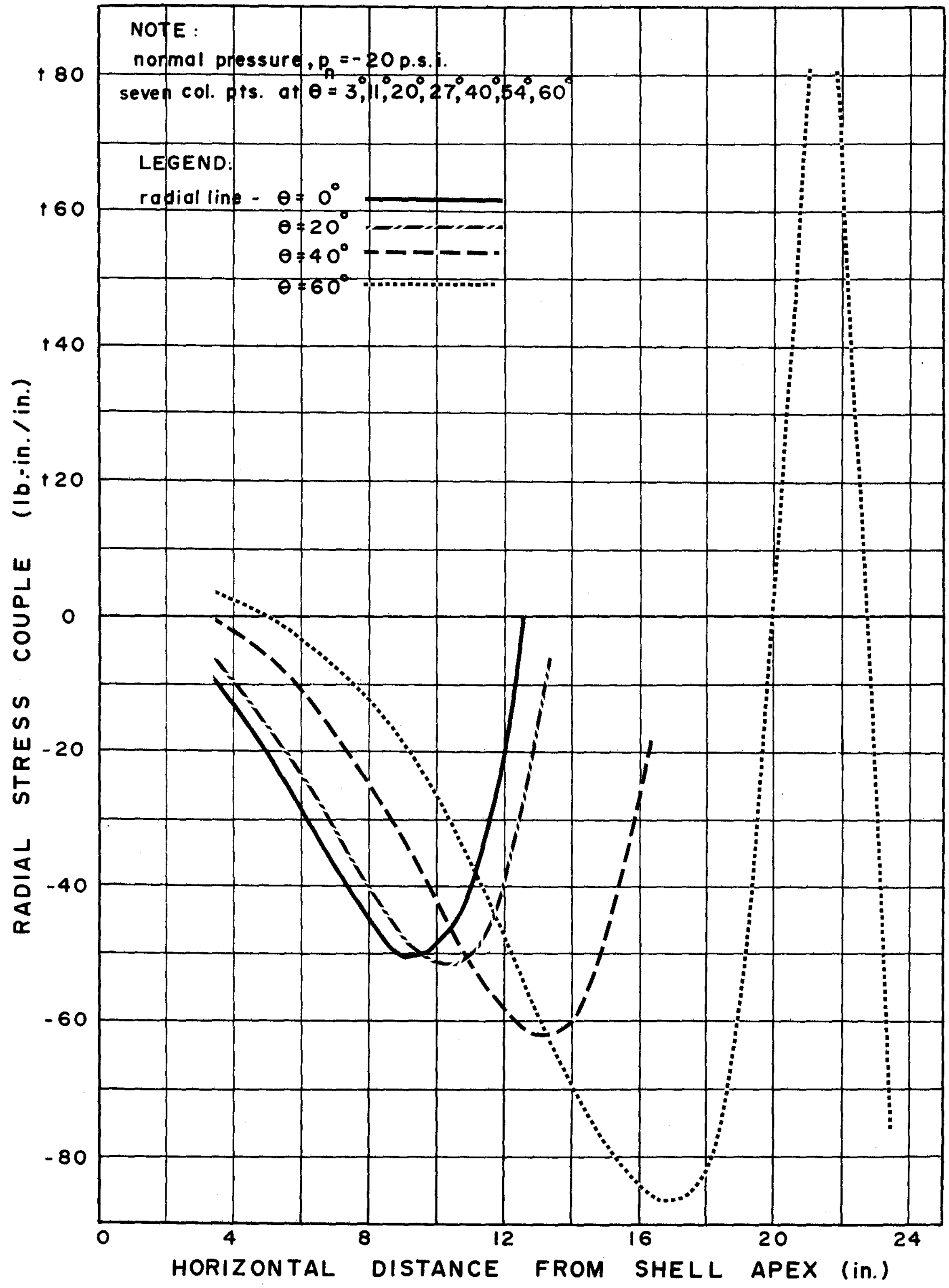

FIGURE 56

PLOT SHOWING THEORETICAL "$M_{\theta r}(\sigma)$"
for SHELL on TRIANGULAR BASE

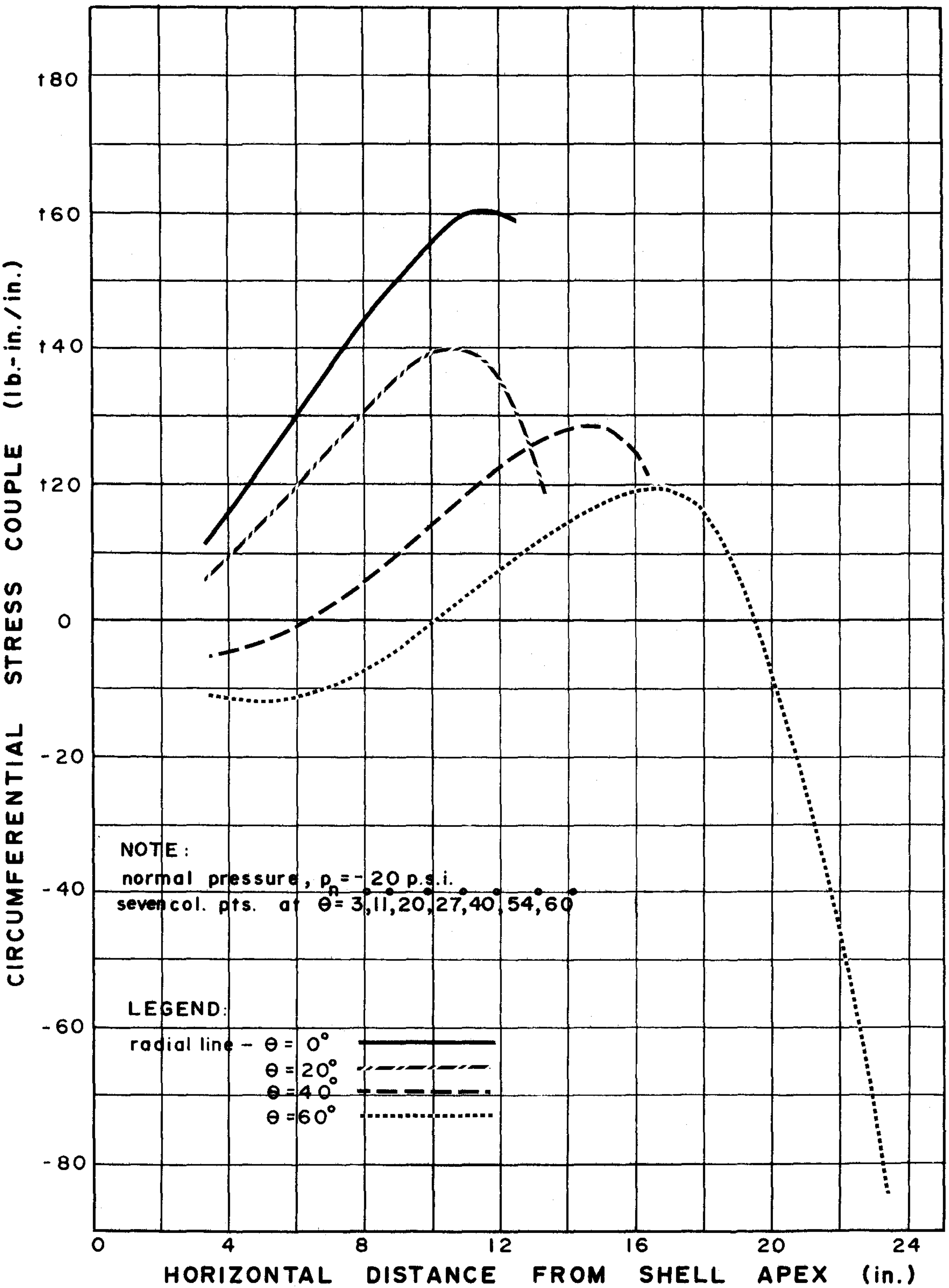

FIGURE 57

CHAPTER V

SUMMARY

The intent of this thesis was realized when it was substantiated that the approximate solution given by ORAVAS in 1957 for shallow, spherical, calotte shells enclosing polygonal base does indeed yield reliable results for the purposes of practical design.

The problems encountered in this collocative solution were largely numerical in nature as the computations tended to be very extensive and involved numbers which had widely varying orders of magnitude. Consequently the use of McMaster's I.B.M. 7040 computer was essential in the practical execution of the solution. Techniques had to be devised to overcome computer limitations and to maintain the greatest possible number of significant figures in all the computations.

The most detailed attempt to verify the reliability of the theoretical results was made in the comparison of the theoretical and experimental results obtained for a spherical shell enclosing an hexagonal base. The results were as compatible as could be expected since the experimental shell was naturally subject to physical limitations both in its construction as well as its boundary conditions. The experimental shell structure exhibited a considerable degree of unperiodicity in its deformation and, therefore, the experimental results can serve merely as an indication for the general nature of the structural behaviour of the shell.

Another attempt to verify the theoretical results was made for a spherical shell enclosing a rectangular base through a comparison with a solution given by DIKOVICH for a similar shell. The normal stress resultants were in satisfactory agreement in the two solutions even though slightly different boundary conditions were employed in the two methods. The normal displacement and stress couples in the collocation solution were markedly larger in magnitude.

A solution for a spherical shell enclosing a triangular base was included in the investigation since shells of this type have been constructed in practice.

The results for the three shells demonstrate that the periodic polygonal boundary of a spherical shell introduces periodic perturbations emanating from its nonrotationally symmetric boundary in the rotationally symmetrical solution. The extent of the penetration of these perturbations towards the shell's apex, where the rotationally symmetric solution associated with the zero order terms of the truncated series solution dominates, depends upon the degree by which the polygonal boundary deviates from the circular boundary of the rotational spherical shell enclosing the polygonal shell.

The consistency of the results for the three shells, which enclosed bases of differing periodic symmetries, indicates that the solution by the collocation method is consistent for all thin calotte shells which satisfy the conditions of shallowness. The discrete satisfaction of boundary conditions tends to accumulate larger magnitude errors near the corners of the polygonal calotte shell and, therefore, it is to be expected that the collocative solution deviates more from the actual solution in the neighbourhood of the corners of the shell.

Since the numerical solution is very sensitive to the degree of accuracy employed in the calculations, it is considered to be good practice to solve any shell using two independent sets of boundary collocation points in order to verify the consistency of the results. The accuracy employed in the theoretical computations of this investigation permitted the introduction of a maximum of seven boundary collocation points for one of the rotationally periodic segments of the shell. It is considered that this represents a sufficient number of boundary collocation points in order to provide reliable practical solutions for shells with as little as triple periodicity.

APPENDIX A

THEORY OF SHALLOW SHELLS

A detailed theoretical solution by the collocation method for a spherical calotte shell over a polygonal base was first given by ORAVAS in a paper of 1957 (1) which however contains a number of misprints. Consequently, it is necessary to give only a brief outline of the method and the correct relations used in the solution of the problem.

The stress resultant tensor

$$\bar{\bar{F}}(\sigma) = F_{11}(\sigma)\bar{e}_1\bar{e}_1 + F_{12}(\sigma)\bar{e}_1\bar{e}_2 + F_{1n}(\sigma)\bar{e}_1\bar{e}_n$$
$$+F_{21}(\sigma)\bar{e}_2\bar{e}_1 + F_{22}(\sigma)\bar{e}_2\bar{e}_2 + F_{2n}(\sigma)\bar{e}_2\bar{e}_n$$

and the stress couple tensor

$$\bar{\bar{M}}(\sigma) = M_{11}(\sigma)\bar{e}_1\bar{e}_1 + M_{12}(\sigma)\bar{e}_1\bar{e}_2$$
$$+M_{21}(\sigma)\bar{e}_2\bar{e}_1 + M_{22}(\sigma)\bar{e}_2\bar{e}_2$$

for shallow shells are related by the force and moment equilibrium equations. The expressions for $F_{1n}(\sigma)$ and $F_{2n}(\sigma)$ obtained from the moment equilibrium equations can be simplified using the first two kinematic compatibility equations. An auxiliary stress function F is introduced in order to satisfy the first two force equilibrium equations identically. Then the third force equilibrium equation becomes a fourth order differential equation in u_n and F. For shallow shells of spherical

VECTOR DIAGRAM SHOWING RELATION OF BOUNDARY COORDINATES n,s TO SHELL INTERIOR COORDINATES r, θ

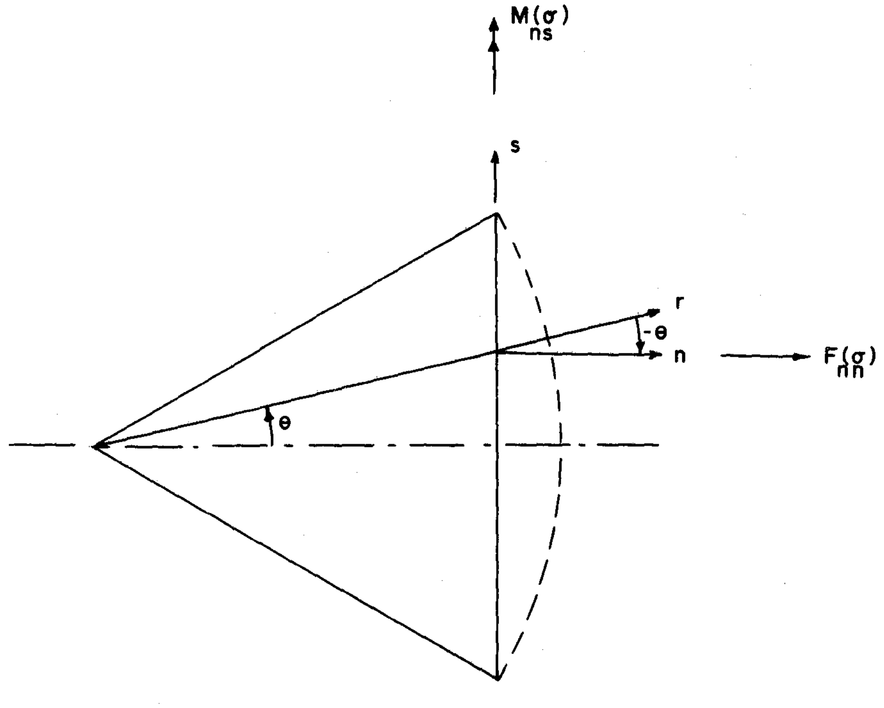

FIGURE 58

middle surface, this equation becomes

$$D\nabla^4 u_n + \frac{1}{R}\nabla^2 F = p_n \tag{A-1}$$

where

$D = Eh^3/12(1-\nu^2)$,

ν = POISSON's ratio,

$$\nabla^2 = \frac{d}{d\bar{r}_0} \cdot \frac{d}{d\bar{r}_0} = \frac{\partial^2}{\partial r^2} + \frac{1}{r}\frac{\partial}{\partial r} + \frac{1}{r^2}\frac{\partial^2}{\partial \theta^2}$$

and R = radius of curvature of the middle surface.

The third kinematic compatibility equation becomes the second fourth order differential equation in u_n and F and can be written as

$$\nabla^4 F - \frac{Eh}{R}\nabla^2 u_n = 0 \tag{A-2}$$

for shallow spherical shells.

These two fundamental fourth order differential equations (A-1) and (A-2) were given by MUSHTARI and VLASOV. MARGUERRE also gave similar shallow shell equations in 1939.

The solution of (A-1) and (A-2) under certain restrictions can be reduced to the solution of a set of three differential equations.

$$\nabla^2 [\nabla^2 - i\lambda^2] V_0 = \frac{p_n}{D} \tag{A-3}$$

$$[\nabla^2 - i\lambda^2]\nabla^2 V_1 = \nabla^2 V_1 = 0 \tag{A-4}$$

$$\nabla^2 V_2 - i\lambda^2 V_2 = 0 \tag{A-5}$$

where

$$V = u_n + i\omega F = V_0 + V_1 + V_2 \quad ,$$

$$\omega = \frac{\sqrt{12(1-\nu^2)}}{Eh^2} \quad ,$$

$$\lambda^2 = \frac{\sqrt{12(1-\nu^2)}}{Rh}$$

and V_0, V_1 and V_2 represent three linearly independent particular solutions.

Solution of (A-3), (A-4) and (A-5) yields the approximate normal displacement u_n and stress function F for a spherical shell of k-tuple symmetry. Since the shells which were investigated possessed no inner boundaries, terms containing $ker_n(x)$, $kei_n(x)$ and r^{-n} were omitted from the solution because of their singular nature at the origin. Finally the solution becomes:

$$u_n = \frac{p_n R^2}{Eh} + A_0^1 ber_0(\lambda r) + A_0^2 bei_0(\lambda r) + E_0^1 + \sum_{n=1}^{\infty}\Big[A_{kn}^1 ber_{kn}(\lambda r) + A_{kn}^2 bei_{kn}(\lambda r) + C_{kn}^1 r^{kn}\Big]\cos(kn\theta) \qquad \text{(A-6)}$$

$$F = \frac{p_n R r^2}{4} + \frac{1}{\omega}\Big\{A_0^1 bei_0(\lambda r) - A_0^2 ber_0(\lambda r) + E_0^2 + \sum_{n=1}^{\infty}\Big[A_{kn}^1 bei_{kn}(\lambda r) - A_{kn}^2 ber_{kn}(\lambda r) + C_{kn}^2 r^{kn}\Big]\cos(kn\theta)\Big\} \qquad \text{(A-7)}$$

Boundary Conditions

At the outer boundary TÖLKE's Boundary Collocation Procedure, introduced by TÖLKE in 1934 and employed in this work, restricts idealized boundary conditions to be satisfied only at discrete boundary points instead of along the entire length of the boundary. Five different boundary conditions were utilized in this investigation in which three distinct shallow calotte shells were studied.

These boundary conditions were given by ORAVAS in 1957 and are listed below:

1. Stress resultants normal to the boundary vanish:

$$F(\sigma)_{nn} = 0$$

2. The boundary undergoes no rotation:

$$\delta\left(\frac{\partial u_n}{\partial n}\right) = 0$$

3. The boundary undergoes no normal displacement:

$$u_n = 0$$

4. The boundary of the shell is fully restrained and consequently undergoes no linear strain:

$$\epsilon_{ss} = 0$$

5. The tangential stress couple vector vanishes along the boundary edge:

$$M(\sigma)_{ns} = 0$$

The boundary conditions 1 to 5 can be expressed in terms of the normal displacement u_n and stress resultant function F as :

$$A_o^1\Psi_1 + A_o^2\Psi_2 + \sum_{n=1}^{\infty}\left[A_{kn}^1\Psi_3 + A_{kn}^2\Psi_4 \qquad + C_{kn}^2\Psi_5\right] = \frac{-p_n R}{2} \tag{A- 8}$$

$$A_o^1\Psi_6 + A_o^2\Psi_7 + \sum_{n=1}^{\infty}\left[A_{kn}^1\Psi_8 + A_{kn}^2\Psi_9 + C_{kn}^1\Psi_{10} \qquad \right] = 0 \tag{A- 9}$$

$$A_o^1\Psi_{11} + A_o^2\Psi_{12} + E_o^1 + \sum_{n=1}^{\infty}\left[A_{kn}^1\Psi_{13} + A_{kn}^2\Psi_{14} + C_{kn}^1\Psi_{15} \qquad \right] = \frac{-p_n R^2}{Eh} \tag{A-10}$$

$$A_o^1\Psi_{16} + A_o^2\Psi_{17} + \sum_{n=1}^{\infty}\left[A_{kn}^1\Psi_{18} + A_{kn}^2\Psi_{19} \qquad + C_{kn}^2\Psi_{20}\right] = -(1-\nu)\frac{p_n R}{2} \tag{A-11}$$

$$A_o^1\Psi_{21} + A_o^2\Psi_{22} + \sum_{n=1}^{\infty}\left[A_{kn}^1\Psi_{23} + A_{kn}^2\Psi_{24} + C_{kn}^1\Psi_{25} \qquad \right] = 0 \tag{A-12}$$

The coefficients in the equations (A-8) to (A-12) are:

$$\Psi_1 = \frac{\lambda}{\omega\bar{r}}\,\mathrm{bei}_o'(\lambda\bar{r})\cos^2\bar{\theta} + \frac{\lambda^2}{\omega}\,\mathrm{bei}_o''(\lambda\bar{r})\sin^2\bar{\theta}$$

$$\Psi_2 = -\frac{\lambda}{\omega\bar{r}}\,\mathrm{ber}_o'(\lambda\bar{r})\cos^2\bar{\theta} + \frac{\lambda^2}{\omega}\,\mathrm{ber}_o''(\lambda\bar{r})\sin^2\bar{\theta}$$

$$\Psi_3 = \left\{\frac{\lambda}{\omega\bar{r}} \operatorname{bei}'_{kn}(\lambda\bar{r})\cos^2\bar{\theta} - \frac{(kn)^2}{\omega\bar{r}^2} \operatorname{bei}_{kn}(\lambda\bar{r})\cos^2\bar{\theta}\right.$$

$$\left. + \frac{\lambda^2}{\omega} \operatorname{bei}''_{kn}(\lambda\bar{r})\sin^2\bar{\theta}\right\} \cos(kn\bar{\theta})$$

$$+ \left\{\frac{kn}{\omega\bar{r}^2} \operatorname{bei}_{kn}(\lambda\bar{r})\sin 2\bar{\theta} - kn\left(\frac{\lambda}{\omega\bar{r}}\right)\operatorname{bei}'_{kn}(\lambda\bar{r})\sin 2\bar{\theta}\right\} \sin(kn\bar{\theta})$$

$$\Psi_4 = \left\{-\frac{\lambda}{\omega\bar{r}} \operatorname{ber}'_{kn}(\lambda\bar{r})\cos^2\bar{\theta} + \frac{(kn)^2}{\omega\bar{r}^2} \operatorname{ber}_{kn}(\lambda\bar{r})\cos^2\bar{\theta}\right.$$

$$\left. - \frac{\lambda^2}{\omega} \operatorname{ber}''_{kn}(\lambda\bar{r})\sin^2\bar{\theta}\right\} \cos(kn\bar{\theta})$$

$$+ \left\{-\frac{kn}{\omega\bar{r}^2} \operatorname{ber}_{kn}(\lambda\bar{r}) + \frac{\lambda kn}{\omega\bar{r}} \operatorname{ber}'_{kn}(\lambda\bar{r})\right\} \sin 2\bar{\theta} \quad \sin(kn\bar{\theta})$$

$$\Psi_5 = \frac{kn}{\omega}(kn-1)\,\bar{r}^{kn-2}\left[(\sin^2\bar{\theta} - \cos^2\bar{\theta})\cos(kn\bar{\theta}) - \sin 2\bar{\theta}\sin(kn\bar{\theta})\right]$$

$$\Psi_6 = -\lambda \operatorname{ber}'_0(\lambda\bar{r})\cos\bar{\theta}$$

$$\Psi_7 = -\lambda \operatorname{bei}'_0(\lambda\bar{r})\cos\bar{\theta}$$

$$\Psi_8 = -\left[\frac{kn}{\bar{r}} \operatorname{ber}_{kn} \sin\bar{\theta}\right]\sin(kn\bar{\theta}) - \left[\lambda \operatorname{ber}'_{kn}(\lambda\bar{r})\cos\bar{\theta}\right]\cos(kn\bar{\theta})$$

$$\Psi_9 = -\left[\frac{kn}{\bar{r}} \operatorname{bei}_{kn} \sin\bar{\theta}\right]\sin(kn\bar{\theta}) - \left[\lambda \operatorname{bei}'_{kn}(\lambda\bar{r})\cos\bar{\theta}\right]\cos(kn\bar{\theta})$$

$$\psi_{10} = -\left[kn\bar{r}^{kn-1}\sin\bar{\theta}\right]\sin(kn\bar{\theta}) - \left[kn\bar{r}^{kn-1}\cos\bar{\theta}\right]\cos(kn\bar{\theta})$$

$$\psi_{11} = \operatorname{ber}_{o}(\lambda\bar{r})$$

$$\psi_{12} = \operatorname{bei}_{o}(\lambda\bar{r})$$

$$\psi_{13} = \operatorname{ber}_{kn}(\lambda\bar{r})\cos(kn\bar{\theta})$$

$$\psi_{14} = \operatorname{bei}_{kn}(\lambda\bar{r})\cos(kn\bar{\theta})$$

$$\psi_{15} = \bar{r}^{kn}\cos(kn\bar{\theta})$$

$$\psi_{16} = \left[\frac{\lambda}{\omega\bar{r}}\operatorname{bei}_{o}'(\lambda\bar{r}) - \frac{\nu\lambda^2}{\omega}\operatorname{bei}_{o}''(\lambda\bar{r})\right]\sin^2\bar{\theta} + \left[\frac{\lambda^2}{\omega}\operatorname{bei}_{o}''(\lambda\bar{r}) - \frac{\nu\lambda}{\omega\bar{r}}\operatorname{bei}_{o}'(\lambda\bar{r})\right]\cos^2\bar{\theta}$$

$$\psi_{17} = \left[-\frac{\lambda}{\omega\bar{r}}\operatorname{ber}_{o}'(\lambda\bar{r}) + \frac{\nu\lambda^2}{\omega}\operatorname{ber}_{o}''(\lambda\bar{r})\right]\sin^2\bar{\theta} + \left[-\frac{\lambda^2}{\omega}\operatorname{ber}_{o}''(\lambda\bar{r}) + \frac{\nu\lambda}{\omega\bar{r}}\operatorname{ber}_{o}'(\lambda\bar{r})\right]\cos^2\bar{\theta}$$

$$\psi_{18} = \left\{\left[\frac{\lambda}{\omega\bar{r}}\operatorname{bei}_{kn}'(\lambda\bar{r}) - \frac{1}{\omega}\left(\frac{kn}{\bar{r}}\right)^2\operatorname{bei}_{kn}(\lambda\bar{r}) - \frac{\nu\lambda^2}{\omega}\operatorname{bei}_{kn}''(\lambda\bar{r})\right]\sin^2\bar{\theta}\right.$$

$$\left. + \left[-\frac{\nu\lambda}{\omega\bar{r}}\operatorname{bei}_{kn}'(\lambda\bar{r}) + \frac{\nu}{\omega}\left(\frac{kn}{\bar{r}}\right)^2\operatorname{bei}_{kn}(\lambda\bar{r}) + \frac{\lambda^2}{\omega}\operatorname{bei}_{kn}''(\lambda\bar{r})\right]\cos^2\bar{\theta}\right\}\cos(kn\bar{\theta})$$

$$+ \left\{(1+\nu)\frac{kn}{\omega}\left[\frac{\lambda}{\bar{r}}\operatorname{bei}_{kn}'(\lambda\bar{r}) - \frac{1}{\bar{r}^2}\operatorname{bei}_{kn}(\lambda\bar{r})\right]\sin 2\bar{\theta}\right\}\sin(kn\bar{\theta})$$

$$\Psi_{19} = \Big\{\Big[-\tfrac{\lambda}{\omega\bar{r}}\,\mathrm{ber}'_{kn}(\lambda\bar{r}) + \tfrac{1}{\omega}\Big(\tfrac{kn}{\bar{r}}\Big)^2 \mathrm{ber}_{kn}(\lambda\bar{r}) + \tfrac{\nu\lambda^2}{\omega}\,\mathrm{ber}''_{kn}(\lambda\bar{r})\Big]\sin^2\bar{\theta}$$

$$+\Big[\tfrac{\nu\lambda}{\omega\bar{r}}\,\mathrm{ber}'_{kn}(\lambda\bar{r}) - \tfrac{\nu}{\omega}\Big(\tfrac{kn}{\bar{r}}\Big)^2 \mathrm{ber}_{kn}(\lambda\bar{r}) - \tfrac{\lambda^2}{\omega}\,\mathrm{ber}''_{kn}(\lambda\bar{r})\Big]\cos^2\bar{\theta}\Big\}\cos(kn\bar{\theta})$$

$$+\Big\{(1+\nu)\tfrac{kn}{\omega}\Big[\tfrac{1}{\bar{r}^2}\,\mathrm{ber}_{kn}(\lambda\bar{r}) - \tfrac{\lambda}{\bar{r}}\,\mathrm{ber}'_{kn}(\lambda\bar{r})\Big]\sin 2\bar{\theta}\Big\}\sin(kn\,\bar{\theta})$$

$$\Psi_{20} = \tfrac{1+\nu}{\omega}\,kn(kn-1)\,\bar{r}^{\,kn-2}\Big\{\Big[\cos^2\bar{\theta} - \sin^2\bar{\theta}\Big]\cos(kn\,\bar{\theta}) + \sin 2\bar{\theta}\,\sin(kn\,\bar{\theta})\Big\}$$

$$\Psi_{21} = \Big[\lambda^2\,\mathrm{ber}''_0(\lambda\bar{r}) + \tfrac{\nu\lambda}{\bar{r}}\,\mathrm{ber}'_0(\lambda\bar{r})\Big]\cos^2\bar{\theta}$$

$$+\Big[\tfrac{\lambda}{\bar{r}}\,\mathrm{ber}'_0(\lambda\bar{r}) + \nu\lambda^2\,\mathrm{ber}''_0(\lambda\bar{r})\Big]\sin^2\bar{\theta}$$

$$\Psi_{22} = \Big[\lambda^2\,\mathrm{bei}''_0(\lambda\bar{r}) + \tfrac{\nu\lambda}{\bar{r}}\,\mathrm{bei}'_0(\lambda\bar{r})\Big]\cos^2\bar{\theta}$$

$$+\Big[\tfrac{\lambda}{\bar{r}}\,\mathrm{bei}'_0(\lambda\bar{r}) + \nu\lambda^2\,\mathrm{bei}''_0(\lambda\bar{r})\Big]\sin^2\bar{\theta}$$

$$\Psi_{23} = \Big\{\Big[\lambda^2\,\mathrm{ber}''_{kn}(\lambda\bar{r}) - \nu\Big(\tfrac{kn}{\bar{r}}\Big)^2\mathrm{ber}_{kn}(\lambda\bar{r}) + \tfrac{\nu\lambda}{\bar{r}}\,\mathrm{ber}'_{kn}(\lambda\bar{r})\Big]\cos^2\bar{\theta}$$

$$+\Big[-\tfrac{(kn)^2}{\bar{r}^2}\,\mathrm{ber}_{kn}(\lambda\bar{r}) + \tfrac{\lambda}{\bar{r}}\,\mathrm{ber}'_{kn}(\lambda\bar{r}) + \nu\lambda^2\,\mathrm{ber}''_{kn}(\lambda\bar{r})\Big]\sin^2\bar{\theta}\Big\}\cos(kn\,\bar{\theta})$$

$$+\Big\{\tfrac{kn}{\bar{r}}(1-\nu)\Big[\lambda\,\mathrm{ber}'_{kn}(\lambda\bar{r}) - \tfrac{1}{\bar{r}}\,\mathrm{ber}_{kn}(\lambda\bar{r})\Big]\sin 2\bar{\theta}\Big\}\sin(kn\,\bar{\theta})$$

$$\Psi_{24} = \left\{\left[\lambda^2 \mathrm{bei}''_{kn}(\lambda\bar{r}) - \nu\left(\frac{kn}{\bar{r}}\right)^2 \mathrm{bei}_{kn}(\lambda\bar{r}) + \frac{2\lambda}{\bar{r}} \mathrm{bei}'_{kn}(\lambda\bar{r})\right]\cos^2\bar{\theta}\right.$$

$$+\left[-\frac{(kn)^2}{\bar{r}^2} \mathrm{bei}_{kn}(\lambda\bar{r}) + \frac{\lambda}{\bar{r}} \mathrm{bei}'_{kn}(\lambda\bar{r}) + \nu\lambda^2 \mathrm{bei}''_{kn}(\lambda\bar{r})\right]\sin^2\bar{\theta}\left.\right\}\cos(kn\,\bar{\theta})$$

$$+\left\{\frac{kn}{\bar{r}}(1-\nu)\left[\lambda\,\mathrm{bei}'_{kn}(\lambda\bar{r}) - \frac{1}{\bar{r}}\,\mathrm{bei}_{kn}(\lambda\bar{r})\right]\sin 2\bar{\theta}\right\}\sin(kn\,\bar{\theta})$$

$$\Psi_{25} = kn(kn-1)(1-\nu)\bar{r}^{\,kn-2}\left[\sin 2\bar{\theta}\ \sin(kn\bar{\theta}) + (2\cos^2\bar{\theta}-1)\cos(kn\bar{\theta})\right]$$

where $\bar{r}$, $\bar{\theta}$ are the coordinates of collocation points.

Simplified expressions for the stress resultants and stress couples can be obtained by utilizing stress-strain, moment-curvature, strain-displacement and curvature-displacement relations and by enforcing the condition

$$u_n \gg u_1\,,\ u_2$$

wherever it is expedient for simplification purposes:

$$F_{\theta\theta}^{(\sigma)} = \frac{\partial^2 F}{\partial r^2}$$

$$F_{rr}^{(\sigma)} = \frac{1}{r}\frac{\partial F}{\partial r} + \frac{1}{r^2}\frac{\partial^2 F}{\partial \theta^2} \qquad \text{(A-13)}$$

$$F_{r\theta}^{(\sigma)} = F_{\theta r}^{(\sigma)} = -\frac{\partial}{\partial r}\left(\frac{1}{r}\frac{\partial F}{\partial \theta}\right)$$

and

$$M_{r\theta}^{(\sigma)} = -D\left[\frac{\partial^2 u_n}{\partial r^2} + \nu\left(\frac{1}{r^2}\frac{\partial^2 u_n}{\partial \theta^2} + \frac{1}{r}\frac{\partial u_n}{\partial r}\right)\right]$$

$$M_{\theta r}^{(\sigma)} = D\left[\frac{1}{r^2}\frac{\partial^2 u_n}{\partial \theta^2} + \frac{1}{r}\frac{\partial u_n}{\partial r} + \nu\frac{\partial^2 u_n}{\partial r^2}\right] \qquad \text{(A-14)}$$

$$M_{rr}^{(\sigma)} = -M_{\theta\theta}^{(\sigma)} = \frac{\mu h^3}{6}\left[\frac{\partial}{\partial r}\left(\frac{1}{r}\frac{\partial u_n}{\partial \theta}\right)\right]$$

Substitution of the expressions for u_n from (A-6) and F from (A-7) in (A-13) and (A-14) yields the sectional resultants :

$$F_{rr}(\sigma) = \frac{p_n R}{2} + A_0^1\left[\frac{\lambda}{\omega r}\mathrm{bei}_0'(\lambda r)\right] + A_0^2\left[-\frac{\lambda}{\omega r}\mathrm{ber}_0'(\lambda r)\right]$$

$$+\sum_{n=1}^{\infty}\Big\{A_{\kappa n}^1\left[\frac{\lambda}{\omega r}\mathrm{bei}_{\kappa n}'(\lambda r) - \frac{1}{\omega}\left(\frac{\kappa n}{r}\right)^2\mathrm{bei}_{\kappa n}(\lambda r)\right]$$

$$+A_{\kappa n}^2\left[-\frac{\lambda}{\omega r}\mathrm{ber}_{\kappa n}'(\lambda r) + \frac{1}{\omega}\left(\frac{\kappa n}{r}\right)^2\mathrm{ber}_{\kappa n}(\lambda r)\right]$$

$$-C_{\kappa n}^2\frac{\kappa n(\kappa n-1)}{\omega}r^{\kappa n-2}\Big\}\cos(\kappa n\theta)$$

$$F_{\theta\theta}(\sigma) = \frac{p_n R}{2} + A_0^1\left[\frac{\lambda^2}{\omega}\mathrm{bei}_0''(\lambda r)\right] + A_0^2\left[-\frac{\lambda^2}{\omega}\mathrm{ber}_0''(\lambda r)\right]$$

$$+\sum_{n=1}^{\infty}\left\{A_{kn}^1\left[\frac{\lambda^2}{\omega}\mathrm{bei}_{kn}''(\lambda r)\right] + A_{kn}^2\left[-\frac{\lambda^2}{\omega}\mathrm{ber}_{kn}''(\lambda r)\right]\right.$$

$$\left.+C_{kn}^2\left[\frac{kn}{\omega}(kn-1)r^{kn-2}\right]\right\}\cos(kn\theta)$$

$$M_{r\theta}(\sigma) = D\Big[A_0^1\left[-\lambda^2\mathrm{ber}_0''(\lambda r) - \frac{\nu}{r}\lambda\,\mathrm{ber}_0'(\lambda r)\right]$$

$$+A_0^2\left[-\lambda^2\mathrm{bei}_0''(\lambda r) - \frac{\nu}{r}\lambda\,\mathrm{bei}_0'(\lambda r)\right]$$

$$+\sum_{n=1}^{\infty}\left\{A_{kn}^1\left[-\lambda^2\mathrm{ber}_{kn}''(\lambda r) + \nu\left(\frac{kn}{r}\right)^2\mathrm{ber}_{kn}(\lambda r) - \frac{\nu}{r}\lambda\,\mathrm{ber}_{kn}'(\lambda r)\right]\right.$$

$$+A_{kn}^2\left[-\lambda^2\mathrm{bei}_{kn}''(\lambda r) + \nu\left(\frac{kn}{r}\right)^2\mathrm{bei}_{kn}(\lambda r) - \frac{\nu}{r}\lambda\,\mathrm{bei}_{kn}'(\lambda r)\right]$$

$$\left.+C_{kn}^1\left[-kn(kn-1)(1-\nu)r^{kn-2}\right]\right\}\cos(kn\theta)\Big]$$

$$M_{\theta r}(\sigma)=D\Big[A_0^1\Big[\tfrac{\lambda}{r}\,ber_0'(\lambda r)+\nu\lambda^2\,ber_0''(\lambda r)\Big]$$

$$+A_0^2\Big[\tfrac{\lambda}{r}\,bei_0'(\lambda r)+\nu\lambda^2\,bei_0''(\lambda r)\Big]$$

$$+\sum_{n=1}^{\infty}\Big\{A_{kn}^1\Big[-\left(\tfrac{kn}{r}\right)^2 ber_{kn}(\lambda r)+\tfrac{\lambda}{r}\,ber_{kn}'(\lambda r)+\nu\lambda^2\,ber_{kn}''(\lambda r)\Big]$$

$$+A_{kn}^2\Big[-\left(\tfrac{kn}{r}\right)^2 bei_{kn}(\lambda r)+\tfrac{\lambda}{r}\,bei_{kn}'(\lambda r)+\nu\lambda^2\,bei_{kn}''(\lambda r)\Big]$$

$$+C_{kn}^1\Big[-kn(kn-1)(1-\nu)\,r^{kn-2}\Big]\Big\}\cos(kn\theta)\Big]$$

First derivatives of KELVIN functions of kn-th order with respect to λr can be expressed by

$$ber_{kn}'(\lambda r) = -\tfrac{1}{\sqrt{2}}\Big[ber_{kn-1}(\lambda r)+bei_{kn-1}(\lambda r)\Big]-\Big[kn\;ber_{kn}(\lambda r)\Big]$$

$$bei_{kn}'(\lambda r) = \tfrac{1}{\sqrt{2}}\Big[ber_{kn-1}(\lambda r)-bei_{kn-1}(\lambda r)\Big]-\Big[kn\;bei_{kn}(\lambda r)\Big].$$

Second derivatives of KELVIN functions of kn-th order with respect to λr can be expressed by

$$ber_{kn}''(\lambda r) = -\tfrac{1}{\lambda r}ber_{kn}'(\lambda r)+\left(\tfrac{kn}{\lambda r}\right)^2 ber_{kn}(\lambda r)-bei_{kn}(\lambda r)$$

$$bei_{kn}''(\lambda r) = -\tfrac{1}{\lambda r}bei_{kn}'(\lambda r)+\left(\tfrac{kn}{\lambda r}\right)^2 bei_{kn}(\lambda r)+ber_{kn}(\lambda r).$$

APPENDIX B

KELVIN FUNCTIONS

One of the differential equations arising in the theoretical solution of shallow, elastic, spherical shells subjected to isothermal deformation is the modified BESSEL equation

$$z^2 \frac{d^2y}{dz^2} + z\frac{dy}{dz} + \left[i^2(z)^2 - n^2\right]y = 0$$

where $n = 0,1,2,\ldots$.

The standard solution of this BESSEL equation is

$$y = Z_n\left[i(z)\right] = A_n J_n\left[i(z)\right] + B_n Y_n\left[i(z)\right]$$

where

J_n is the standardized n-th order BESSEL function of the first kind,

Y_n is the standardized n-th order BESSEL function of the second kind

and A_n and B_n are complex constants.

See the book by FARRELL and ROSS of 1963.

This solution can also be written in the form

$$y = C_n I_n(z) + D_n K_n(z)$$

where

I_n is the standardized modified n-th order BESSEL function of the first kind,

K_n is the standardized modified n-th order BESSEL function of the second kind,

the complex constants

$$C_n = i^n A_n - i^{n-1} B_n$$

and $$D_n = \frac{2}{\pi} i^{-(n+2)} B_n$$

See the McLACHLAN text of 1955.

Substitution for $z = \sqrt{i}\,\lambda r$ yields

$$y = E_n[\mathrm{ber}_n(\lambda r) + i\,\mathrm{bei}_n(\lambda r)] + G_n[\mathrm{ker}_n(\lambda r) + i\,\mathrm{kei}_n(\lambda r)]$$

where

$\mathrm{ber}_n(\lambda r)$ and $\mathrm{bei}_n(\lambda r)$ are KELVIN functions of n-th order of the first kind,

$\mathrm{ker}_n(\lambda r)$ and $\mathrm{kei}_n(\lambda r)$ are KELVIN functions of n-th order of the second kind,

the complex constants

$$E_n = i^{-n} C_n = A_n - i^{-1} B_n$$

and $$G_n = i^n D_n = \frac{2}{\pi} i^{-2} B_n .$$

The shells under investigation possess no inner boundary, hence KELVIN functions of the second kind, $\mathrm{ker}_n(\lambda r)$

and $kei_n(\lambda r)$ which pertain to the inner boundary effect, are not pertinent. Therefore the solution germane to the shell problems investigated becomes

$$y = E_n\left[ber_n(\lambda r) + i\,bei_n(\lambda r)\right] \quad . \tag{B-1}$$

The most facile method to procure KELVIN functions of the first kind for any order n is to employ the "Backward Recurrence Technique" devised by J.C.P. MILLER and outlined by MICHELS in 1964.

Backward Recurrence Technique

KELVIN functions of the first kind f_n decrease rapidly in order of magnitude with their increasing order n. Forward recurrence techniques result in a loss of one significant figure in f_{n+1} when it is computed from f_n for each power of ten of the ratio f_n / f_{n+1} . Consequently it is exceedingly difficult to obtain accurate higher order KELVIN functions of the first kind from computed lower order functions by means of forward recurrence techniques.

MILLER devised a scheme of Backward Recurrence by which the number of significant figures in the calculated functions would actually increase with each successive application of the recurrence relation. The standardized

BESSEL functions J_n, Y_n as well as the standardized modified BESSEL functions I_n, K_n obey the recurrence relation

$$F_{n+1}(z) + F_{n-1}(z) = \frac{2n}{z} F_n(z) \qquad \text{(B-2)}$$

where $F_n^{(z)}$ represents a series of functions of argument z.

The collocation solution is concerned only with the modified BESSEL function $I_n(z)$. Since both $I_n(z)$ and $F_n(z)$ satisfy equation (B-2), a linear relationship between the two functions,

$$F_n(z) = \alpha I_n(z) \qquad \text{(B-3)}$$

where α represents a complex constant, exists.

For any known value of the complex constant α, the modified BESSEL function $I_n(z)$ can be calculated for any particular order n for which the function $F_n(z)$ has been computed.

Since $F_n(z)$ is a linear function of $I_n(z)$, its magnitude also decreases with increasing order n. Hence, computing $F_n(z)$ by means of a backward recurrence relation starting at some arbitrary order n = m, gives increasing accuracy for each successive recurrence computation.

MICHELS states that for single precision computation routine (eight figure accuracy) it is safe to start the backward recurrence at some order n = m, such that the ratio of the value of the BESSEL function at which the recurrence was begun to the value of the BESSEL function of order h, where h is the highest functional order required in the solution, should satisfy

$$\frac{I_m(z)}{I_h(z)} < 10^{-5}$$

This ratio should be even smaller to obtain double precision accuracy (17 figure accuracy) in $I_n(z)$.

Since $F_n(z)$ is an arbitrary functional-series governed only by the recurrence relation (B-2), it can be determined numerically by assigning arbitrary values to two successive terms, F_n and F_{n+1}, such that $|F_n| > |F_{n+1}|$. Starting the backward recurrence at some order n = m - 1 and using

$$F_m(z) = 0$$

$$F_{m-1}(z) = a$$

where "a" is any arbitrary real constant, the recurrence relation (B-2) yields :

$$F_{m-2}(z) = \frac{2a}{z}(m-1)$$

$$F_{m-3}(z) = a\left[\frac{4(m-1)(m-2)}{z^2} - 1\right]$$

$$F_{m-4}(z) = a\left[\frac{8(m-1)(m-2)(m-3)}{z^3} - \frac{2(m-3)}{z} - \frac{2(m-1)}{z}\right]$$

. . .

The backward recurrence is repeated until the functional-series F_n has been calculated for all orders n, ranging from n = 0 to n = m.

The constant α may be calculated from equation (B-3). Thus

$$F_n(z) = \alpha I_n(z) = \alpha[\mathrm{ber}_n(\lambda r) + i\,\mathrm{bei}_n(\lambda r)]$$

where

$$z = \sqrt{i}\,\lambda r = x + iy = \frac{1}{\sqrt{2}}(1+i)\lambda r .$$

Since α is not a function of n and $\mathrm{ber}_o(\lambda r)$, $\mathrm{bei}_o(\lambda r)$ are tabulated to a high order of accuracy, it is expedient to set n = 0 :

$$F_o(z) = \alpha[\mathrm{ber}_o(\lambda r) + i\,\mathrm{bei}_o(\lambda r)] .$$

Substituting

$$F_o(z) = \mathcal{R}[F_o(z)] + i\,\mathcal{I}[F_o(z)] ,$$

where

$\mathcal{R}[F_o(z)]$ = real part of $F_o(z)$

and $\mathcal{I}[F_o(z)]$ = imaginary part of $F_o(z)$,

in the relation above yields

$$\mathcal{R}[F_o(z)] + i\,\mathcal{I}[F_o(z)] = [\alpha_r + i\alpha_i]\,[\mathrm{ber}_o(\lambda r) + i\,\mathrm{bei}_o(\lambda r)]$$

or

$$\alpha_r + i\alpha_i = \left\{ \frac{\mathcal{R}[F_o(z)]\,\mathrm{ber}_o(\lambda r) + \mathcal{I}[F_o(z)]\,\mathrm{bei}_o(\lambda r)}{\mathrm{ber}_o^2(\lambda r) + \mathrm{bei}_o^2(\lambda r)} \right\} + i\left\{ \frac{\mathcal{I}[F_o(z)]\,\mathrm{ber}_o(\lambda r) - \mathcal{R}[F_o(z)]\,\mathrm{bei}_o(\lambda r)}{\mathrm{ber}_o^2(\lambda r) + \mathrm{bei}_o^2(\lambda r)} \right\}. \qquad \text{(B-3*)}$$

Consequently the constant α can be determined by equating the real and imaginary parts of the equation (B-3*), as:

$$\alpha_r = \frac{\mathcal{R}[F_o(z)]\,\mathrm{ber}_o(\lambda r) + \mathcal{I}[F_o(z)]\,\mathrm{bei}_o(\lambda r)}{[\mathrm{ber}_o^2(\lambda r) + \mathrm{bei}_o^2(\lambda r)]} \qquad \text{(B-4)}$$

$$\alpha_i = \frac{\mathcal{I}[F_o(z)]\,\mathrm{ber}_o(\lambda r) - \mathcal{R}[F_o(z)]\,\mathrm{bei}_o(\lambda r)}{[\mathrm{ber}_o^2(\lambda r) + \mathrm{bei}_o^2(\lambda r)]} \qquad \text{(B-5)}$$

Equating real and imaginary parts of equation (B-3*) yields:

$$\alpha_i \mathcal{R}[F_n(z)] = \alpha_i \alpha_r \,\mathrm{ber}_n(\lambda r) - \alpha_i^2 \,\mathrm{bei}_n(\lambda r)$$

$$\alpha_r \mathcal{I}[F_n(z)] = \alpha_i \alpha_r \,\mathrm{ber}_n(\lambda r) + \alpha_r^2 \,\mathrm{bei}_n(\lambda r)$$

Rearranging yields:

$$\mathrm{ber}_n(\lambda r) = \frac{\alpha_i \mathcal{I}[F_n(z)] + \alpha_r \mathcal{R}[F_n(z)]}{(\alpha_i^2 + \alpha_r^2)} \qquad \text{(B-6)}$$

$$\mathrm{bei}_n(\lambda r) = \frac{\alpha_r \mathcal{I}[F_n(z)] - \alpha_i \mathcal{R}[F_n(z)]}{(\alpha_i^2 + \alpha_r^2)} \qquad \text{(B-7)}$$

Now $\mathrm{ber}_n(\lambda r)$, $\mathrm{bei}_n(\lambda r)$ can be calculated for any order n, for which $F_n(Z)$ is computed.

It should be noted that both α and F_n are functions of the constant "a", so that "a" is eliminated in equations (B-6) and (B-7) and has no influence whatsoever on the values of

$ber_n(\lambda r)$ and $bei_n(\lambda r)$.

Numerical Calculations of KELVIN Functions

An important purpose of this investigation was to ascertain whether the numerical solution was consistent for various numbers of boundary collocation points. KELVIN functions, $ber_n(x)$ and $bei_n(x)$, were calculated accurately from orders 0 to 36 for arguments ranging from 3.0 to 10.0 to give a maximum range of seven collocation points for the characteristic boundary segment of the shell enclosing an hexagonal base. Consequently, the shell of quadruple periodicity enclosing a rectangular base had a maximum range of ten collocation points and the shell of triple symmetry enclosing a triangular base had a maximum range of twelve collocation points.

Double precision techniques were used throughout the KELVIN function calculations.

LOWELL's Tables of 1959 gave zero order KELVIN functions to 12 - 14 figure accuracy. The backward recurrence was begun at the order 51 to insure the accuracy of higher order KELVIN functions. For a typical boundary point of argument 9.0, the ratio of $ber_m(\lambda r)$ to $ber_h(\lambda r)$ was

$$\frac{ber_{49}(9.0)}{ber_{36}(9.0)} \approx 10^{-12}$$

It was considered that the accuracy employed in the backward recurrence computations would permit $ber_n(\lambda r)$ and $bei_n(\lambda r)$, for n ranging from 0 to 36, to have the same 10 to 12 figure accuracy as the initial zero order functions from which they were calculated.

It was essential to use a different constant "a" for each functional-argument, λr, in order to overcome the floating point underflow (numbers less than 10^{-38} are set equal to zero) and overflow (numbers greater than 10^{+38} cause the termination of the computer calculations) limitations of the I.B.M. 7040 computer. The constant "a" ranged from 10^{-37} to 10^{-15} (see FIGURE 59) for arguments ranging from 3.0 to 10.0.

Since values of higher order KELVIN functions were less than 10^{-38} for arguments smaller than 3.0 (see TABLES 1 and 2 and FIGURE 60), it was impossible to accurately calculate sectional resultants close to the shell's apex.

The distributions of $ber_n(\lambda r)$, as functions of arguments λr ranging from 0.5 to 10.0, are given in FIGURES 61 to 76 for orders n ranging from 0 to 36. It was observed that $ber_n(\lambda r)$ are slowly oscillating functions of λr which decrease rapidly in magnitude for increasing order n. Comparison of TABLES 1 and 2 indicate that the behaviour of $ber_n(\lambda r)$ and $bei_n(\lambda r)$ is quite similar. See also the tables by YOUNG and KIRK of 1964.

$BER_n(x)$

ARG.	ØRDER 0	ØRDER 6	ØRDER 12	ØRDER 18	ØRDER 24	ØRDER 30	ØRDER 36
0.50	0.9990234640D 00	-0.3027510137D-08	-0.1244338331D-15	0.7476612613D-29	0.5726024934D-38	0.0000000000D-38	0.0000000000D-38
0.60	0.9979751139D 00	-0.1301761306D-07	-0.1109451772D-14	0.2866349061D-27	0.4551994523D-36	0.0000000000D-38	0.0000000000D-38
0.70	0.9962488284D 00	-0.4467851525D-07	-0.7054425700D-14	0.6255523784D-26	0.1840443018D-34	0.0000000000D-38	0.0000000000D-38
0.80	0.9936011377D 00	-0.1300240405D-06	-0.3502292283D-13	0.9038592220D-25	0.4536548614D-33	0.0000000000D-38	0.0000000000D-38
0.90	0.9897513567D 00	-0.3336017718D-06	-0.1439342913D-12	0.9531222046D-24	0.7662684739D-32	0.0000000000D-38	0.0000000000D-38
1.00	0.9843817821D 00	-0.7749374753D-06	-0.5095989370D-12	0.7839614261D-23	0.9606242617D-31	0.0000000000D-38	0.0000000000D-38
1.10	0.9771379732D 00	-0.1661035756D-05	-0.1599212302D-11	0.5274039747D-22	0.9461681119D-30	0.0000000000D-38	0.0000000000D-38
1.20	0.9676291558D 00	-0.3331571716D-05	-0.4542797646D-11	0.3005439923D-21	0.7636265887D-29	0.0000000000D-38	0.0000000000D-38
1.30	0.9554287468D 00	-0.6319705490D-05	-0.1186889527D-10	0.1489847263D-20	0.5213810619D-28	0.0000000000D-38	0.0000000000D-38
1.40	0.9400750567D 00	-0.1143174077D-04	-0.2887706019D-10	0.6558806214D-20	0.3087216410D-27	0.0000000000D-38	0.0000000000D-38
1.50	0.9210721835D 00	-0.1984912712D-04	-0.6607247334D-10	0.2606610352D-19	0.1616809824D-26	-0.1221566084D-37	0.0000000000D-38
1.60	0.8978911386D 00	-0.3325657078D-04	-0.1433025682D-09	0.9476206710D-19	0.7608817475D-26	-0.9634512265D-37	0.0000000000D-38
1.70	0.8699712370D 00	-0.5400026584D-04	-0.2965288792D-09	0.3185619685D-18	0.3259673741D-25	-0.6704217109D-36	0.0000000000D-38
1.80	0.8367217942D 00	-0.8528048271D-04	-0.5885587459D-09	0.9991771381D-18	0.1284976934D-24	-0.4175356436D-35	0.0000000000D-38
1.90	0.7975241670D 00	-0.1313829486D-03	-0.1125573047D-08	0.2946029572D-17	0.4703148500D-24	-0.2355471027D-34	0.0000000000D-38
2.00	0.7517341827D 00	-0.1979536185D-03	-0.2081942317D-08	0.8217373412D-17	0.1610497910D-23	-0.1215933107D-33	0.0000000000D-38
2.10	0.6986850014D 00	-0.2923215606D-03	-0.3736651294D-08	0.2180127312D-16	0.5193155232D-23	-0.5793653038D-33	0.0000000000D-38
2.20	0.6376904571D 00	-0.4238747546D-03	-0.6525680167D-08	0.5527219648D-16	0.1585730798D-22	-0.2567105923D-32	0.0000000000D-38
2.30	0.5680489261D 00	-0.6044936245D-03	-0.1111595027D-07	0.1344499705D-15	0.4607421266D-22	-0.1064606782D-31	0.0000000000D-38
2.40	0.4890477721D 00	-0.8490470805D-03	-0.1850796455D-07	0.3149001472D-15	0.1279237280D-21	-0.4155621257D-31	-0.1904010632D-38
2.50	0.3999684171D 00	-0.1175955725D-02	-0.3017609110D-07	0.7123358255D-15	0.3406579181D-21	-0.1534374201D-30	-0.8276527130D-38
2.60	0.3000920903D 00	-0.1607826675D-02	-0.4825758326D-07	0.1560558549D-14	0.8729309496D-21	-0.5382322495D-30	-0.3396129680D-37
2.70	0.1887063040D 00	-0.2172161340D-02	-0.7580393183D-07	0.3319006736D-14	0.2158709171D-20	-0.1800657549D-29	-0.1321196208D-36
2.80	0.6511210843D-01	-0.2902159460D-02	-0.1171110312D-06	0.6867580852D-14	0.5165144282D-20	-0.5765168661D-29	-0.4891933499D-36
2.90	-0.7136782583D-01	-0.3837563890D-02	-0.1781479325D-06	0.1385170589D-13	0.1198526990D-19	-0.1771949149D-28	-0.1729935195D-35
3.00	-0.2213802496D 00	-0.5025646447D-02	-0.2671076680D-06	0.2728083463D-13	0.2702657112D-19	-0.5242657090D-28	-0.5860947284D-35
3.10	-0.3855314550D 00	-0.6522238699D-02	-0.3951077665D-06	0.5254652826D-13	0.5933674993D-19	-0.1496914007D-27	-0.1907716770D-34
3.20	-0.5643764305D 00	-0.8392866968D-02	-0.5770726312D-06	0.9912309467D-13	0.1270517311D-18	-0.4133979874D-27	-0.5980964619D-34
3.30	-0.7584070121D 00	-0.1071397165D-01	-0.8328348932D-06	0.1833605659D-12	0.2657221700D-18	-0.1106512333D-26	-0.1810260396D-33
3.40	-0.9680389953D 00	-0.1357421138D-01	-0.1188498142D-05	0.3329992183D-12	0.5435904489D-18	-0.2875881936D-26	-0.5300718665D-33
3.50	-0.1193598180D 01	-0.2603740712D-03	-0.1502769048D-05	-0.8712259764D-12	0.9282660669D-18	0.2123896427D-25	-0.1259980356D-32
3.60	-0.1435305322D 01	0.1236480303D-02	-0.2001646320D-05	-0.1657019033D-11	0.1718762246D-17	0.5529112521D-25	-0.3259791578D-32
3.70	-0.1693259984D 01	0.3031799411D-02	-0.2617922023D-05	-0.2987984560D-11	0.3093384100D-17	0.1361285216D-24	-0.8118878209D-32
3.80	-0.1967423273D 01	0.5090064200D-02	-0.3362357396D-05	-0.5152411247D-11	0.5414615700D-17	0.3190587581D-24	-0.1948608132D-31
3.90	-0.2257594466D 01	0.7345371411D-02	-0.4240538126D-05	-0.8539690692D-11	0.9221027497D-17	0.7148935718D-24	-0.4510494810D-31
4.00	-0.2563416557D 01	0.9694959043D-02	-0.5250274557D-05	-0.1364411232D-10	0.1528111834D-16	0.1535235259D-23	-0.1007531681D-30
4.10	-0.2884305732D 01	-0.5937732016D-01	-0.1094573426D-04	0.1402599075D-10	0.4824564619D-16	-0.1147864012D-23	-0.4465501221D-30
4.20	-0.3219479832D 01	-0.7169668486D-01	-0.1454162672D-04	0.2269515179D-10	0.8590636935D-16	-0.2481199330D-23	-0.1062547954D-29
4.30	-0.3567910863D 01	-0.8615201297D-01	-0.1918015652D-04	0.3630648917D-10	0.1508817915D-15	-0.5266755760D-23	-0.2477082849D-29
4.40	-0.3928306622D 01	-0.1030391876D 00	-0.2512396098D-04	0.5745295771D-10	0.2615543865D-15	-0.1098745082D-22	-0.5663081914D-29
4.50	-0.4299086552D 01	-0.1226835648D 00	-0.3269165708D-04	0.8997618068D-10	0.4477668868D-15	-0.2254552954D-22	-0.1270763139D-28
4.60	-0.4678356937D 01	-0.1454412839D 00	-0.4226742050D-04	0.1395165852D-09	0.7574274170D-15	-0.4553536884D-22	-0.2801108069D-28
4.70	-0.5063885587D 01	-0.1717003873D 00	-0.5431170100D-04	0.2142844101D-09	0.1266625104D-14	-0.9058515107D-22	-0.6069874407D-28
4.80	-0.5453076175D 01	-0.2018816966D 00	-0.6937310165D-04	0.3261319993D-09	0.2094971186D-14	-0.1776073982D-21	-0.1293970010D-27
4.90	-0.5842942442D 01	-0.2354393876D 00	-0.8810142035D-04	0.4920341720D-09	0.3428647699D-14	-0.3434155853D-21	-0.2715527345D-27
5.00	-0.6230082479D 01	-0.2758611986D 00	-0.1112618150D-03	0.7361175764D-09	0.5554725300D-14	-0.6552049074D-21	-0.5613615176D-27
5.10	-0.6610653357D 01	-0.3206682014D 00	-0.1397500049D-03	0.1092423782D-08	0.8911818700D-14	-0.1234130998D-20	-0.1143790451D-26
5.20	-0.6980346403D 01	-0.3714140554D 00	-0.1746083616D-03	0.1608646898D-08	0.1416423543D-13	-0.2296084014D-20	-0.2298302621D-26
5.30	-0.7334363435D 01	-0.4286836593D 00	-0.2170426659D-03	0.2351157726D-08	0.2230964302D-13	-0.4221431502D-20	-0.4556723632D-26
5.40	-0.7667394351D 01	-0.4930911063D 00	-0.2684392171D-03	0.3411716444D-08	0.3483419546D-13	-0.7673063808D-20	-0.8918622586D-26
5.50	-0.7973596451D 01	-0.5652768420D 00	-0.3303818702D-03	0.4916388983D-08	0.5393436549D-13	-0.1379418370D-19	-0.1724032528D-25
5.60	-0.8246575962D 01	-0.6459039146D 00	-0.4046684419D-03	0.7037323615D-08	0.8283186956D-13	-0.2453649618D-19	-0.3292968456D-25
5.70	-0.8479372252D 01	-0.7356532026D 00	-0.4933257712D-03	0.1000822203D-07	0.1262176153D-12	-0.4319967778D-19	-0.6217355572D-25
5.80	-0.8664445263D 01	-0.8352174931D 00	-0.5986225328D-03	0.1414455183D-07	0.1908732742D-12	-0.7531014256D-19	-0.1160838623D-24
5.90	-0.8793666753D 01	-0.9452942806D 00	-0.7230786856D-03	0.1986982759D-07	0.2865358012D-12	-0.1300400388D-18	-0.2144119849D-24
6.00	-0.8858315966D 01	-0.1066577146D 01	-0.8694701856D-03	0.2774960391D-07	0.4270921434D-12	-0.2224793157D-18	-0.3919151468D-24
6.10	-0.8849080413D 01	-0.1199745569D 01	-0.1040827301D-02	0.3853523836D-07	0.6322199391D-12	-0.3772441281D-18	-0.7091657498D-24
6.20	-0.8756062474D 01	-0.1345453028D 01	-0.1240424534D-02	0.5321996738D-07	0.9296269957D-12	-0.6341624950D-18	-0.1270737401D-23
6.30	-0.8568792593D 01	-0.1504313220D 01	-0.1471759772D-02	0.7311043417D-07	0.1358089942D-11	-0.1057164846D-17	-0.2255532285D-23
6.40	-0.8276249873D 01	-0.1676884252D 01	-0.1738519859D-02	0.9991752397D-07	0.1971553371D-11	-0.1748083536D-17	-0.3966923989D-23
6.50	-0.7866890928D 01	-0.1863650632D 01	-0.2044529281D-02	0.1358712231D-06	0.2844628273D-11	-0.2867918911D-17	-0.6914976699D-23
6.60	-0.7328687885D 01	-0.2065002890D 01	-0.2393678130D-02	0.1838652473D-06	0.4079926540D-11	-0.4669385036D-17	-0.1195017720D-22
6.70	-0.6649176463D 01	-0.2281214686D 01	-0.2789824863D-02	0.2476384150D-06	0.5817791502D-11	-0.7546383480D-17	-0.2047925785D-22
6.80	-0.5815515115D 01	-0.2512417209D 01	-0.3236668733D-02	0.3320011829D-06	0.8249138342D-11	-0.1210872000D-16	-0.3481086309D-22
6.90	-0.4814556200D 01	-0.2758570741D 01	-0.3737585970D-02	0.4431175090D-06	0.1163230945D-10	-0.1929422989D-16	-0.5870509941D-22
7.00	-0.3632930243D 01	-0.3019433218D 01	-0.4295422990D-02	0.5888541961D-06	0.1631508578D-10	-0.3053600752D-16	-0.9824096710D-22
7.10	-0.2257144280D 01	-0.3294525650D 01	-0.4912238976D-02	0.7792122718D-06	0.2276328498D-10	-0.4801033134D-16	-0.1631760067D-21
7.20	-0.6736953791D 00	-0.3583094282D 01	-0.5588989192D-02	0.1026857716D-05	0.3159773010D-10	-0.7500208874D-16	-0.2690629989D-21
7.30	0.1130799653D 01	-0.3884069374D 01	-0.6325139317D-02	0.1347772079D-05	0.4364180075D-10	-0.1164403446D-15	-0.4405234586D-21
7.40	0.3169457312D 01	-0.4196020533D 01	-0.7118199906D-02	0.1762047256D-05	0.5998229306D-10	-0.1796789571D-15	-0.7162774940D-21
7.50	0.5454962184D 01	-0.4517108517D 01	-0.7963168859D-02	0.2294853007D-05	0.8204693008D-10	-0.2756282679D-15	-0.1156823811D-20
7.60	0.7999382494D 01	-0.4845033493D 01	-0.8851868447D-02	0.2977610756D-05	0.1117025934D-09	-0.4203872027D-15	-0.1856094240D-20
7.70	0.1081396548D 02	-0.5176979762D 01	-0.9772162024D-02	0.3849412857D-05	0.1513792048D-09	-0.6375850863D-15	-0.2959033737D-20
7.80	0.1390891171D 02	-0.5509556991D 01	-0.1070703412D-01	0.4958733004D-05	0.2042251871D-09	-0.9617251344D-15	-0.4687963343D-20
7.90	0.1729312765D 02	-0.5838738066D 01	-0.1163351604D-01	0.6365480737D-05	0.2743015893D-09	-0.1442934998D-14	-0.7381887915D-20
8.00	0.2097395561D 02	-0.6159793715D 01	-0.1252143748D-01	0.8143461335D-05	0.3668232816D-09	-0.2153684652D-14	-0.1155477690D-19
8.10	0.2495688080D 02	-0.6467224140D 01	-0.1333198320D-01	0.1038331162D-04	0.4884571179D-09	-0.3198242604D-14	-0.1798150292D-19
8.20	0.2924521480D 02	-0.6754687933D 01	-0.1401603196D-01	0.1319599268D-04	0.6476886233D-09	-0.4725926759D-14	-0.2782388400D-19
8.30	0.3383975543D 02	-0.7014928670D 01	-0.1451225336D-01	0.1671693200D-04	0.8552705853D-09	-0.6949591065D-14	-0.4281457309D-19
8.40	0.3873842296D 02	-0.7239699647D 01	-0.1474493688D-01	0.2111092048D-04	0.1124768873D-08	-0.1017130599D-13	-0.6552396201D-19
8.50	0.4393587275D 02	-0.7419687325D 01	-0.1462152540D-01	0.2657788373D-04	0.1473222849D-08	-0.1481788240D-13	-0.9974561852D-19
8.60	0.4942308498D 02	-0.7544434151D 01	-0.1402982459D-01	0.3335966267D-04	0.1921939796D-08	-0.2148980996D-13	-0.1510501369D-18
8.70	0.5518693210D 02	-0.7602261571D 01	-0.1283485803D-01	0.4174795519D-04	0.2497444720D-08	-0.3102840472D-13	-0.2275771120D-18
8.80	0.6120972522D 02	-0.7580194143D 01	-0.1087533685D-01	0.5209358860D-04	0.3232608634D-08	-0.4460757864D-13	-0.3411621929D-18
8.90	0.6746874085D 02	-0.7463885831D 01	-0.7959712085D-02	0.6481731228D-04	0.4167979657D-08	-0.6385877629D-13	-0.5059334317D-18
9.00	0.7393572986D 02	-0.7237549686D 01	-0.3861777413D-02	0.8042232009D-04	0.5353341807D-08	-0.9104042399D-13	-0.7555618561D-18
9.10	0.8057641115D 02	-0.6883892312D 01	0.1684210035D-02	0.9950873404D-04	0.6849525719D-08	-0.1292668999D-12	-0.1116419888D-17
9.20	0.8734995267D 02	-0.6384054651D 01	0.8988922629D-02	0.1227903026D-03	0.8730493312D-08	-0.1828168105D-12	-0.1641993864D-17
9.30	0.9420844336D 02	-0.5717560854D 01	0.1841389959D-01	0.1511135902D-03	0.1108571390D-07	-0.2575465659D-12	-0.2404021232D-17
9.40	0.1010963597D 03	-0.4862277134D 01	0.3037805755D-01	0.1854799566D-03	0.1402284156D-07	-0.3614432847D-12	-0.3503989663D-17
9.50	0.1079500319D 03	-0.3794382778D 01	0.4536480046D-01	0.2270706481D-03	0.1767069179D-07	-0.5053614357D-12	-0.5084851386D-17
9.60	0.1146971142D 03	-0.2488355639D 01	0.6392975114D-01	0.2772753421D-03	0.2218249810D-07	-0.7040009728D-12	-0.7347115125D-17
9.70	0.1212560663D 03	-0.9169746822D 00	0.8670912221D-01	0.3377245064D-03	0.2773940446D-07	-0.9772018427D-12	-0.1057082954D-16
9.80	0.1275356515D 03	0.9486576024D 00	0.1144287375D 00	0.4103259504D-03	0.3455411581D-07	-0.1351651633D-11	-0.1514551905D-16
9.90	0.1334344603D 03	0.3139069907D 01	0.1479137080D 00	0.4973059560D-03	0.4287458250D-07	-0.1863131024D-11	-0.2161075830D-16
10.00	0.1388404659D 03	0.5686350658D 01	0.1880987563D 00	0.6012553809D-03	0.5298753399D-07	-0.2559457164D-11	-0.3071094452D-16

TABLE I

NOTE: $D\text{-}00 = \times 10^{-00}$

$BEI_n(x)$

ARG.	ORDER 0	ØRDER 6	ØRDER 12	ØRDER 18	ØRDER 24	ØRDER 30	ØRDER 36
0.50	0.6249321838D-01	0.3390723751D-06	-0.5982441474D-18	-0.2272882075D-26	-0.0000000000D-38	-0.0000000000D-38	0.0000000000D-38
0.60	0.8997975041D-01	0.1012426775D-05	-0.7680941506D-17	-0.6051136309D-25	0.1638725083D-38	-0.0000000000D-38	0.0000000000D-38
0.70	0.1224489390D 00	0.2552804624D-05	-0.6647634486D-16	-0.9702311253D-24	0.9018242850D-37	-0.0000000000D-38	0.0000000000D-38
0.80	0.1598862295D 00	0.5687588602D-05	-0.4310729171D-15	-0.1073307575D-22	0.2903430644D-35	-0.0000000000D-38	0.0000000000D-38
0.90	0.2022693635D 00	0.1152878542D-04	-0.2242233012D-14	-0.8942538007D-22	0.6206910001D-34	-0.0000000000D-38	0.0000000000D-38
1.00	0.2495660400D 00	0.2168927944D-04	-0.9801176310D-14	-0.5957764629D-21	0.9606561934D-33	-0.0000000000D-38	0.0000000000D-38
1.10	0.3017312692D 00	0.3841392625D-04	-0.3721909387D-13	-0.3312341440D-20	0.1144919118D-31	-0.0000000000D-38	0.0000000000D-38
1.20	0.3587044199D 00	0.6472502614D-04	-0.1258324109D-12	-0.1586015486D-19	0.1099698078D-30	-0.0000000000D-38	0.0000000000D-38
1.30	0.4204059656D 00	0.1045815381D-03	-0.3858736713D-12	-0.6698805759D-19	0.8812176521D-30	0.9198119266D-38	0.0000000000D-38
1.40	0.4867339336D 00	0.1630511750D-03	-0.1088953869D-11	-0.2542649406D-18	0.6051716918D-29	0.8496209006D-37	0.0000000000D-38
1.50	0.5575600623D 00	0.2464942551D-03	-0.2860673583D-11	-0.8801990313D-18	0.3638434361D-28	0.6731449046D-36	-0.0000000000D-38
1.60	0.6327256770D 00	0.3627578688D-03	-0.7060546360D-11	-0.2812189860D-17	0.1948281688D-27	0.4666055151D-35	-0.0000000000D-38
1.70	0.7120372924D 00	0.5213785527D-03	-0.1649698956D-10	-0.8373389103D-17	0.9423073197D-27	0.2876030026D-34	-0.0000000000D-38
1.80	0.7952619548D 00	0.7337912369D-03	-0.3671881362D-10	-0.2342335552D-16	0.4164778553D-26	0.1597612937D-33	-0.0000000000D-38
1.90	0.8821223406D 00	0.1013541744D-02	-0.7826532021D-10	-0.6197524500D-16	0.1698572435D-25	0.8088533006D-33	-0.0000000000D-38
2.00	0.9722916273D 00	0.1376499575D-02	-0.1604630091D-09	-0.1559865909D-15	0.6445419764D-25	0.3768087549D-32	-0.0000000000D-38
2.10	0.1065388161D 01	0.1841067086D-02	-0.3176514218D-09	-0.3752937833D-15	0.2291663031D-24	0.1628368794D-31	-0.0000000000D-38
2.20	0.1160969944D 01	0.2428380511D-02	-0.6091334865D-09	-0.8667424785D-15	0.7680918571D-24	0.6573549036D-31	-0.0000000000D-38
2.30	0.1258528975D 01	0.3162497479D-02	-0.1134713912D-08	-0.1928500776D-14	0.2439595448D-23	0.2493975380D-30	-0.0000000000D-38
2.40	0.1357485476D 01	0.4070564899D-02	-0.2058458367D-08	-0.4147012031D-14	0.7376543139D-23	0.8939705891D-30	-0.0000000000D-38
2.50	0.1457182044D 01	0.5182960170D-02	-0.3644331948D-08	-0.8642561269D-14	0.2131880679D-22	0.3041624959D-29	-0.0000000000D-38
2.60	0.1556877774D 01	0.6533397690D-02	-0.6308724773D-08	-0.1749866837D-13	0.5909992692D-22	0.9863135076D-29	-0.1552283382D-38
2.70	0.1655742407D 01	0.8158991631D-02	-0.1069662525D-07	-0.3449576280D-13	0.1576484700D-21	0.3059324029D-28	-0.6513045123D-38
2.80	0.1752850564D 01	0.1010026483D-01	-0.1779045201D-07	-0.6633830018D-13	0.4057766561D-21	0.9106248559D-28	-0.2593825948D-37
2.90	0.1847176116D 01	0.1240109245D-01	-0.2906341384D-07	-0.1246670308D-12	0.1010337496D-20	0.2608624621D-27	-0.9840819832D-37
3.00	0.1937586785D 01	0.1510856796D-01	-0.4669286175D-07	-0.2292987608D-12	0.2438961344D-20	0.7210552194D-27	-0.3568483415D-36
3.10	0.2022839042D 01	0.1827277745D-01	-0.7385357492D-07	-0.4133539205D-12	0.5719830145D-20	0.1927640706D-26	-0.1240468402D-35
3.20	0.2101573388D 01	0.2194646733D-01	-0.1151164524D-06	-0.7312433020D-12	0.1305563148D-19	0.4994628119D-26	-0.4144788041D-35
3.30	0.2172310131D 01	0.2618458889D-01	-0.1769848539D-06	-0.1270923426D-11	0.2905175034D-19	0.1256705839D-25	-0.1334415031D-34
3.40	0.2233445750D 01	0.3104370172D-01	-0.2686090616D-06	-0.2172439482D-11	0.6311966573D-19	0.3075930967D-25	-0.4148720017D-34
3.50	0.2283249967D 01	0.3582466904D-01	0.2951372219D-06	-0.3169097520D-11	-0.2942453819D-18	0.6187118478D-25	0.4552122192D-33
3.60	0.2319863655D 01	0.4076937008D-01	0.4963856310D-06	-0.4971099617D-11	-0.6521886228D-18	0.1353753311D-24	0.1396310368D-32
3.70	0.2341297714D 01	0.4581115084D-01	0.7833020544D-06	-0.7617301667D-11	-0.1370465114D-17	0.2865196151D-24	0.4037073212D-32
3.80	0.2345433061D 01	0.5081833914D-01	0.1176779418D-05	-0.1140576012D-10	-0.2749690807D-17	0.5870482698D-24	0.1107227755D-31
3.90	0.2330021882D 01	0.5563240897D-01	0.1696685955D-05	-0.1669132618D-10	-0.5290953139D-17	0.1165072756D-23	0.2892695253D-31
4.00	0.2292690323D 01	0.6006774388D-01	0.2358145405D-05	-0.2387238913D-10	-0.9789289816D-17	0.2240615140D-23	0.7217785254D-31
4.10	0.2230942780D 01	0.8709344930D-01	-0.3665754097D-05	-0.6238067053D-10	0.8187133307D-17	0.8415454859D-23	-0.5093858420D-31
4.20	0.2142167987D 01	0.9880588441D-01	-0.5129304831D-05	-0.9602584856D-10	0.1531258387D-16	0.1732394566D-22	-0.1272465405D-30
4.30	0.2023647069D 01	0.1115255429D 00	-0.7119662860D-05	-0.1462899299D-09	0.2821944087D-16	0.3505892045D-22	-0.3110859636D-30
4.40	0.1872563796D 01	0.1252453633D 00	-0.9806686459D-05	-0.2206625019D-09	0.5127732906D-16	0.6980250882D-22	-0.7450410068D-30
4.50	0.1686017204D 01	0.1399396527D 00	-0.1340888107D-04	-0.3296979441D-09	0.9192917140D-16	0.1368294565D-21	-0.1749630118D-29
4.60	0.1461036836D 01	0.1555549734D 00	-0.1820563362D-04	-0.4881469772D-09	0.1627001761D-15	0.2642522068D-21	-0.4032302798D-29
4.70	0.1194600797D 01	0.1720105642D 00	-0.2455210372D-04	-0.7164618598D-09	0.2844255652D-15	0.5031104403D-21	-0.9127485840D-29
4.30	0.8836568537D 00	0.1891907719D 00	-0.3289725628D-04	-0.1042784160D-08	0.4913819454D-15	0.9448686211D-21	-0.2030806279D-28
4.90	0.5251468109D 00	0.2069399699D 00	-0.4380559089D-04	-0.1505551479D-08	0.8393630113D-15	0.1751396695D-20	-0.4444398118D-28
5.00	0.1160343816D 00	0.2250564436D 00	-0.5798320047D-04	-0.2156892683D-08	0.1418266461D-14	0.3205748491D-20	-0.9573564806D-28
5.10	-0.3466632176D 00	0.2432857254D 00	-0.7630887630D-04	-0.3067021060D-08	0.2371530613D-14	0.5797214619D-20	-0.2031059329D-27
5.20	-0.8658397275D 00	0.2613133665D 00	-0.9987106884D-04	-0.4329882240D-08	0.3925881466D-14	0.1036227081D-19	-0.4246350127D-27
5.30	-0.1444260151D 01	0.2787571388D 00	-0.1300116123D-03	-0.6070369827D-08	0.6436470458D-14	0.1831576739D-19	-0.8753760319D-27
5.40	-0.2084516693D 01	0.2951586622D 00	-0.1683772267D-03	-0.8453487440D-08	0.1045480521D-13	0.3202640255D-19	-0.1780274587D-26
5.50	-0.2788980155D 01	0.3099744658D 00	-0.2169799242D-03	-0.1169591234D-07	0.1683015210D-13	0.5542073954D-19	-0.3573617627D-26
5.60	-0.3559746593D 01	0.3225664934D 00	-0.2782675634D-03	-0.1608050393D-07	0.2685981978D-13	0.9494598325D-19	-0.7083722028D-26
5.70	-0.4398579112D 01	0.3321920770D 00	-0.3552059168D-03	-0.2197440108D-07	0.4251011323D-13	0.1610910404D-18	-0.1387203035D-25
5.80	-0.5306844640D 01	0.3379934122D 00	-0.4513737454D-03	-0.2985146590D-07	0.6673903048D-13	0.2707690732D-18	-0.2684888800D-25
5.90	-0.6285445623D 01	0.3389865792D 00	-0.5710724975D-03	-0.4031995868D-07	0.1039642189D-12	0.4510186560D-18	-0.5137994021D-25
6.00	-0.7334746541D 01	0.3340501699D 00	-0.7194523759D-03	-0.5415646891D-07	0.1607371114D-12	0.7447073570D-18	-0.9725376030D-25
6.10	-0.8454495270D 01	0.3219135953D 00	-0.9026566424D-03	-0.7234727965D-07	0.2467078467D-12	0.1219253074D-17	-0.1821465863D-24
6.20	-0.9643739286D 01	0.3011451635D 00	-0.1127986139D-02	-0.9613850543D-07	0.3759978207D-12	0.1979859760D-17	-0.3376650809D-24
6.30	-0.1090073683D 02	0.2701400388D 00	-0.1404086116D-02	-0.1270965139D-06	0.5691403265D-12	0.3189458135D-17	-0.6197881010D-24
6.40	-0.1222286313D 02	0.2271082132D 00	-0.1741157532D-02	-0.1671803147D-06	0.8558084078D-12	0.5098535754D-17	-0.1126748680D-23
6.50	-0.1360651200D 02	0.1700626418D 00	-0.2151195082D-02	-0.2188277696D-06	0.1278627573D-11	0.8089454731D-17	-0.2029392703D-23
6.60	-0.1504692299D 02	0.9680772120D-01	-0.2648254214D-02	-0.2850576325D-06	0.1898475564D-11	0.1274185407D-16	-0.3622287366D-23
6.70	-0.1653842454D 02	0.4928313299D-02	-0.3248749430D-02	-0.3695895655D-06	0.2801809922D-11	0.1992854135D-16	-0.6409062019D-23
6.80	-0.1807362361D 02	-0.1082204516D 00	-0.3971786101D-02	-0.4769843675D-06	0.4110746755D-11	0.3095519870D-16	-0.1124378620D-22
6.90	-0.1964399237D 02	-0.2455223307D 00	-0.4839527942D-02	-0.6128066865D-06	0.5996853914D-11	0.4776266920D-16	-0.1956338734D-22
7.00	-0.2123940258D 02	-0.4101077879D 00	-0.5877602122D-02	-0.7838124379D-06	0.8699935042D-11	0.7321809726D-16	-0.3376689239D-22
7.10	-0.2284807860D 02	-0.6053601458D 00	-0.7115543755D-02	-0.9981629832D-06	0.1255348851D-10	0.1115314968D-15	-0.5782977644D-22
7.20	-0.2445647980D 02	-0.8349197062D 00	-0.8587281161D-02	-0.1265667799D-05	0.1801905299D-10	0.1688483719D-15	-0.9829218521D-22
7.30	-0.2604918364D 02	-0.1102685432D 01	-0.1033166287D-01	-0.1598056840D-05	0.2573233229D-10	0.2540880798D-15	-0.1658377107D-21
7.40	-0.2760877052D 02	-0.1412813753D 01	-0.1239302677D-01	-0.2009283013D-05	0.3656486594D-10	0.3801233458D-15	-0.2777988840D-21
7.50	-0.2911571187D 02	-0.1769713997D 01	-0.1482181100D-01	-0.2515854034D-05	0.5170613100D-10	0.5654308687D-15	-0.4621076654D-21
7.60	-0.3054826296D 02	-0.2178039945D 01	-0.1767520556D-01	-0.3137191426D-05	0.7277238484D-10	0.8363890367D-15	-0.7634851271D-21
7.70	-0.3188236236D 02	-0.2642676908D 01	-0.2101784208D-01	-0.3896012294D-05	0.1019503676D-09	0.1230459988D-14	-0.1253080123D-20
7.80	-0.3309153967D 02	-0.3168723738D 01	-0.2492251853D-01	-0.4818726838D-05	0.1421862694D-09	0.1800574112D-14	-0.2043389183D-20
7.90	-0.3414683399D 02	-0.3761469108D 01	-0.2947095342D-01	-0.5935840998D-05	0.1974332483D-09	0.2621141359D-14	-0.3311216959D-20
8.00	-0.3501672516D 02	-0.4426361358D 01	-0.3475456289D-01	-0.7282349199D-05	0.2729743987D-09	0.3796252739D-14	-0.5332809948D-20
8.10	-0.3566708051D 02	-0.5168971165D 01	-0.4087525151D-01	-0.8898096447D-05	0.3758425932D-09	0.5470816136D-14	-0.8537320074D-20
8.20	-0.3606111968D 02	-0.5994946264D 01	-0.4794620549D-01	-0.1082808204D-04	0.5153642511D-09	0.7845604636D-14	-0.1358772186D-19
8.30	-0.3615940062D 02	-0.6909957390D 01	-0.5609267386D-01	-0.1312268839D-04	0.7038610854D-09	0.1119749686D-13	-0.2150263512D-19
8.40	-0.3591982983D 02	-0.7919634586D 01	-0.6545272048D-01	-0.1583764779D-04	0.9575525333D-09	0.1590657479D-13	-0.3383878785D-19
8.50	-0.3529770030D 02	-0.9029493001D 01	-0.7617792542D-01	-0.1903410686D-04	0.1297712256D-08	0.2249223661D-13	-0.5296293073D-19
8.60	-0.3424576064D 02	-0.1024484725D 02	-0.8843401078D-01	-0.2277801271D-04	0.1752145212D-08	0.3166110548D-13	-0.8245506561D-19
8.70	-0.3271431931D 02	-0.1157071344D 02	-0.1024013608D 00	-0.2713942563D-04	0.2357067887D-08	0.4437030158D-13	-0.1277035316D-18
8.80	-0.3065138788D 02	-0.1301169784D 02	-0.1182754015D 00	-0.3219122064D-04	0.3159493894D-08	0.6191063079D-13	-0.1967791118D-18
8.90	-0.2800286754D 02	-0.1457187137D 02	-0.1362667982D 00	-0.3800717285D-04	0.4220251053D-08	0.8601547240D-13	-0.3017130905D-18
9.00	-0.2471278317D 02	-0.1625462889D 02	-0.1566014247D 00	-0.4465922956D-04	0.5617785036D-08	0.1190026726D-12	-0.4603575419D-18
9.10	-0.2072356953D 02	-0.1806253232D 02	-0.1795200485D 00	-0.5221375397D-04	0.7452939721D-08	0.1639586281D-12	-0.6990811840D-18
9.20	-0.1597641420D 02	-0.1999713688D 02	-0.2052776706D 00	-0.6072648108D-04	0.9854946647D-08	0.2249760431D-12	-0.1056659282D-17
9.30	-0.1041166192D 02	-0.2205879941D 02	-0.2341424480D 00	-0.7023587390D-04	0.1298890673D-07	0.3074596396D-12	-0.1589862801D-17
9.40	-0.3969285325D 01	-0.2424646814D 02	-0.2663941201D 00	-0.8075450764D-04	0.1706510822D-07	0.4185174753D-12	-0.2381455947D-17
9.50	0.3410573282D 01	-0.2655745319D 02	-0.3023218476D 00	-0.9225803901D-04	0.2235059736D-07	0.5674595709D-12	-0.3551593539D-17
9.60	0.1178698419D 02	-0.2898717716D 02	-0.3422213631D 00	-0.1046712365D-03	0.2918350491D-07	0.7664303518D-12	-0.5273999113D-17
9.70	0.2121753181D 02	-0.3152890542D 02	-0.3863913208D 00	-0.1178504537D-03	0.3799073374D-07	0.1031207070D-11	-0.7798839727D-17
9.80	0.3175753090D 02	-0.3417345584D 02	-0.4351287192D 00	-0.1315618204D-03	0.4930973427D-07	0.1382202958D-11	-0.1148494611D-16
9.90	0.4345915293D 02	-0.3690888778D 02	-0.4887232598D 00	-0.1454543034D-03	0.6381523733D-07	0.1845721454D-11	-0.1684502625D-16
10.00	0.5637045855D 02	-0.3972017046D 02	-0.5474504874D 00	-0.1590266497D-03	0.8235198155D-07	0.2455516444D-11	-0.2460887935D-16

TABLE 2

NOTE: $D\text{-}00 = \times 10^{-00}$

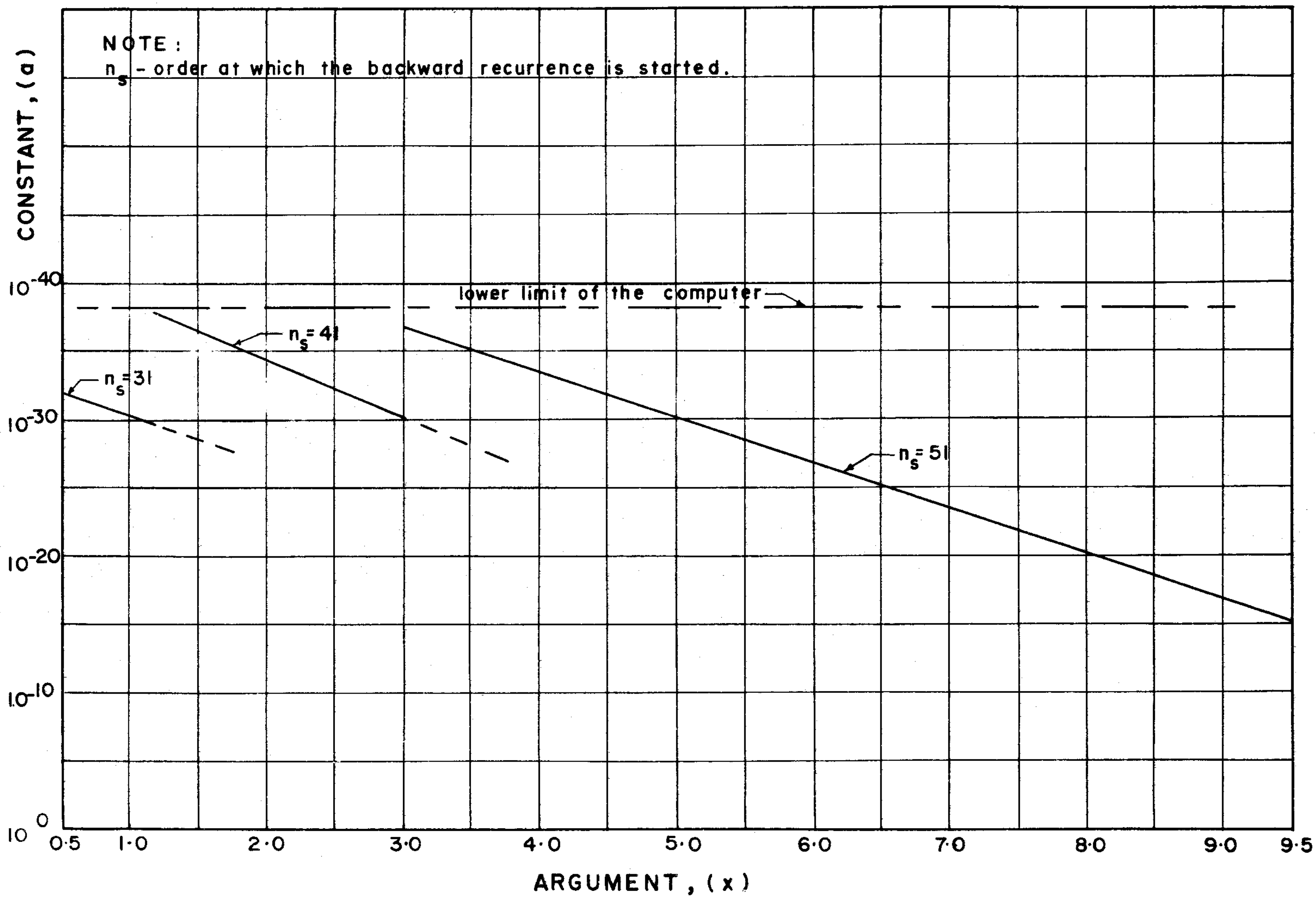

FIGURE 59

PLOT SHOWING RANGE of VALUES of the CONSTANT "a"

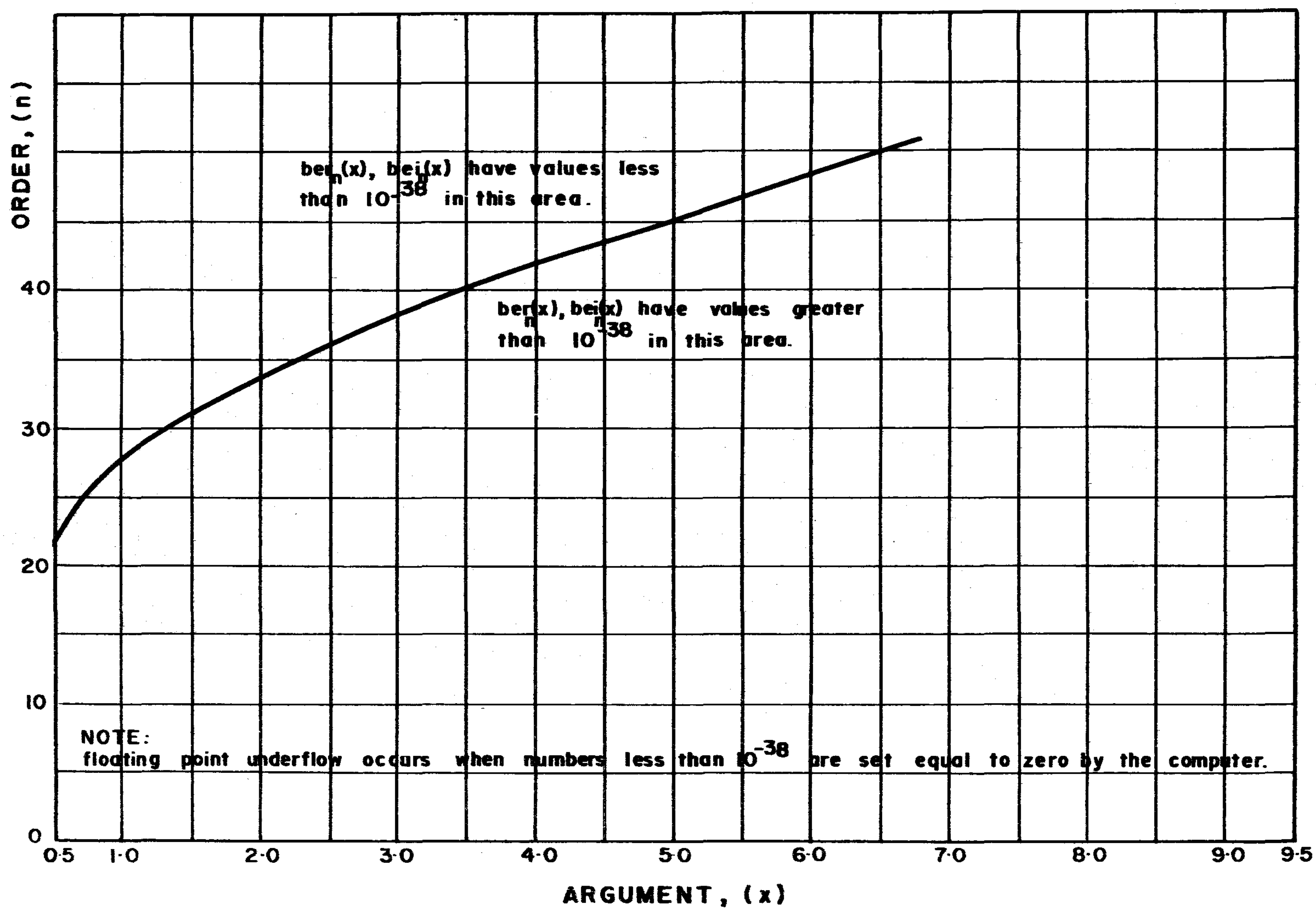

PLOT SHOWING the ORDER of $BER_n(x)$, $BEI_n(x)$ at which FLOATING POINT UNDERFLOW OCCURS

FIGURE 60

PLOT of $BER_0(x)$ and $BER_{12}(x)$

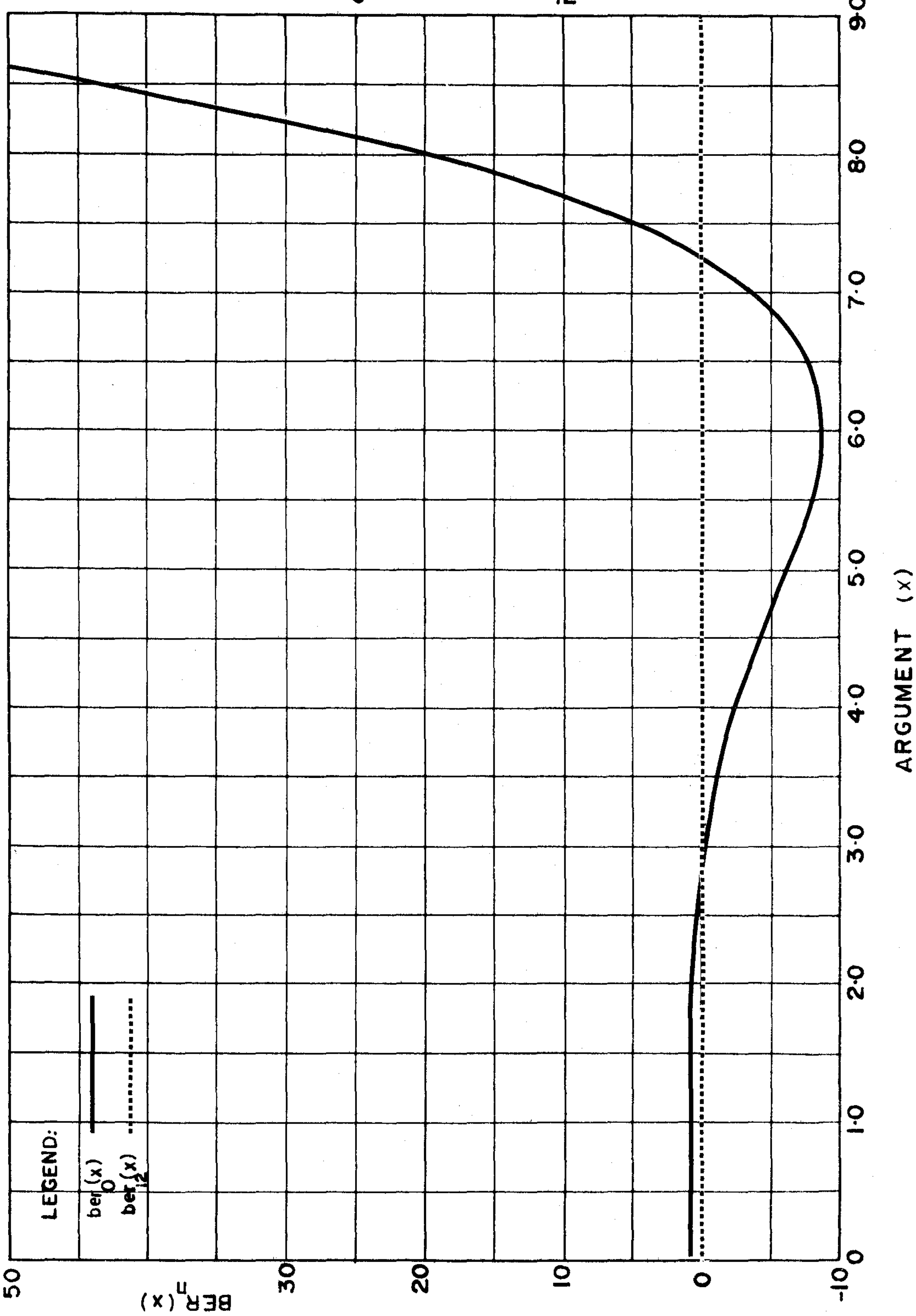

FIGURE 61

PLOT of $BER_0(x)$

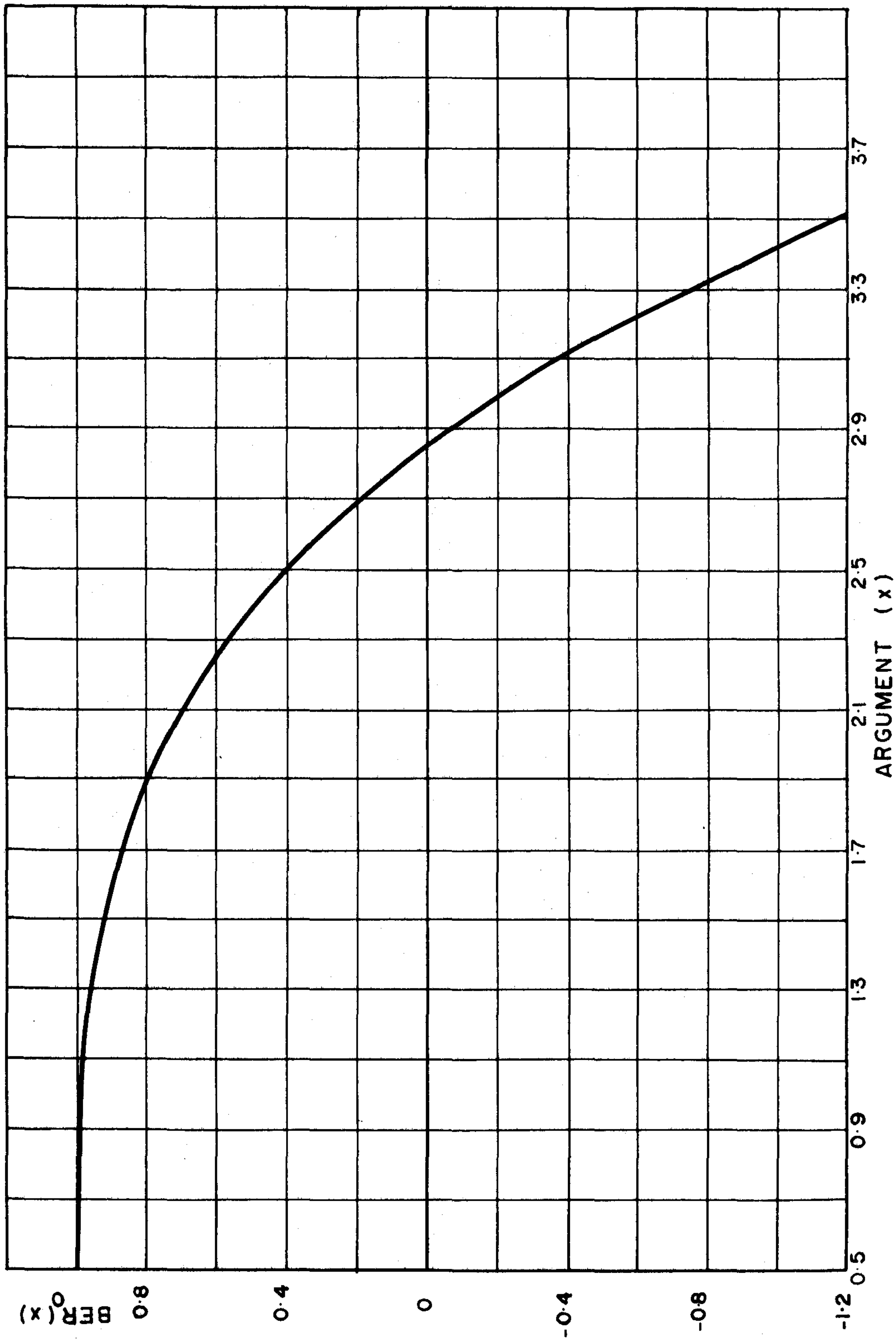

FIGURE 62

PLOT of $BER_0(x)$

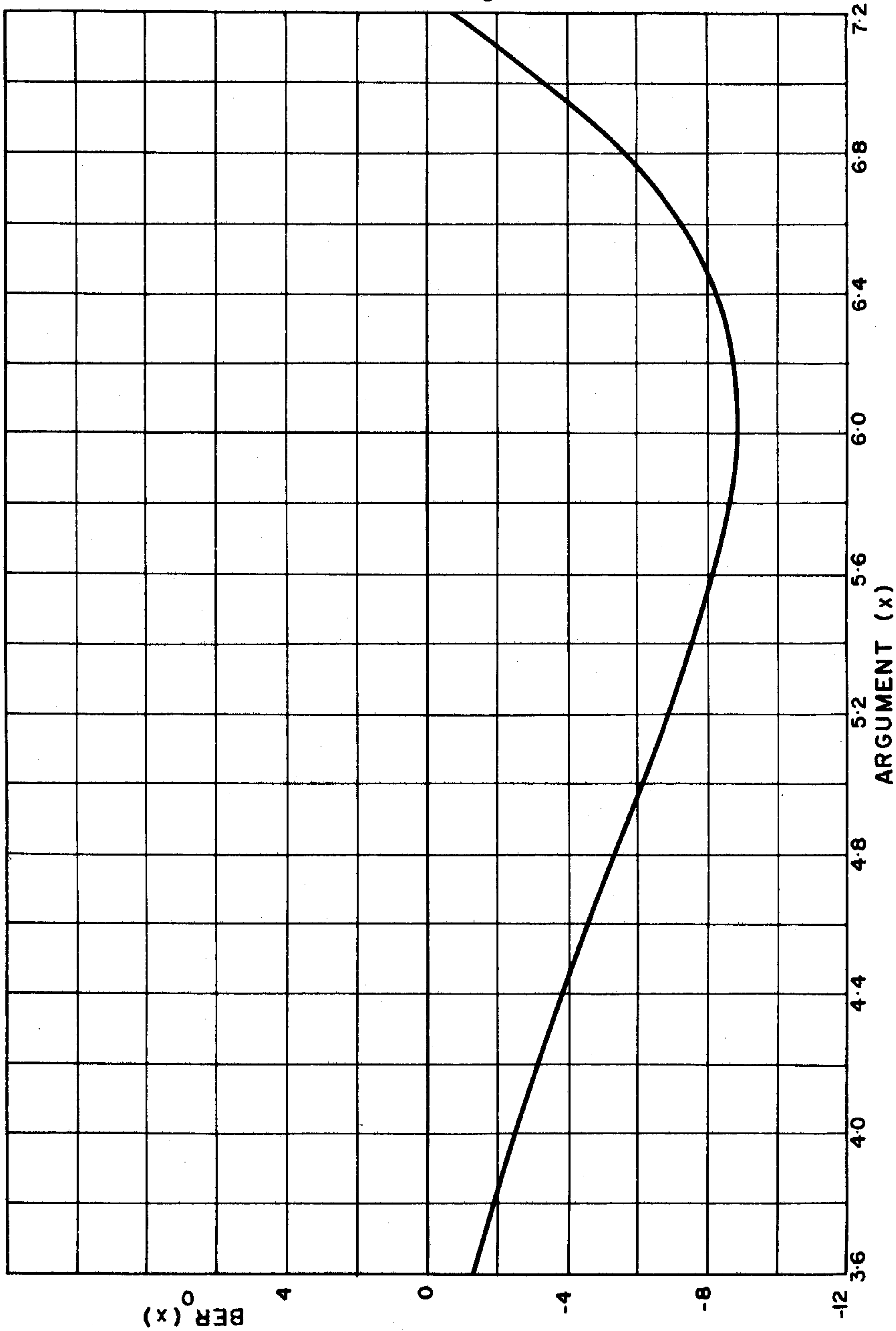

FIGURE 63

PLOT of $BER_0(x)$

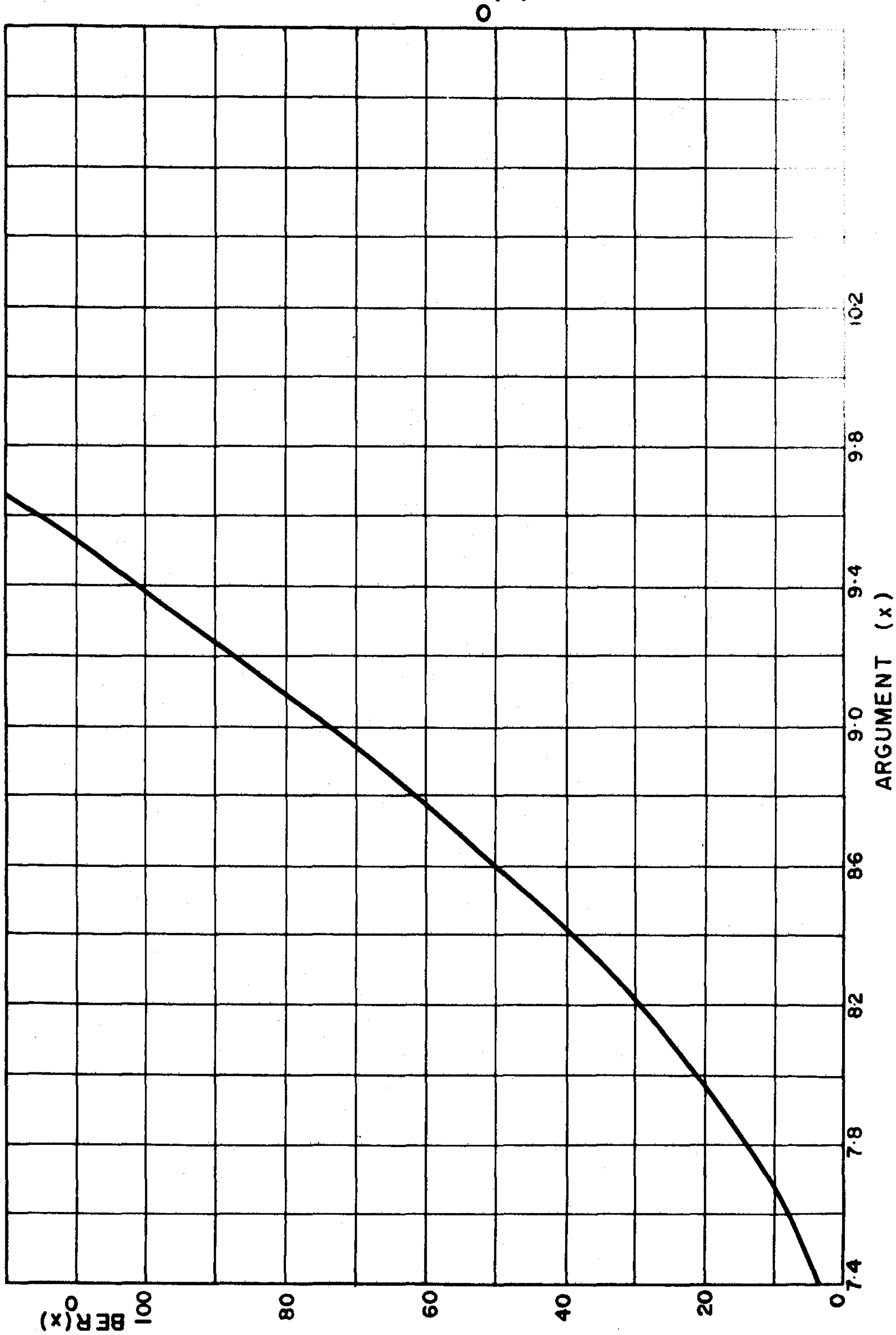

FIGURE 64

PLOT of $BER_{12}(x)$

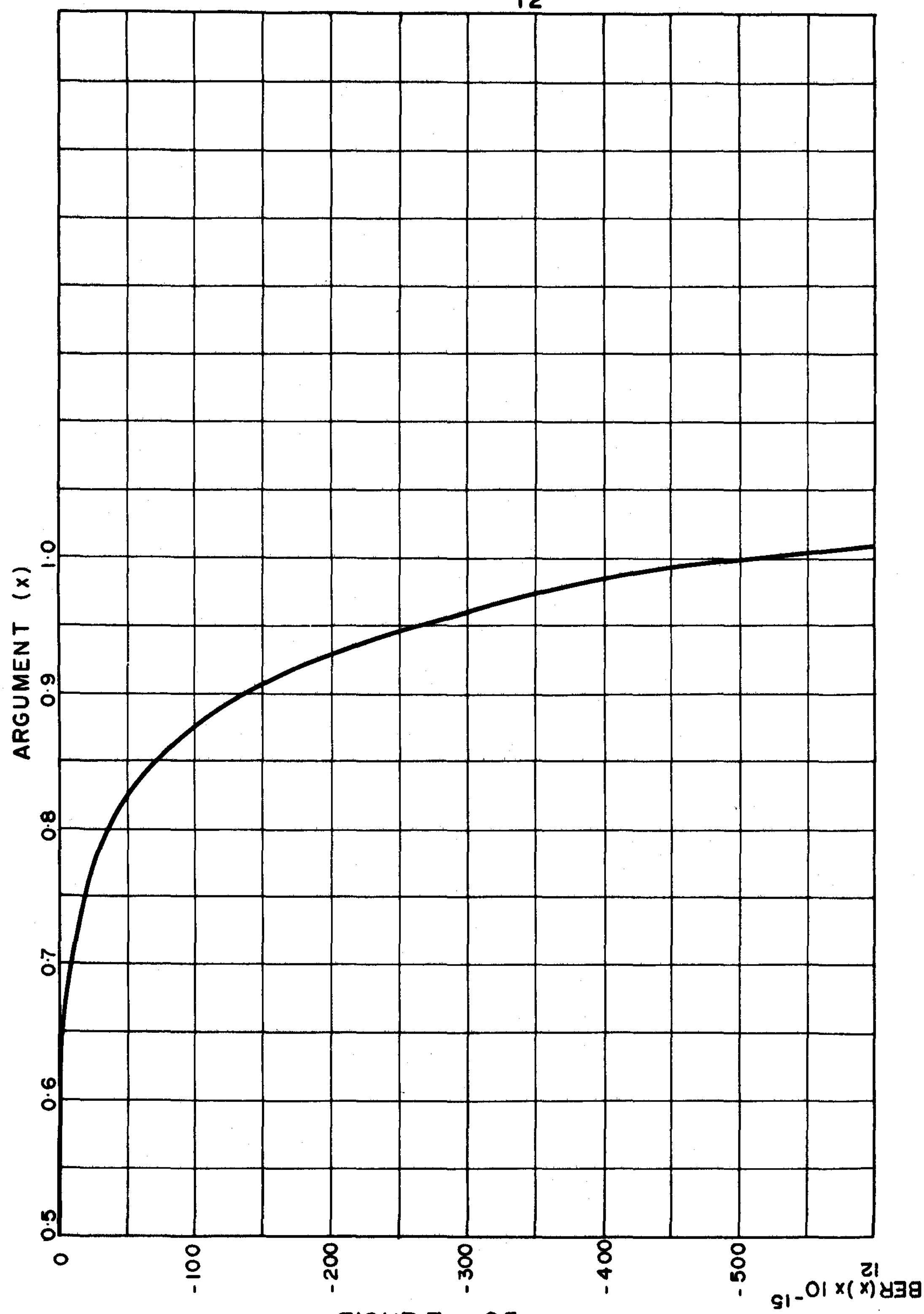

FIGURE 65

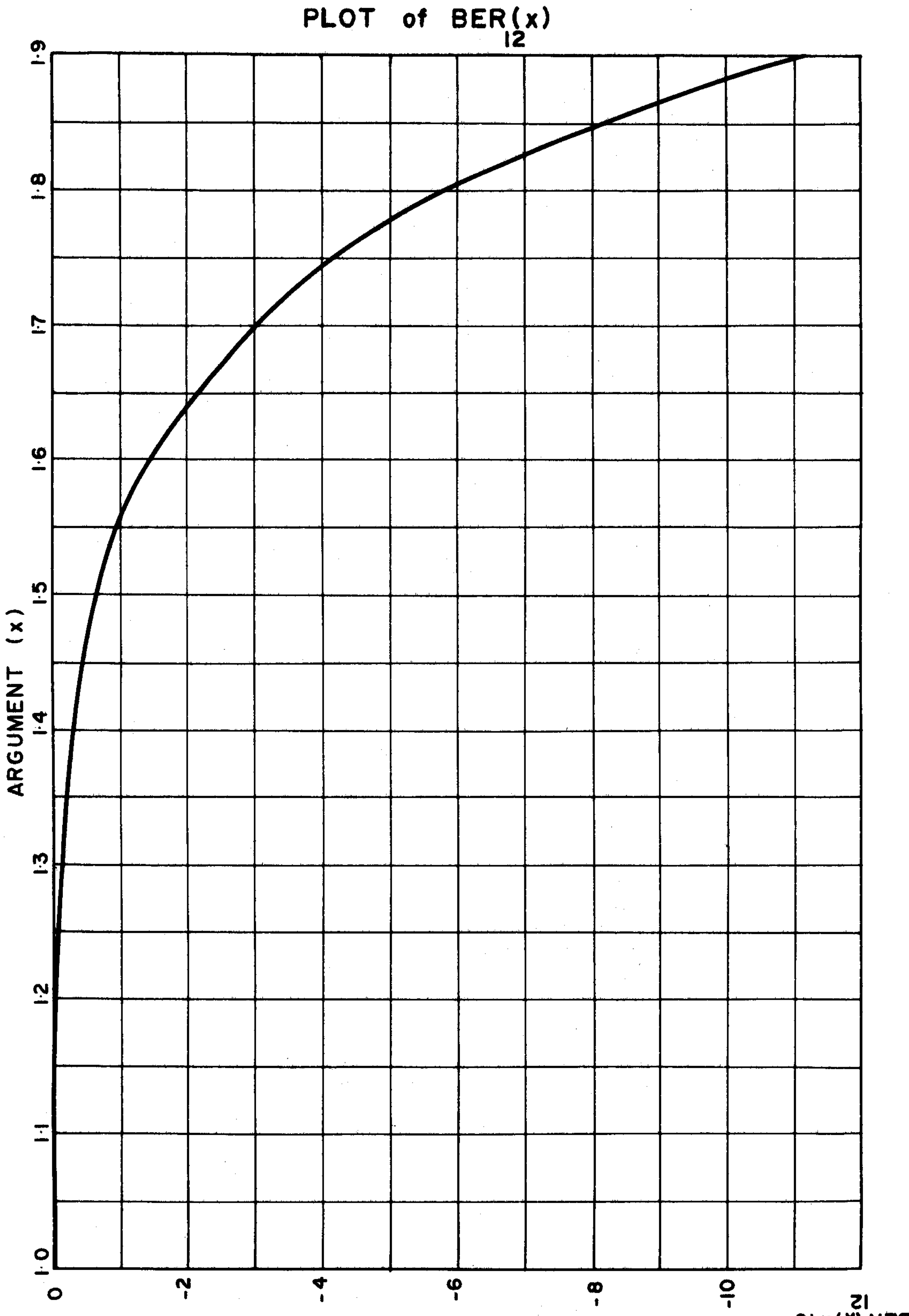
PLOT of BER12(x)
ARGUMENT (x)
1·0
1·1
1·2
1·3
1·4
1·5
1·6
1·7
1·8
1·9
0
-2
-4
-6
-8
-10
BER12(x) x 10^-10

FIGURE 66

PLOT of $BER_{12}(x)$

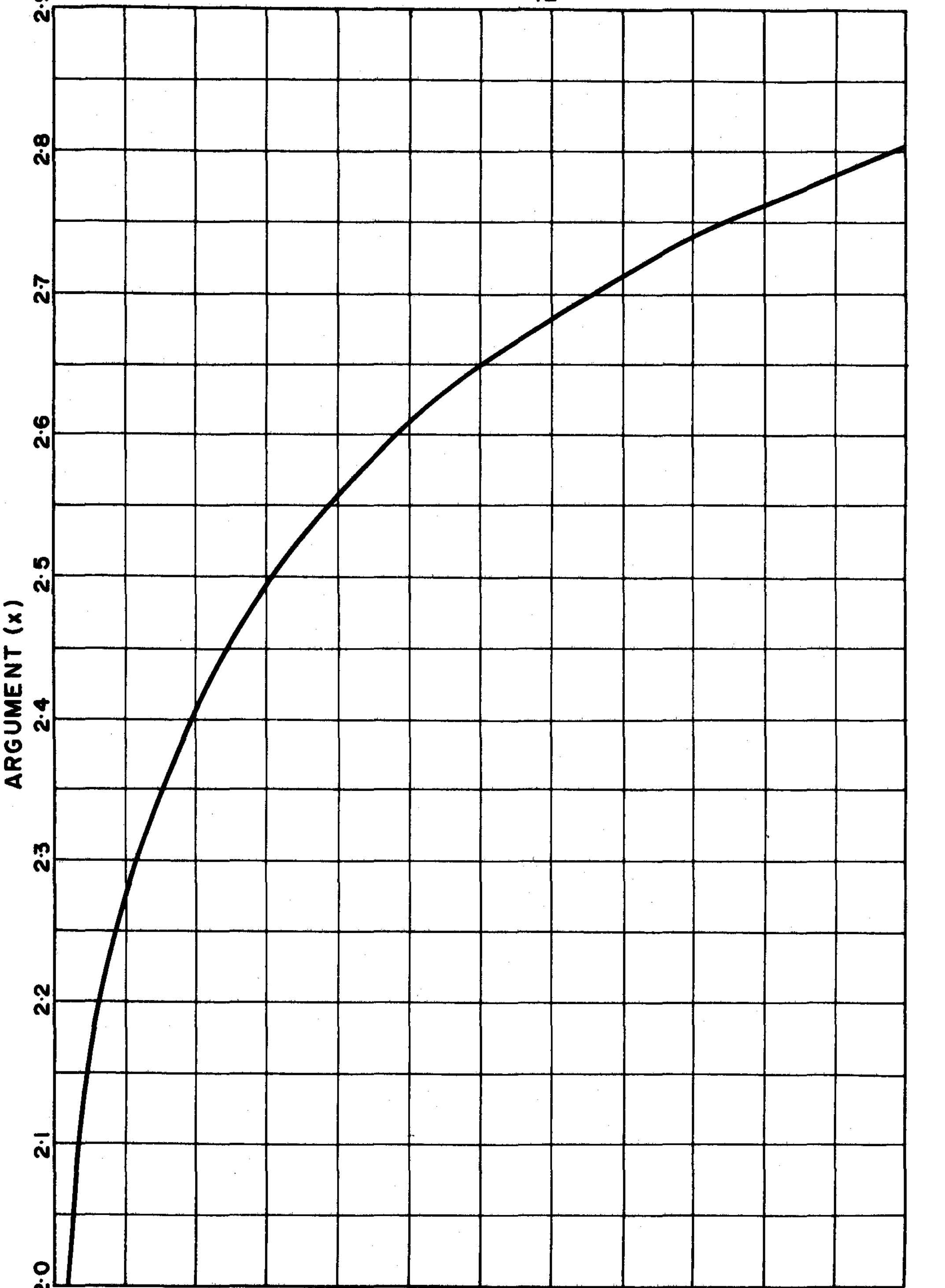

FIGURE 67

PLOT of $BER_{12}(x)$

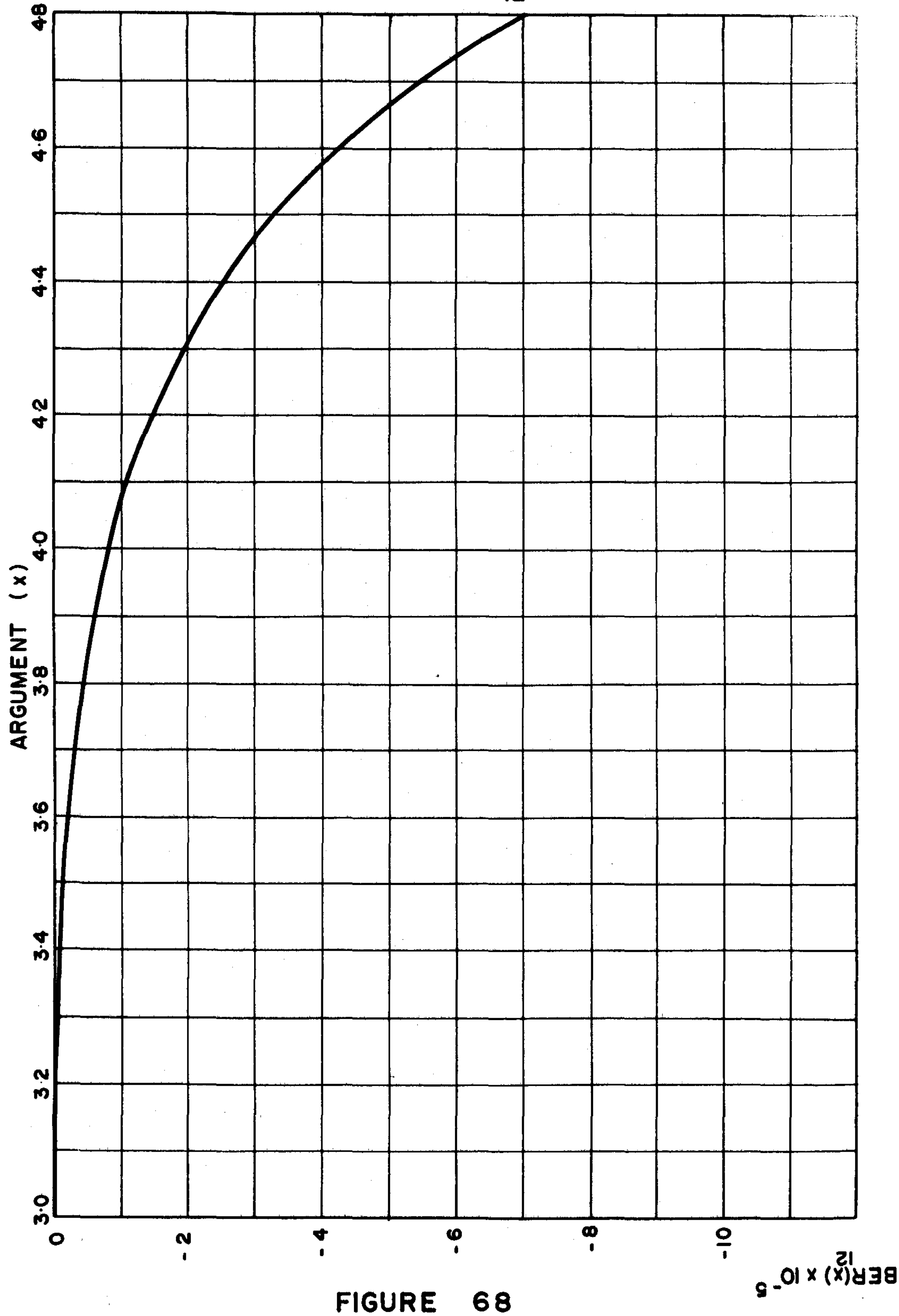

FIGURE 68

PLOT of $BER_{12}(x)$

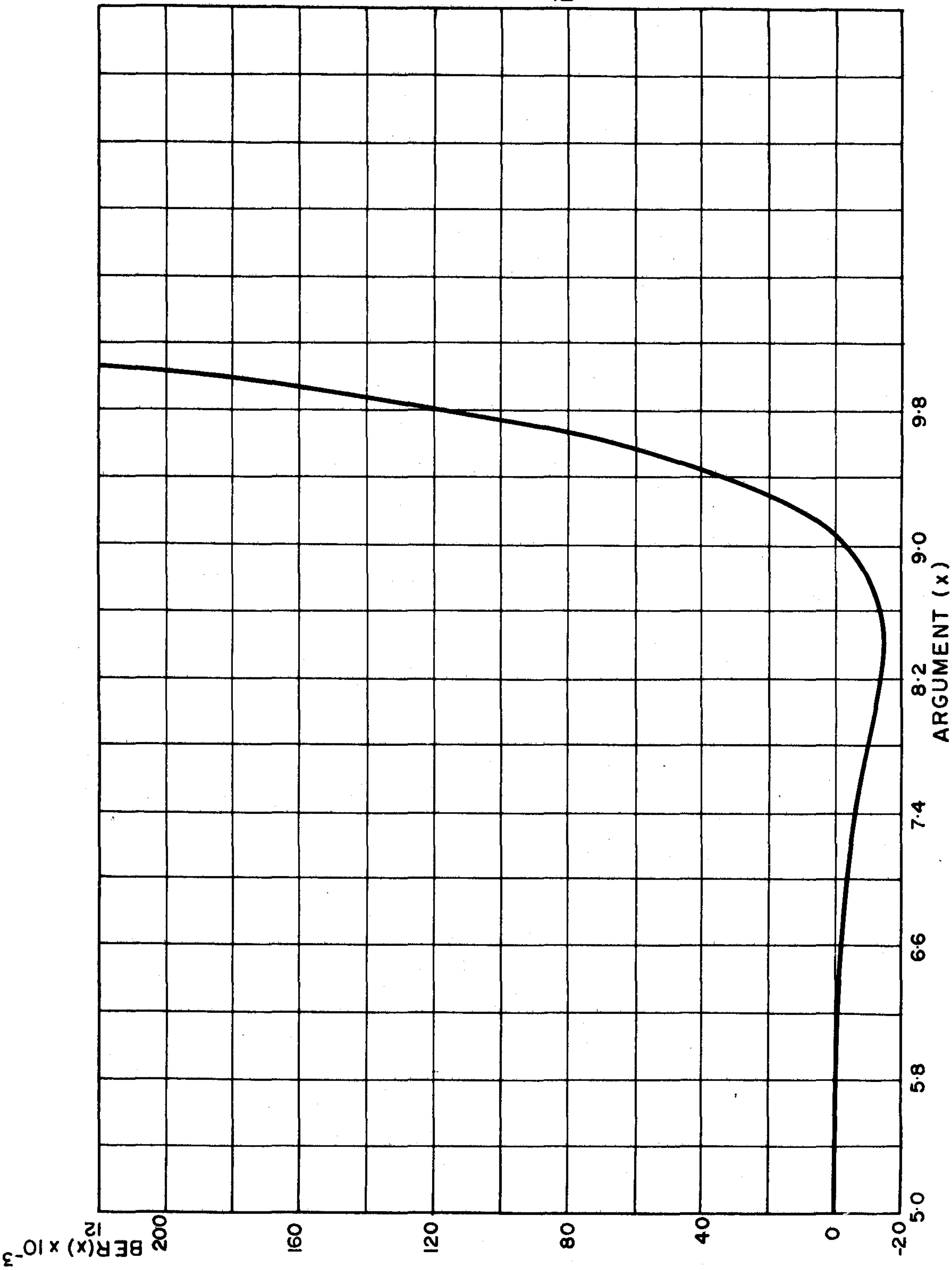

FIGURE 69

PLOT of $BER_{24}(x)$

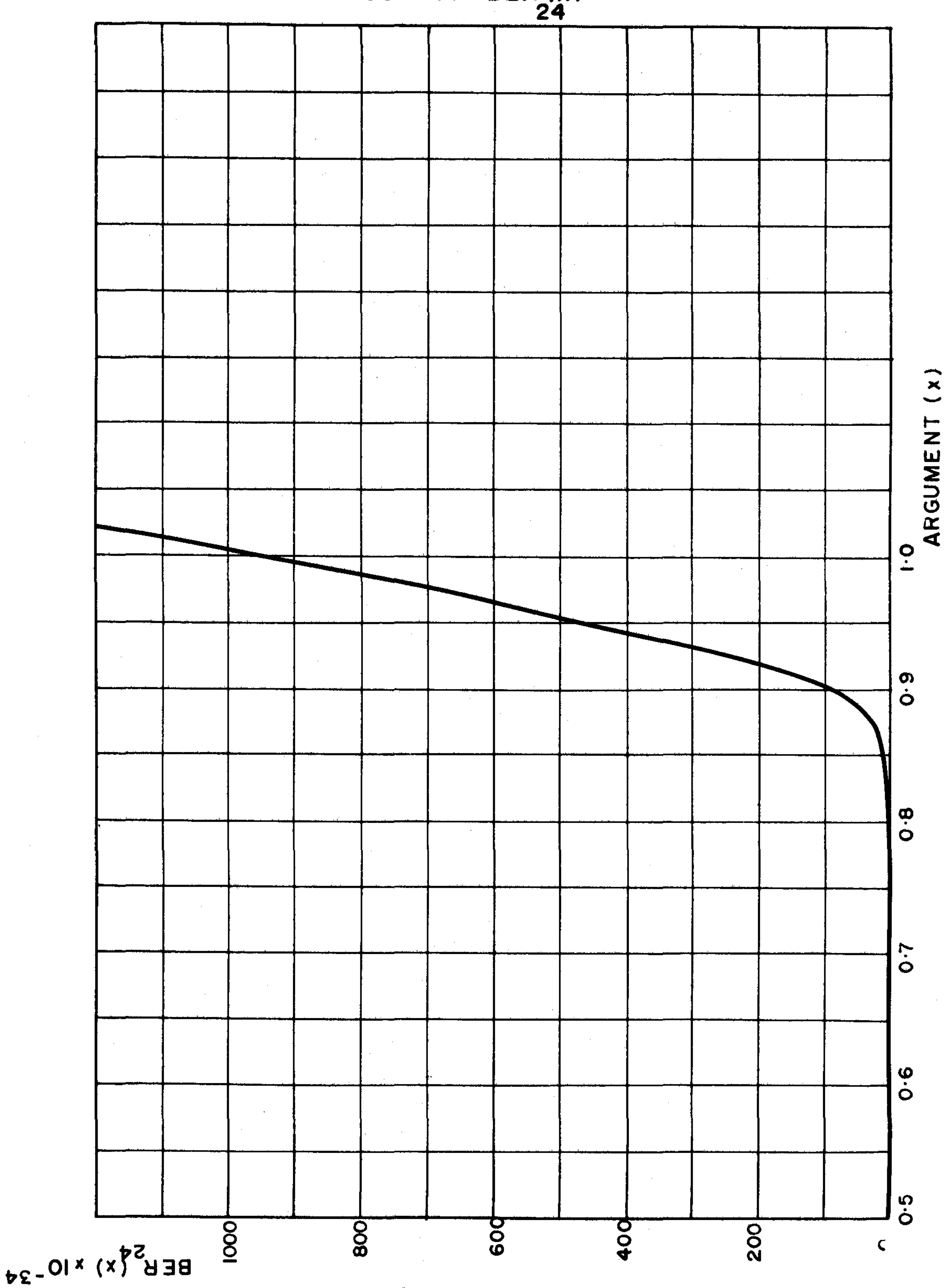

FIGURE 70

PLOT of $BER_{24}(x)$

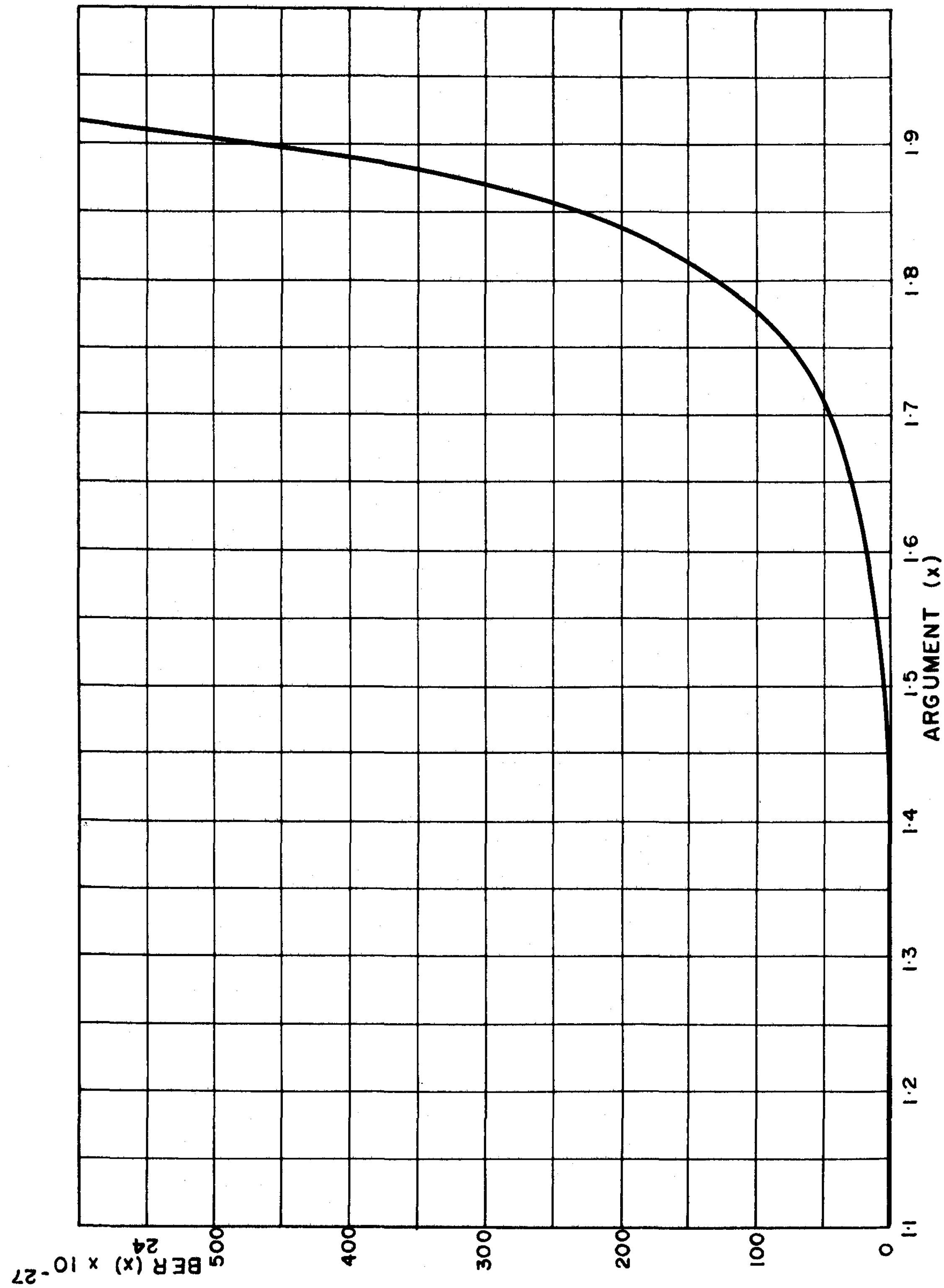

FIGURE 71

PLOT of $BER_{24}(x)$

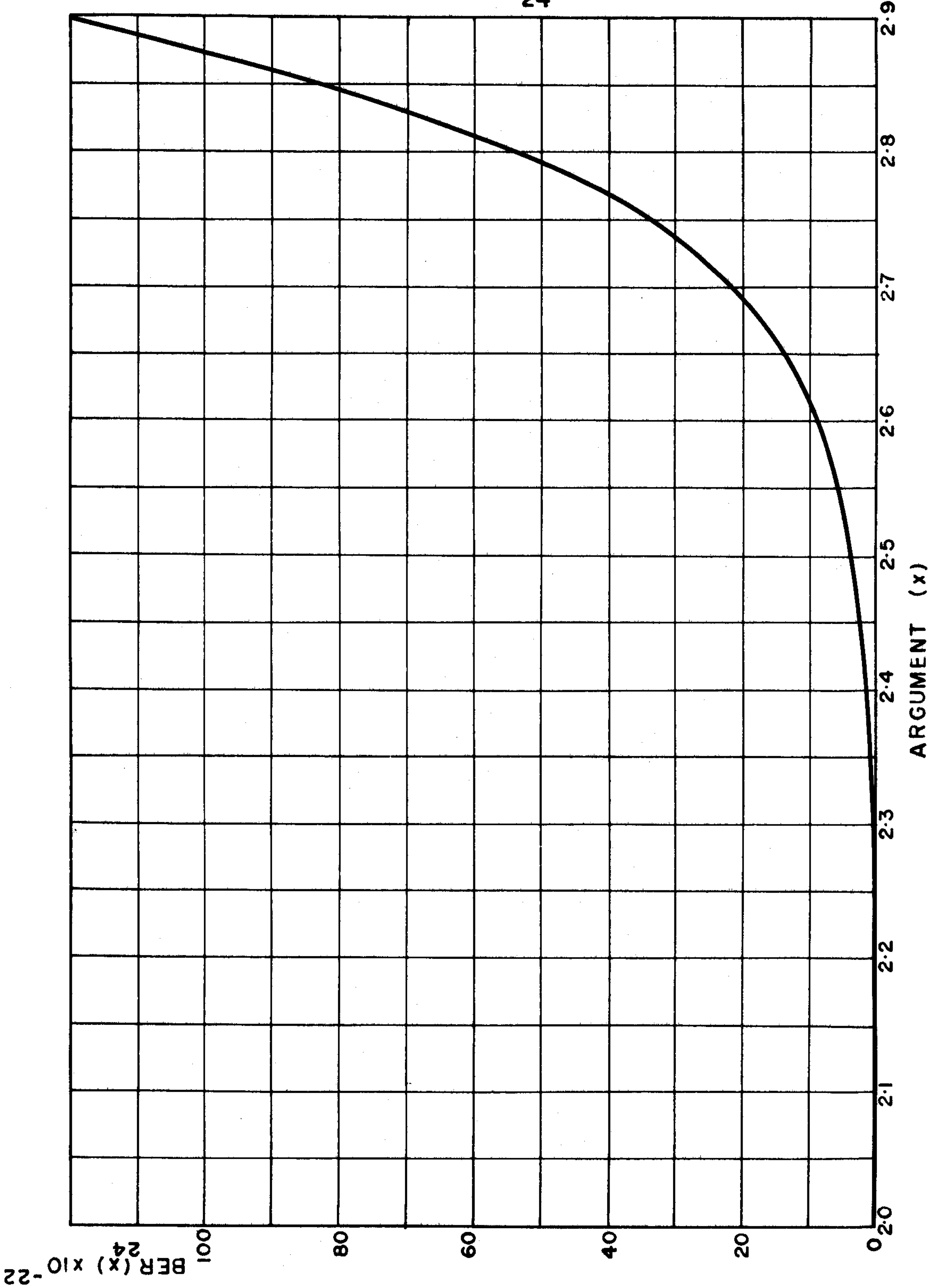

FIGURE 72

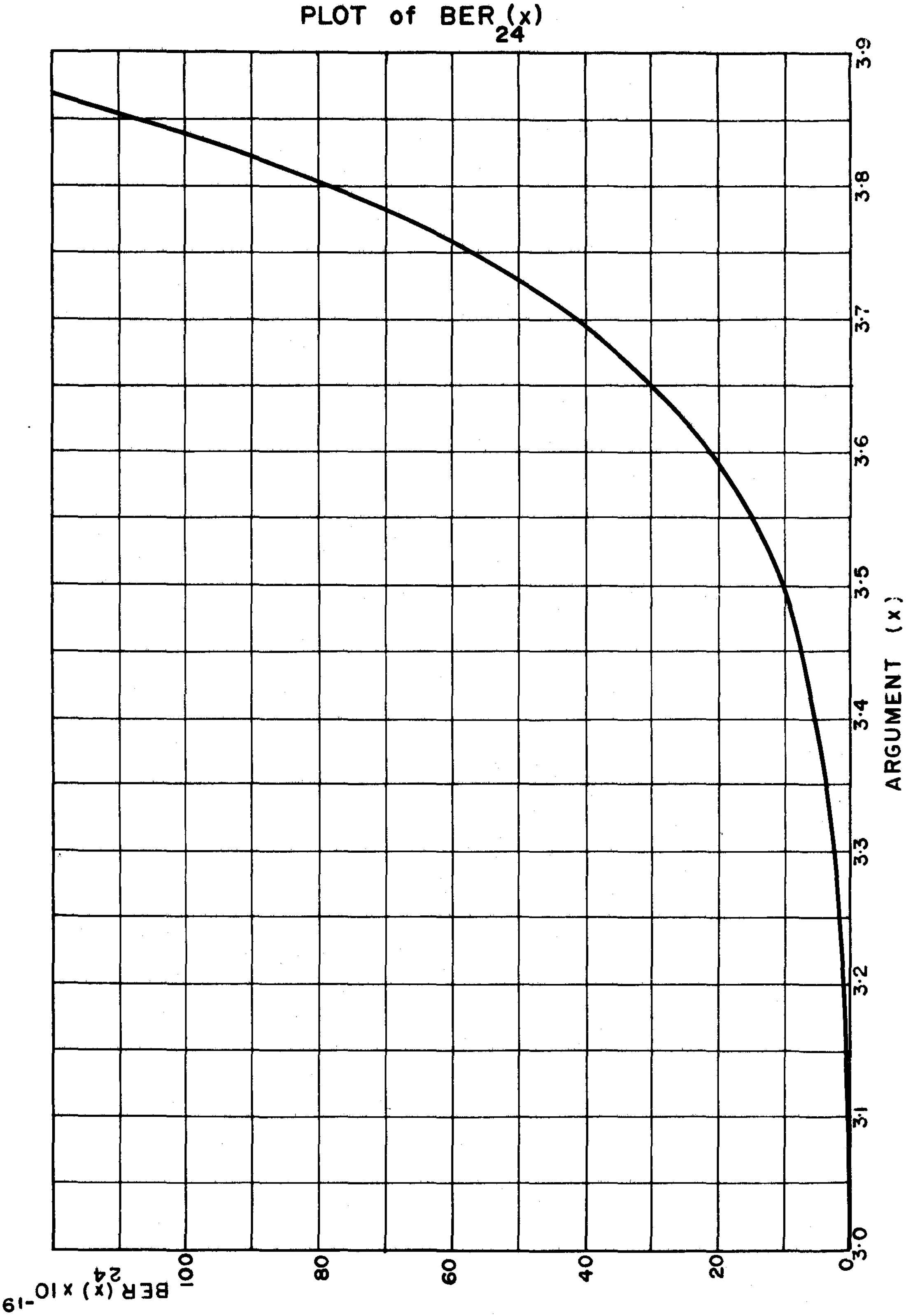
PLOT of $BER_{24}(x)$
3·0
3·1
3·2
3·3
3·4
3·5
3·6
3·7
3·8
3·9
ARGUMENT (x)
0
20
40
60
80
100
$BER_{24}(x) \times 10^{-19}$

FIGURE 73

PLOT of $BER_{24}(x)$

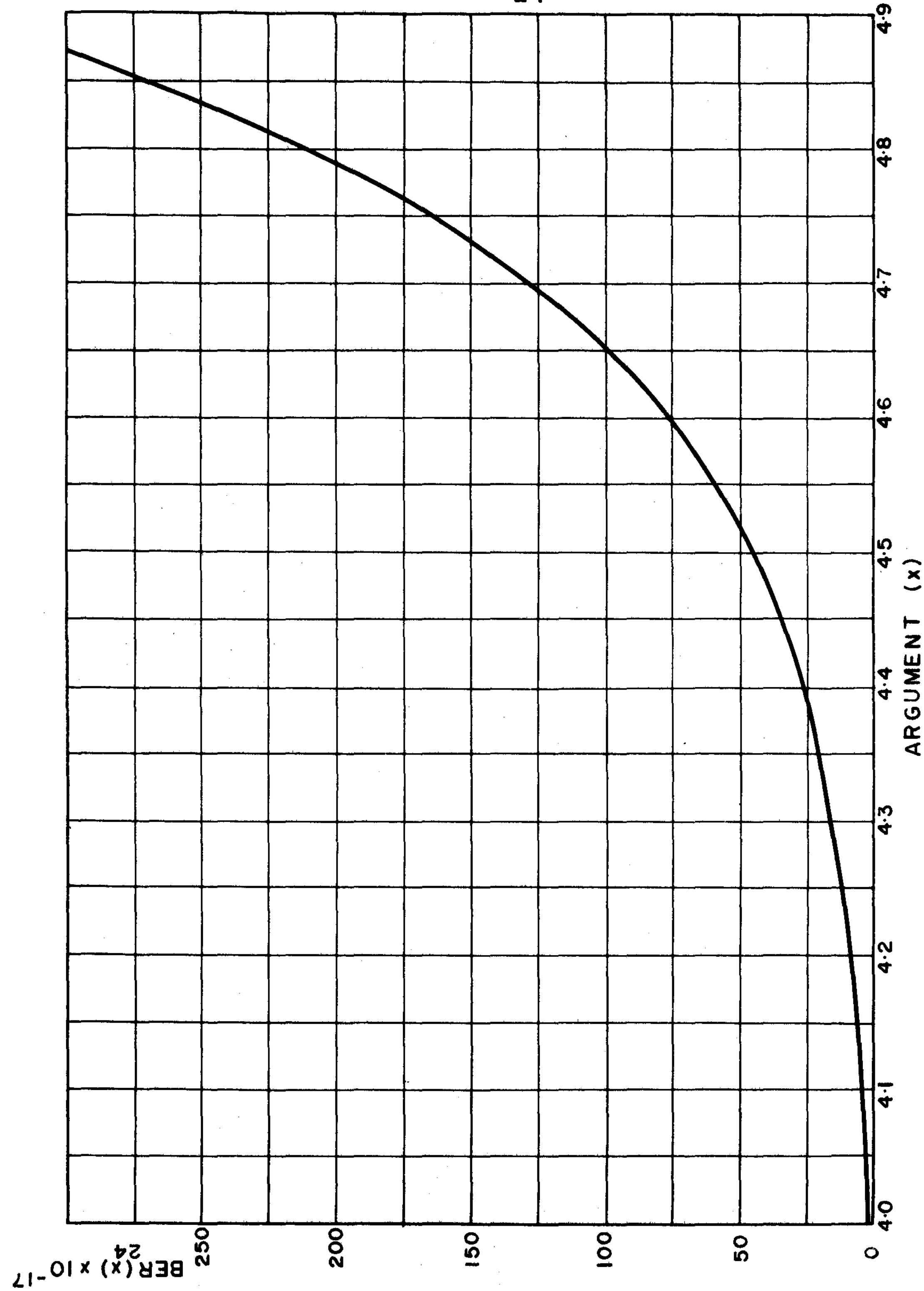

FIGURE 74

PLOT of $BER_{24}(x)$

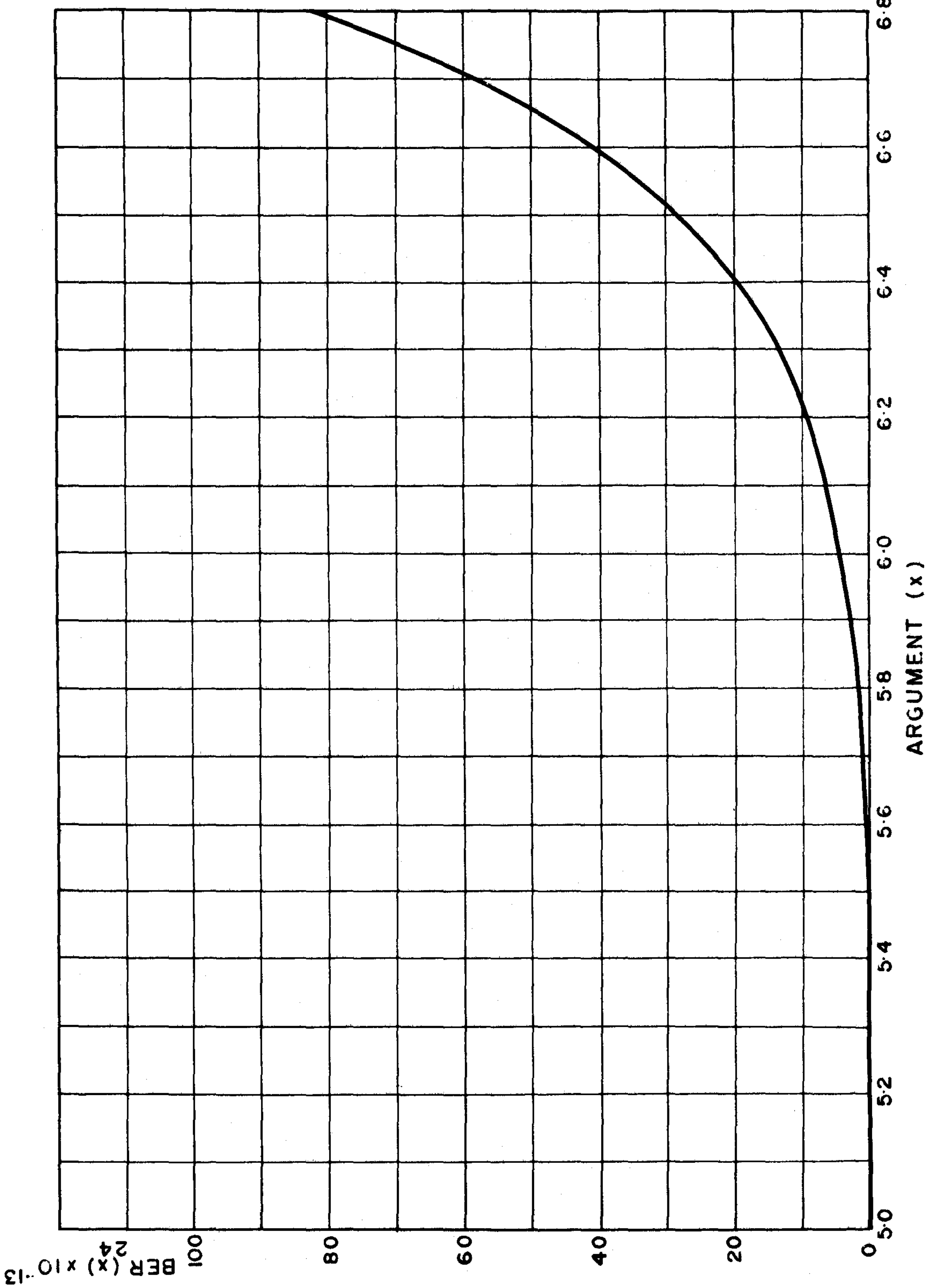

FIGURE 75

PLOT of $BER_{24}(x)$

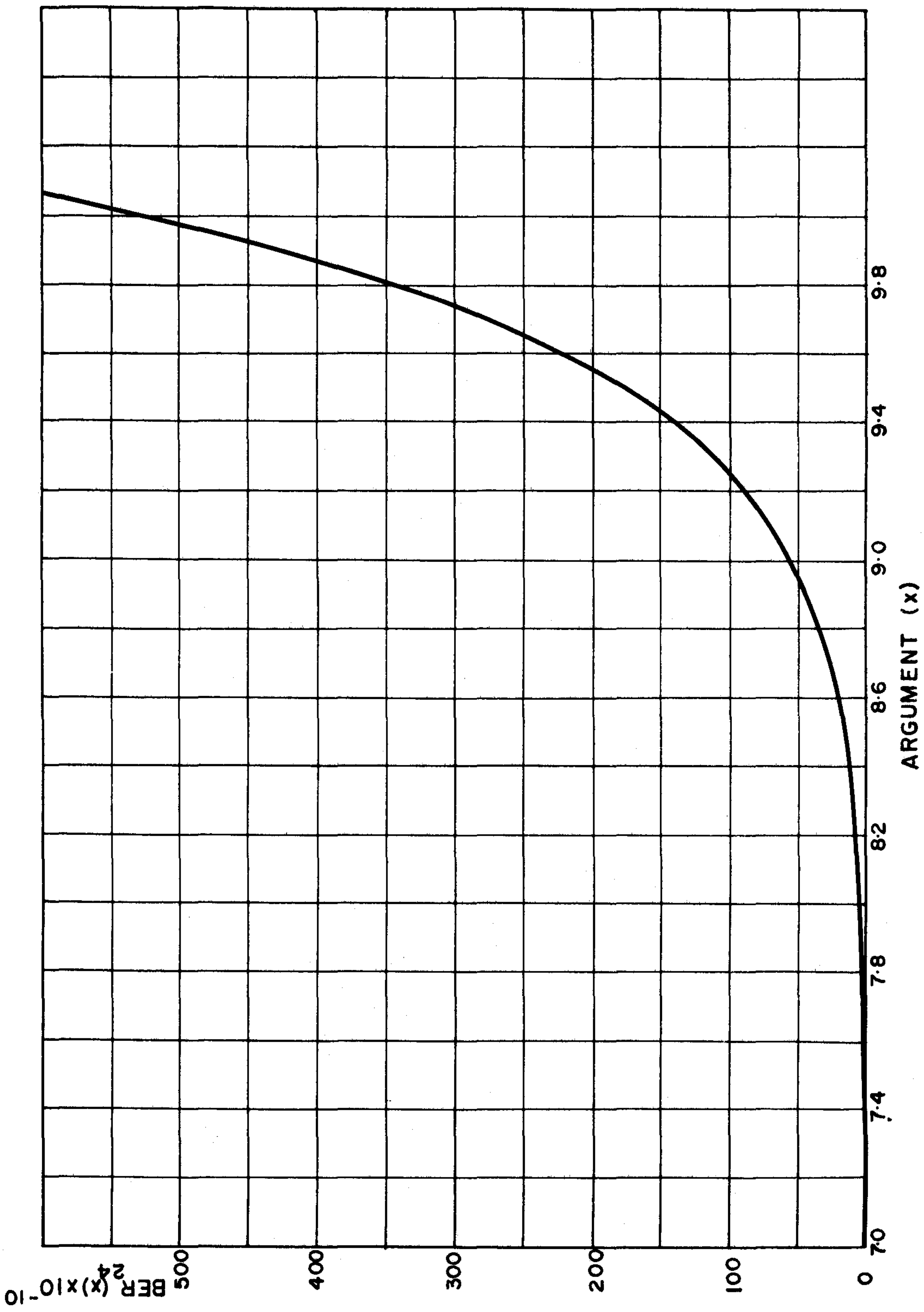

FIGURE 76

BIBLIOGRAPHY

1934 Tölke, F.
"Über Spannungszustände in dünnen Rechteckplatten". Ingenieur-Archiv, vol. 5, p. 187.

1939 Marguerre, K.
"Zur Theorie der gekrümmten Platte grosser Formänderung", Proc. 5th International Congress of Applied Mechanics, Cambridge, Mass., 1938.

1949 Vlasov, V. Z.
"Obshchaya teoriya obolochek i ee prilozheniya v tekhnike", Gostekhizdat, Moscow, 1949, p. 295.

1955 McLachlan, N.W.
"Bessel Functions For Engineers", Oxford at the Clarendon Press, Second Edition.

1957 (1) Oravas, G. Æ.
"Stress and Strain in Thin Shallow Spherical Calotte Shells", International Association for Bridge and Structural Engineers, Zurich.

(2) Oravas, G. Æ.
"Transverse Bending of Thin Shallow Shells of Translation", Österreichisches Ingenieur-Archiv, vol. 11 - 4, p. 264, 1957.

1959 Lowell, H.
"Tables of Bessel-Kelvin Functions ber, bei, ker, kei and their Derivatives for Argument Range 0(0.01) 107.50", Technical Report R - 32, National Aeronautics and Space Administration, Washington, D.C.

1960 Dikovich, V. V.
"Pologie Pryamougol'nye v Plane Obolochki Vrashcheniya", Gos. Izd. Lit. po Stroitel'stvu, Arkhitekture i Stroit Materialam, Moscow - Leningrad.

1963 Farrell, O.J. and Ross, B.
"Solved Problems: Gamma and Beta Functions, Legendre Polynomials, Bessel Functions", The MacMillan Co., New York.

1964 Michels, T. E.
"The Backward Recurrence Method for Computing the Regular Bessel Function", Technical Note D - 2141, National Aeronautics and Space Administration, Washington, D.C.

Young, A. and Kirk, A.
"Bessel Functions Part IV Kelvin Functions", R.S.M.T.C. vol. 10, University Press, Cambridge.

1964 Riley, G. E.
"Stress and Strain in a Shallow Elastic Calotte Shell", Thesis, McMaster University.